THE REACTIONS OF (+)-2- AND (+)-3-CARENES WITH THE RETENTION OF THE BICYCLIC FRAMEWORK

Liudmila Bets, Liudmila Vlad, Fliur Macaev*

Institute of Chemistry of the Academy of Sciences of Moldova,
Academy str. 3, MD-2028, Chisinau, Moldova
Tel +373-22-739-754, Fax +373-22-739-954, E-mail: flmacaev@cc.acad.md

Abstract: Carane-type compounds have attracted attention in recent years due to their practical importance. This review is focused on describing the developments in the synthesis of trimethylbicyclo[4.1.0]heptanes and their unsaturated analogues from monoterpenes (+)-2- and (+)-3-carenes published mostly during the last decade.

Keywords: (+)-2- carene, (+)-3-carene, trimethylbicyclo[4.1.0]heptanes, trimethylbicyclo[4.1.0]hept-3-enes, organic synthesis.

1. Introduction

Progress of modern synthetic organic chemistry is determined by two general tendencies – profound study of biological processes and natural products as the ground for the creation of new effective bioregulators (drugs, pharmaceuticals, diagnostic materials, pesticides et al.) and the use of natural substances as the starting materials (raw materials) for the synthesis of new optically active compounds including bioregulators. The development of new enantiopure compounds, in particular new medicals having chiral centers in a molecule (such substances are found in about, the third part of all drugs and in more than 75% of new pharmaceuticals) is connected with the requirements of obtaining high molecular purity. It is well known that one of the tasks of the synthesis of a bioactive compound is the preparation of the required enantiomer in an optically pure form. Bicyclic monoterpenes (+)-3-carene **1a** and (+)-2-carene **1b** are widely used for resolving this type of problems [1-7]. A structural feature of both compounds is the presence of the reactive C=C double bond and bicyclic bridging system. This fact opens perspectives for a new synthesis with the retention of the bicyclic framework of monoterpenes **1a,b**. The main attention in this review is focused on the articles published during the last decade, and on those not mentioned in the above references. Data on skeleton transformation as well as a gradual fragmentation of the terpenes framework are published in works [8-13] and will be not considered hereafter.

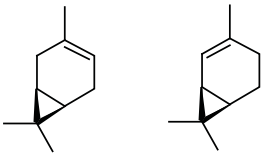

1a **1b**

2. Synthesis on the basis of (+)-3-carene with the retention of the carane framework

Sulfur containing terpenoids derivatives, which have a number of important properties, are not found in nature. The regioselective method for obtaining epimeric sulfides **2** is described in [14] and it is based on the hydrolysis of the product of sulfenyl chloride addition to (+)-3-carene **1a** (scheme 1).

***Scheme* 1**

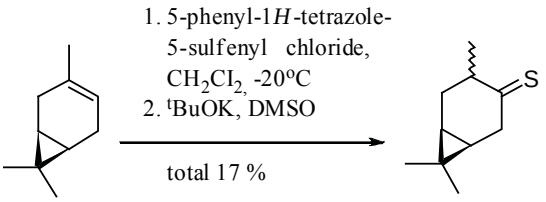

1a **2**

In order to perform the introduction of the thio-group into position 3 of the carane framework it is suggested to use the addition of $(MeS)_2$ to carene **1a** or thio-caranes **4**,**7** (scheme 2).

The $ZnCl_2$ catalyzed addition of $(MeS)_2$ yields a mixture of isomeric products **6a,b** (R=H) [15,16]. For the synthesis of similarly built substances, the α- and β-thio-oxides of 3-carene epoxides **3a** and **3b** have been prepared. The latter gave the carane derivatives **5** and **8** upon the interaction with mercaptans. The respective homologues **6a,b** (R=Me, Et, i-Pr or prenyl) are formed at alkylation of mercaptans in alkaline conditions with alkyl halides.

***Scheme* 2**

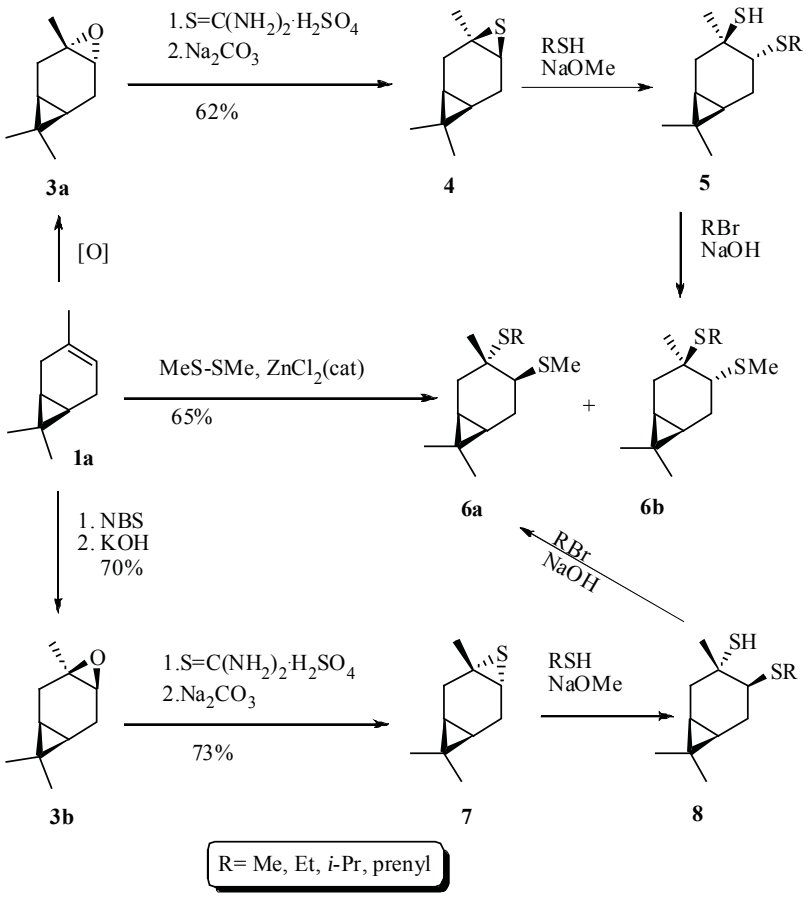

Initial epoxides **3a** can be obtained using peroxy acids, dimethyloxirane, by the oxidization with H_2O_2 or O_2 catalyzed by transition metals [22-50]. One of the most used epoxidation methods is the stoichiometric peracid route using such acids as peracetic acid and *m*-chloroperbenzoic acid. The employment of peroxy acids is not a clean method as equivalent amounts of acid waste are produced. The safety issues associated with handling peracids are also a matter of concern. The use of hydrogen peroxide as a cheap, environmentally clean and easily handled oxidant in conjugation with robust and easily obtainable synthetic metalloporphirins, transition metal Schiff base complexes of various metals, heteropoly acids, transition metal substituted heteropoly acids as catalysts led to procedures, which help to perform epoxidation reaction. However, the chemo- and stereoselectivity of the oxidation reactions were not high. Moreover, the separation of the catalysts is usually troublesome and not economical for application. Dimethyldioxirane epoxidation of (+)-3-carene **1a** gave the corresponding epoxide **3a** (yield 100%). In pilot conditions, carene **1a** is oxidized into epoxide **3a** (yield 93%) by pinane hydroperoxide in the presence of molybdenum catalysts [51]. Epoxide **3b** is synthesized in two steps with a 70% yield [52].

Synthesized tiocaranes as well as (+)-3-carene **1a** itself show an antifungal activity [53].

Hydroxymercaptans and sulfides **9-12,** that are of interest as physiologically active compounds and reagents, have been synthesized from epoxides **3a**,**b** [54,55] (scheme 3).

It has been established that the interaction of oxides **3a**,**b** with thioglycolic acid proceeds along with the formation of isomeric diols **10a,b** in mixture with acids **9a,b**. The given reactions allow the synthesis of disulfide **11** and enantiomers **12a**,**b**. However, the yield of these products is low.

cis-Diol **13** can be synthesized by direct hydroxylation of 3-carene **1** with $KMnO_4$ or OsO_4 [56, 57].

Salakhutdinov *et al* published the synthesis of compound **13** using *cis*-opening of epoxide **3a** [58]. This approach gave *cis*-diol avoiding skeleton rearrangements, which were noticed with β-epoxide **3b**.

We designed and synthesized novel *P**-chiral monodentate phosphite ligands, having five-membered phosphacycles and OMe (or NEt_2) exocyclic substituents (scheme 4) [59, 60].

These can be easily prepared by direct phosphorylation of the appropriate **13** and purified by vacuum distillation. Carene-based compounds **14a,b** are characterized by rather small contents of the minor epimer. The major stereoisomer has the *R* - configuration at the *P** - stereocenter.

***Scheme* 3**

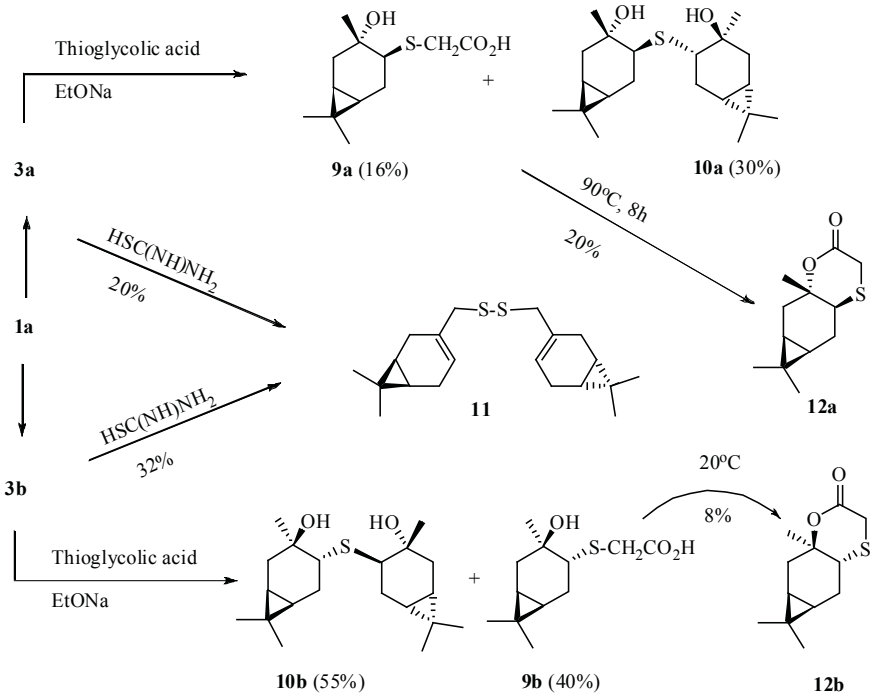

***Scheme* 4**

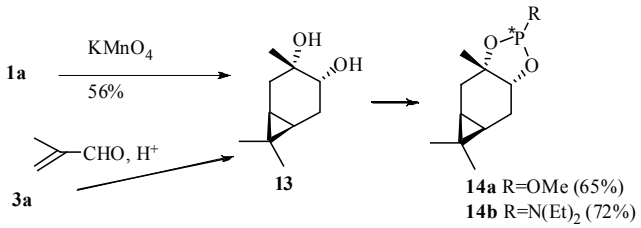

One of the approaches to enhance asymmetrising activity of chiral phosphite-type compounds is the synthesis of the respective *P,N*-bidentate ligands with additional *C** - stereocenters in the side chain *N*-containing group. In particular, oxazolinophosphite **15** has been prepared using phosphoramidite **14b** as a phosphorylating reagent (scheme 5).

***Scheme* 5**

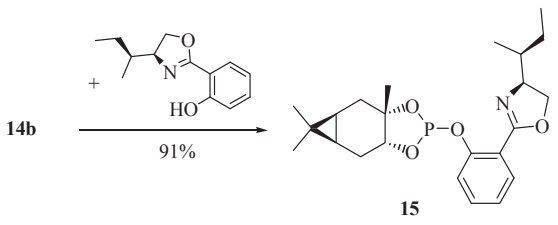

Using these novel ligands, up to 91% *ee* was achieved in the Pd-catalysed asymmetric allylic amination [59, 60].

β-Hydroxyamine **16**, obtained by the interaction of epoxide **3a** with morpholine [61-63], was an effective catalyst in addition of diethylzinc to aromatic aldehydes in the synthesis of optically active alcohols (up to 98% ee) (scheme 6).

***Scheme* 6**

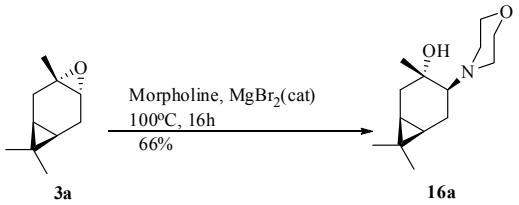

Diastereomeric compound 1**6b** has been synthesized from epoxide **3b** and morpholine [64] (scheme 7).

***Scheme* 7**

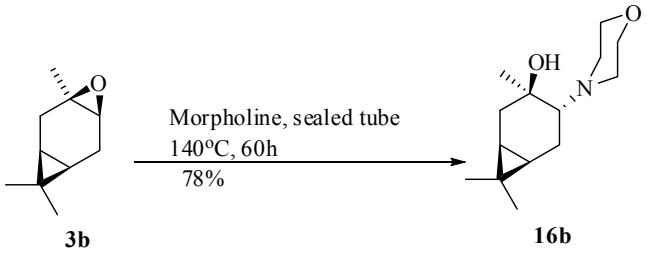

Another, no less interesting group of carane derivatives **7a-d**, has been synthesized from oxide **3a,b** (scheme 8). It should be noted that in most cases the syntheses are not selective, though they have been carried out in various proton solvents during catalysis with inorganic or organic acids, oxides of heavy metals, or under photolysis [57, 43, 65-77].

***Scheme* 8**

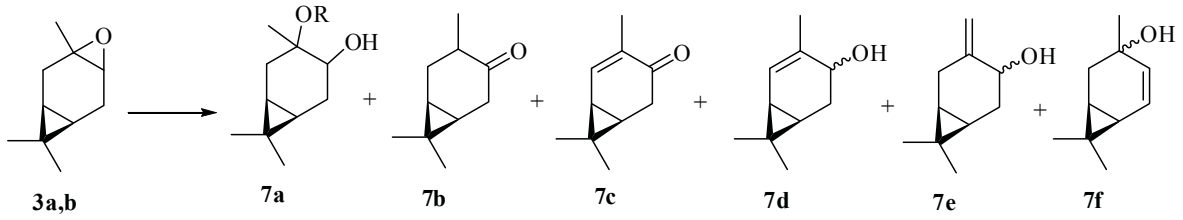

Acid-catalysed opening of the epoxide **3a** involves the cleavage of a more highly substituted C-O bond and affords as a rule compound **7a** accompanied by trace amounts of the opposite 4-alkoxy-3-caranols. The treatment of oxide **3a** with both mineral acids and acetic acid provides 4-caranone **7b**. The rearrangement of epoxide **3a** has been made using boron trifluoride etherate, which resulted in the mixture of the 4-caranone (43%) with menth-3-en-2-one (28%).

***Scheme* 9**

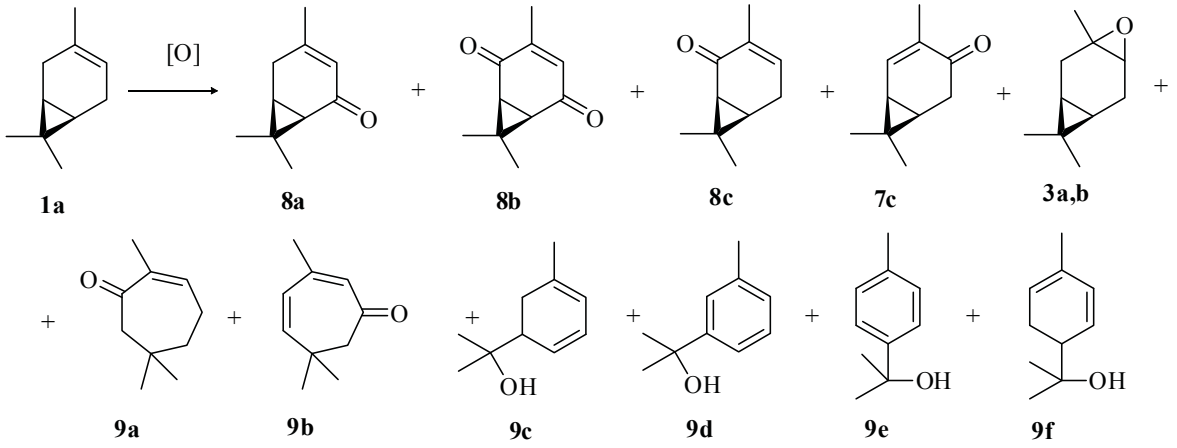

The treatment of the isomeric epoxide **3b** under identical conditions provides product **7b** with 66% yield. In contrast with the epoxide **3a**, which gives major trans-diols **7a** (R=H) on the acid-catalyzed hydrolysis – epoxide **3b** was noted to give both the expected cis- and trans-diols **7a** (R=H) in 26% and 53%, respectively. The repetition of the experiment in acidic MeOH provides both regio-isomeric hydroxy ethers in total yield 80%. The treatment of the isomeric epoxides **7a,b** with oxides of heavy metals or under photosensitized conditions provides the mixture of isomeric carenes **7c-f** .

Liquid-phase oxidative conversions of carene **1a** are technologically perspective but it is difficult to make them, just like the previous ones, due to the low selectivity of the process, which results in a low yield and a difficult identification of the enones **8a-d, 9a,b,** epoxides **3a,b**, diene **9c** and aromatic hydrocarbons **9d-f** [78-80].

The introduction of functional groups in the C4 position of caranes is required for the elaboration of approaches to obtain practically important *gem*-dimethylcyclopropanes, e.g to fragrant substances [81-84].

Overall yield of 4-formylcarane **10** at hydroformylation or carbonylation has not exceeded 40% (scheme 10) [85, 86].

***Scheme* 10**

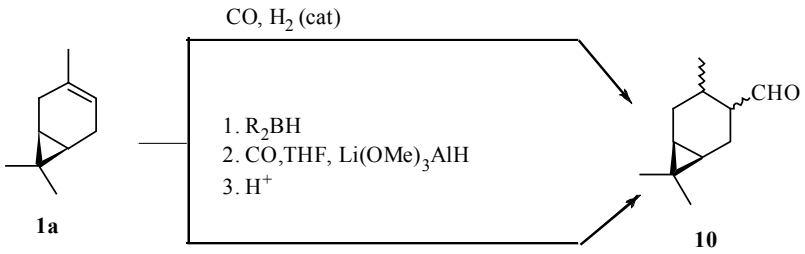

The approach to acetals and ketals **12** [87] has been performed on the basis of the well-known 3β,4β-carandiol **11** [76, 88, 89].

***Scheme* 11**

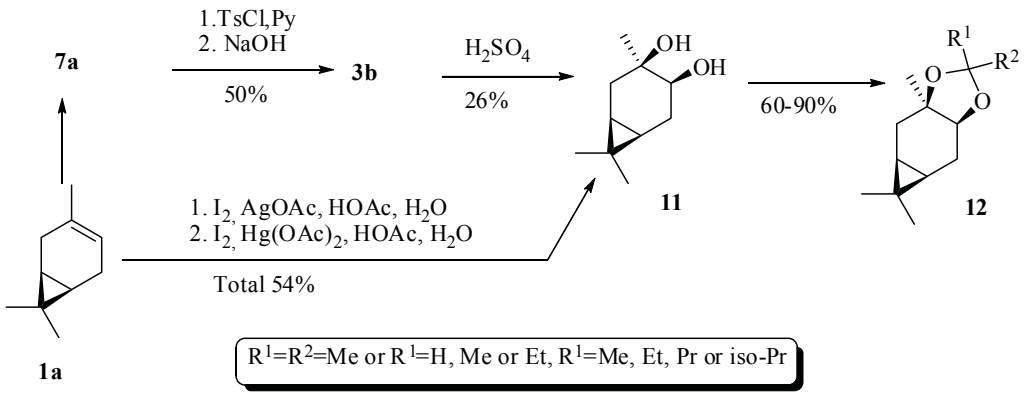

Target products have been obtained by the treatment of diol **11** and the corresponding aldehyde or ketone with catalytic amounts of sulfuric or *p*-toluenesulfonic acids. These acetals and ketals had odour characteristics and in these conditions the *gem*-dialkyl group created pleasant, floral-balsamic or floral-wood odours. Acetals had markedly less odour.

Odorants **14a-c** have been synthesized from 4-hydroxy-3(10)-carene **13** (scheme 12) [90, 91].

Another group [92] has described the stereoselective route from an alcohol **13** to functionalized ketone **15,** olefines **17, 20,** and aldehyde **19**.

3(10)-Caren-4-on **21** [67], 4α-acetyl-2-carene **23** [93], 3-caran-10-al **24** [94-96] and 4-acetyl-3-carene **26** [93] have been selected [97-99] for the construction of intermediates **22, 25, 27, 28** of the optically active tri- and tetracyclic analogues of sesquiterpenes from *Nardostachys jatamansi* and *Aristolochia debilis* [100], and the homologues of some crop protection agents (scheme 13) [5, 101- 103].

***Scheme* 12**

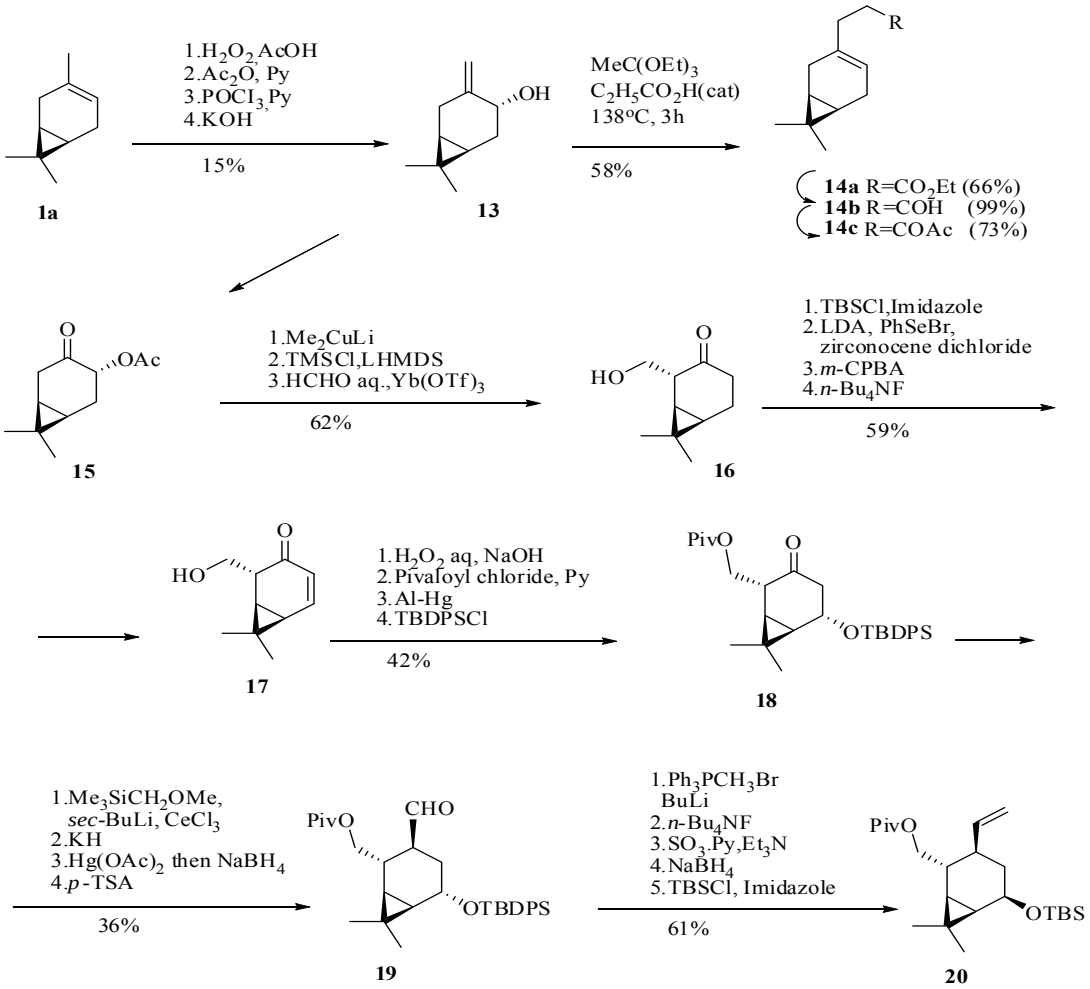

***Scheme* 13**

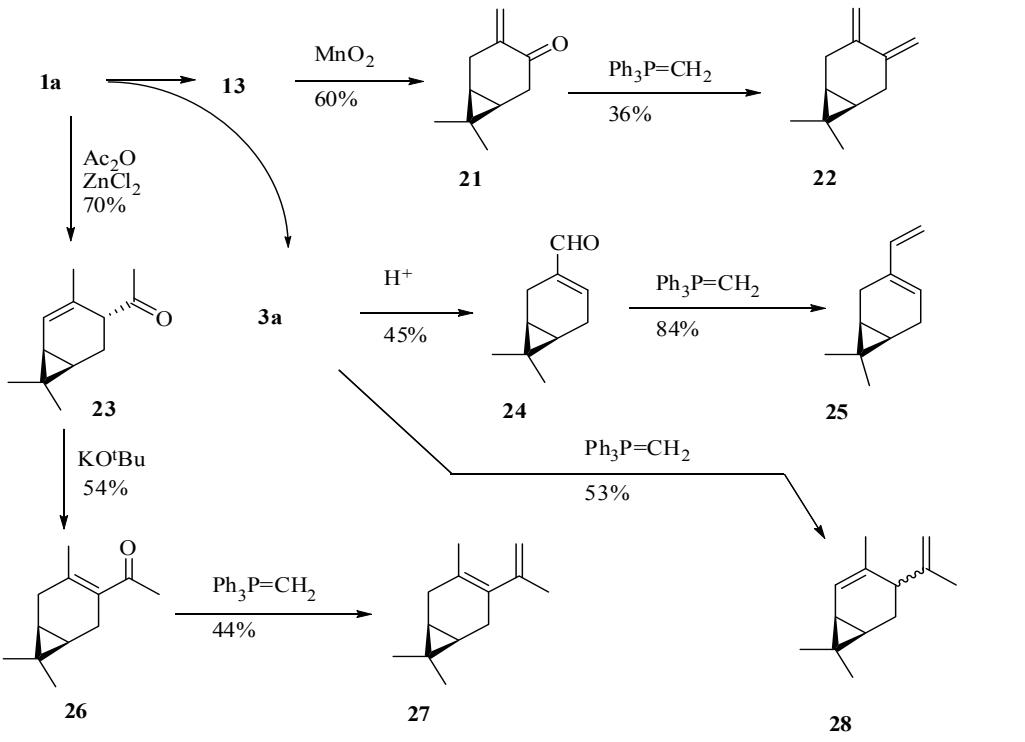

The synthesis of cyclic products on the basis of compounds **22, 25-28** has been discussed in the review [6], so it will not be considered hereafter.

The direct amidocyclopropanation of (+)-3-carene **1a** using organozinc carbenoids gives a single isomer **29** [104-106]

***Scheme* 14**

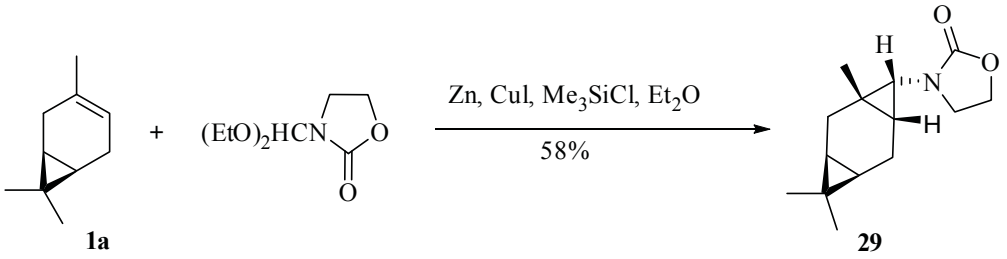

A pathway for preparing optically active lactam functionalized ionic liquid **31** was demonstrated by scheme 15 [107].

***Scheme* 15**

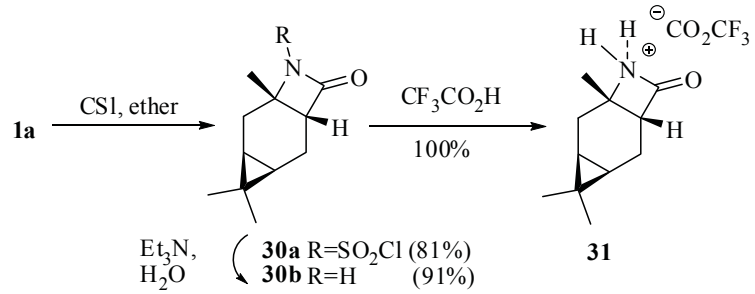

The reaction of chlorosulfonyl isocyanate addition to compound **1a** proceeds regio- and stereoselectively with the formation of β-lactam **30a.** The hydrolysis of compound **30a** has yielded the product **30b** [108].

The synthesis of lactams **34**, **35** included the preliminary constructing of the diol **32a** or the bromohydrine **32b** with following cycloaddition of anhydrides **33a,b** to imines (scheme 16) [109-111].

***Scheme* 16**

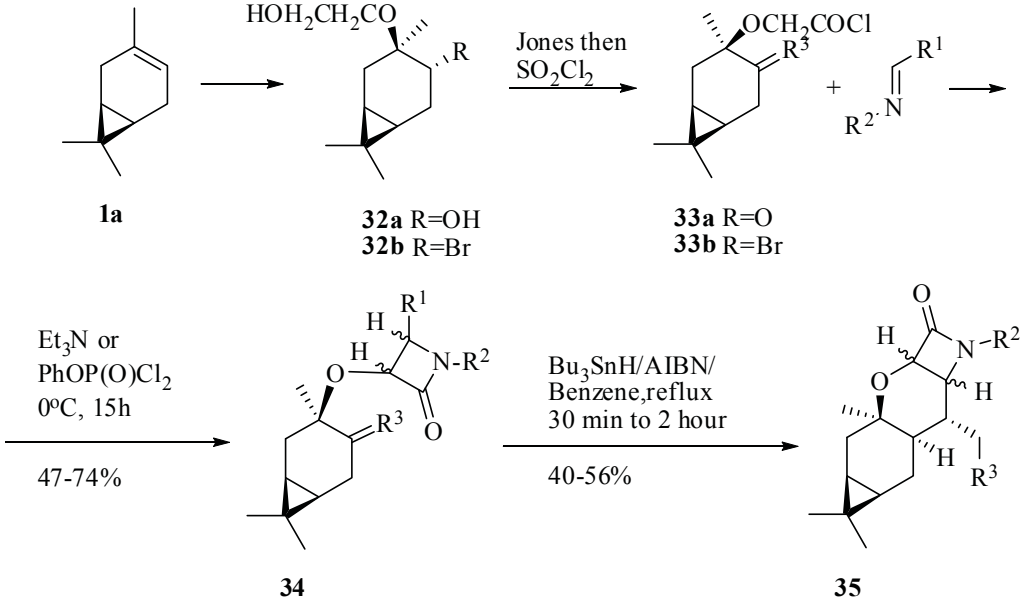

The ketoximes of the carane series should also be mentioned (scheme 17) [112, 115-120].

***Scheme* 17**

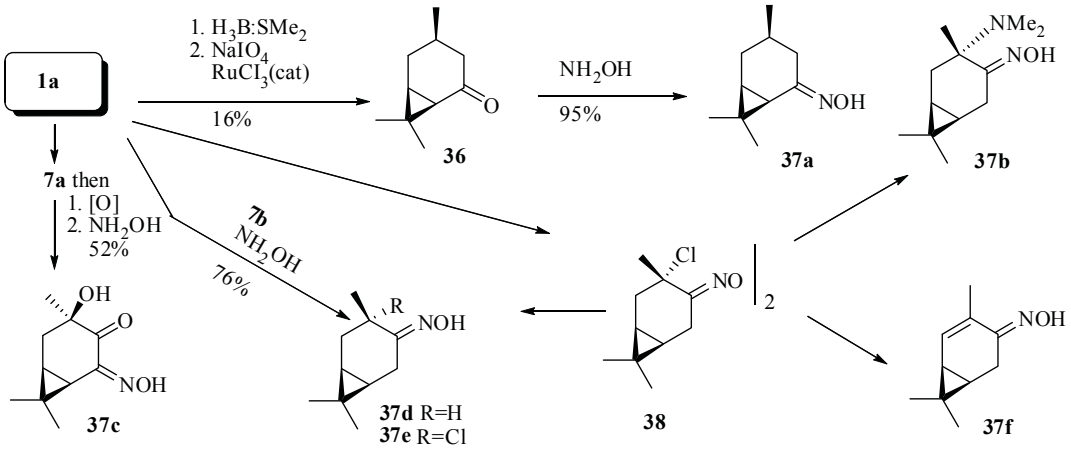

Substances **37a,c,d** have been classically synthesized from ketones **7b** and **36**, while the homologues **37b**,**f** have been obtained on the basis of the adduct **38**.

Asymmetric ring opening of *meso*-epoxide with *B*-halobis(2-isocaranyl)boranes affords chlorohydrine **39** with 19% ee enantioselectivity (scheme 18) [121].

***Scheme* 18**

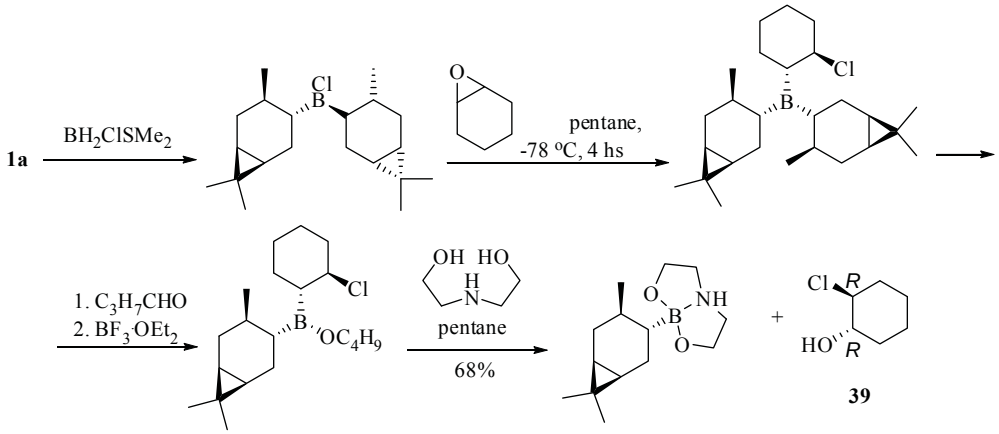

A convenient method for the syntesis of optically active trans-hydroxyselenodes **40a-c, 43** from oxide **3a** on the reactions of sodium selenide or sodium diselenide was described (scheme 19) [122].

***Scheme* 19**

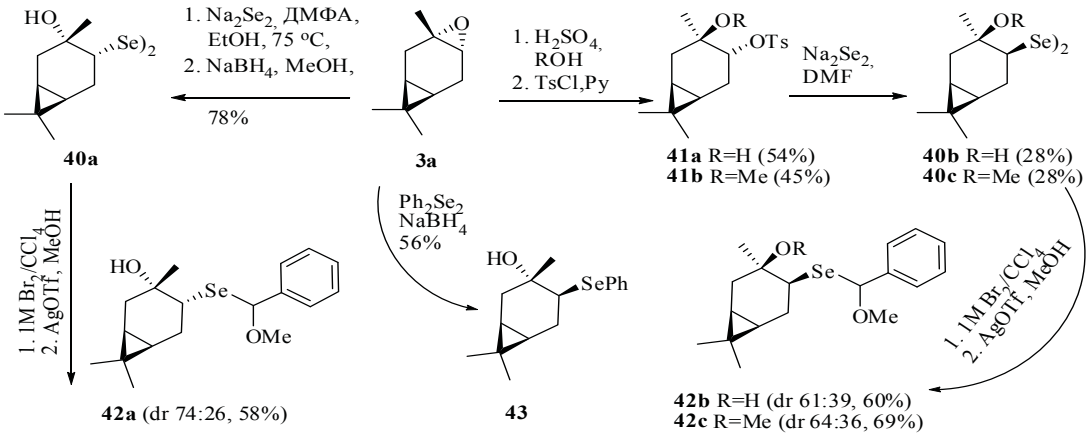

The cis-hydroxy and cis-methoxydiselenides **40b,c** were obtained in the reaction of sodium diselenide with the corresponding hydroxy- and methoxytosylates **41a,b**.

New chiral selenium-caranes **45a,b** as well as **46a,b** can be synthesized from hydroxyselenide **44** [123].

***Scheme* 20**

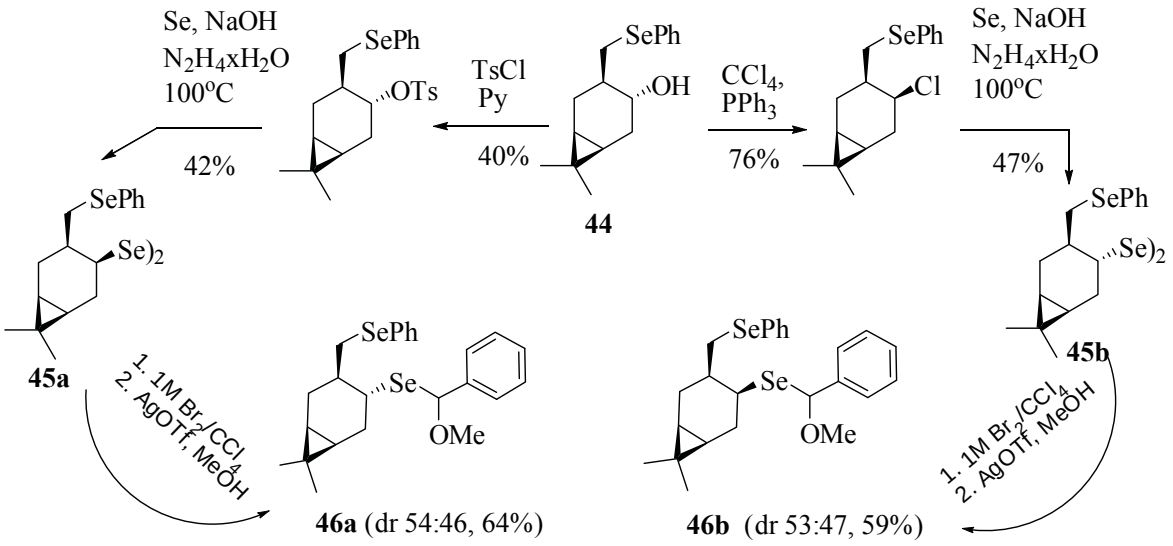

The diselenides were used for asymmetric selenenylation of sterene and selenocyclization with o-allylphenol with moderate yield but low diastereoselectivety.

(+)-3-Carene **1a** has been easily converted into β-azidoselenide **47** by addition of PhSeOTf in the presence of NaN_3 [123].

***Scheme* 21**

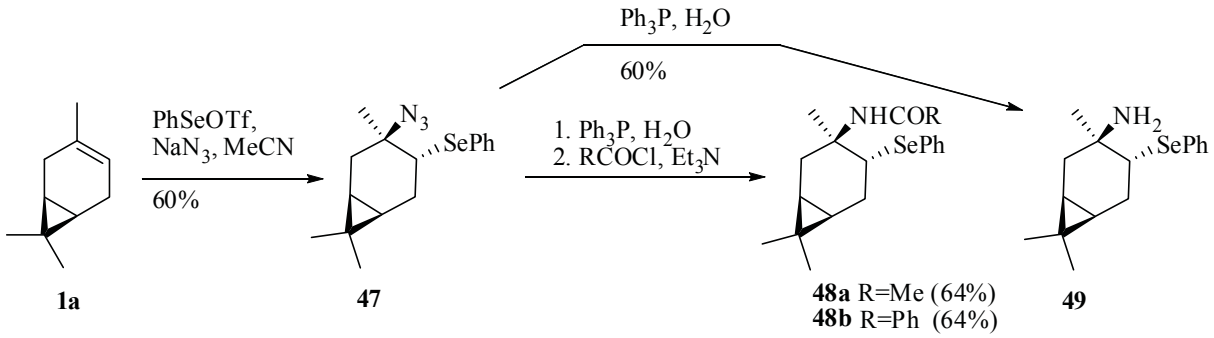

Using classical procedures, compound **47** was converted into amidoselenides **48a,b** and aminoselenide **49**.

The regio- and stereoselective aminohydroxylation of monoterpene **1a** into hydroxytoluenesulfonamide **47** was reported [124].

***Scheme* 22**

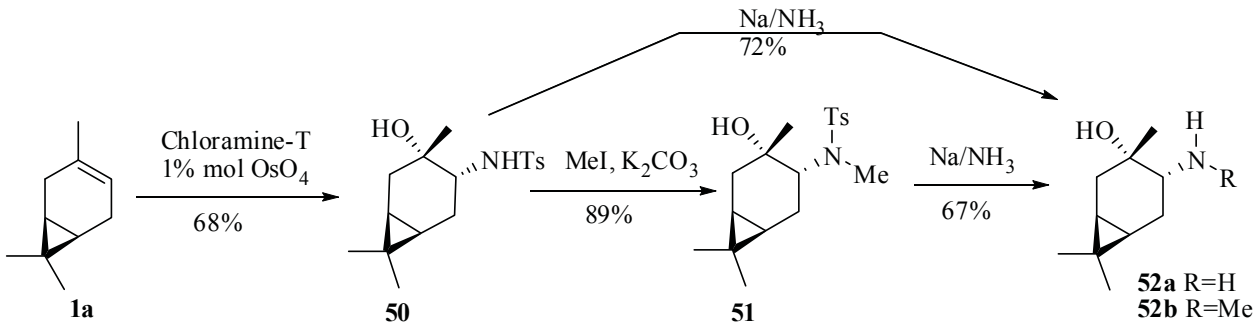

The methylation of compound **50** gives the corresponding product **51.** The sulfonamides **50, 51** were reduced with sodium in liquid ammonia to give the corresponding cis-amino alcohols **52a,b**.

The ionic-liquids **55a-c** [125-128] catalyzed Kondakov and Prince reactions of monoterpene **1a** were described [129].

***Scheme* 23**

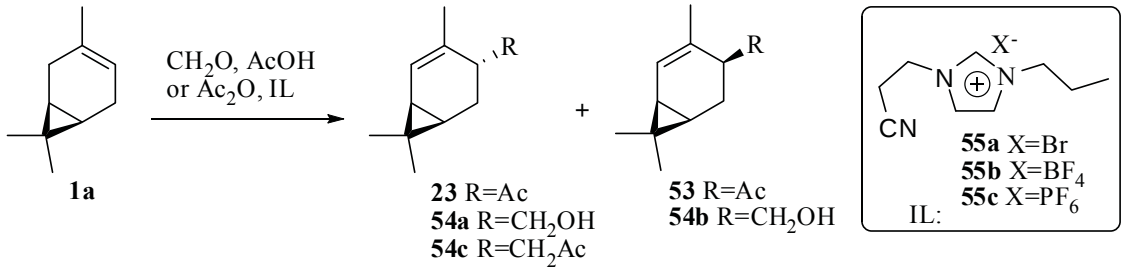

The reaction of carene **1a**, with Ac_2O in the presence of ionic liquid **55a** at 50°C gave the mixture of 4α- and 4β-acetyl-2-carenes **23,54** (ratio 95:5). All the attempts of hydroxymethylation of **1a** using paraformaldehyde in the presence or in the solution of ionic-liquids **55a-c** have failed. Only the addition of the AcOH to the indicated mixture has contributed to the proceeding of Prins's reaction with the formation of 4α-hydroxymethyl-2-carenes **53a,c** and 4α-acetoxymethyl-2-carenes **53b** as well.

The silylation of compound **23** was carried out in both conditions of kinetic and thermodynamic control of the reaction [130-132]. The reaction of compound **23** with chlorotrimethylsilane afforded silyl enol ether **56a** [133,134].

***Scheme* 24**

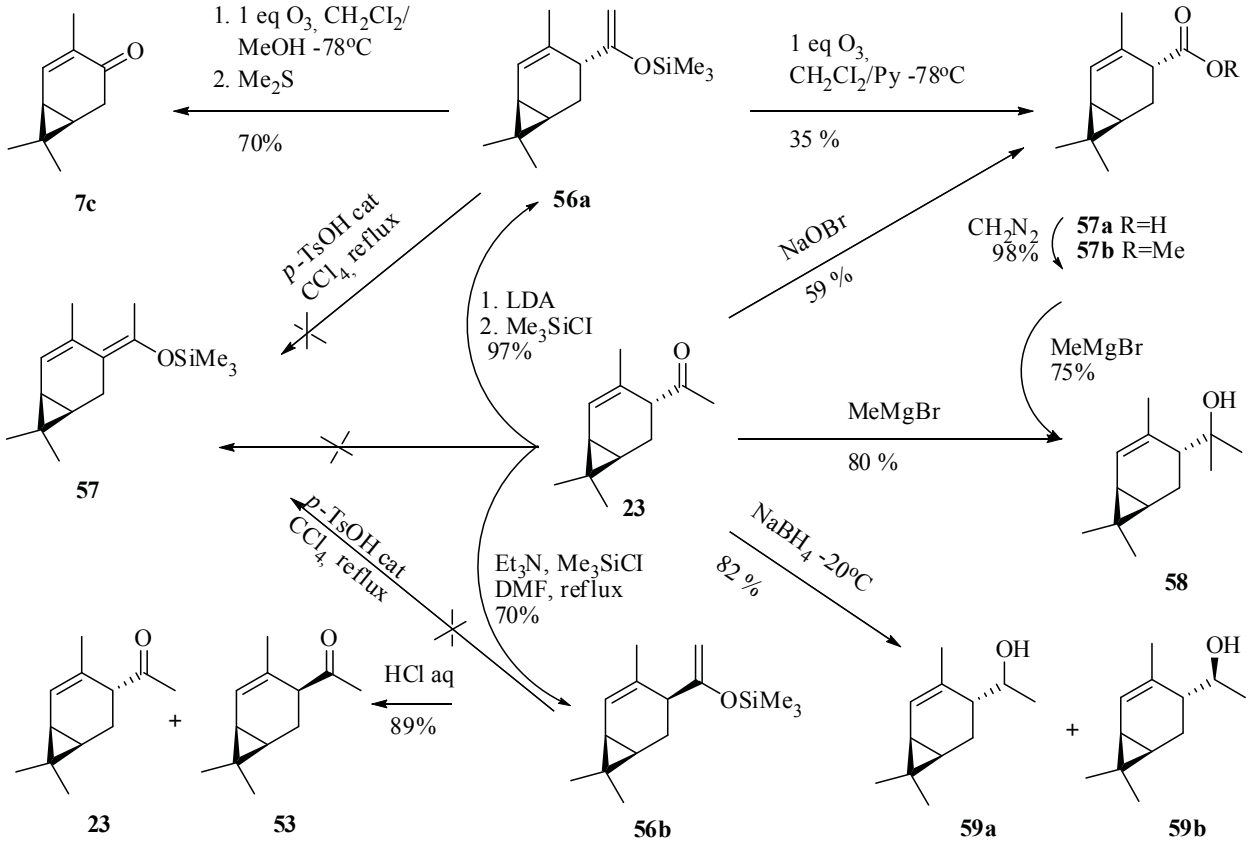

An interaction of ketone **23** with the mixture of Et_3N-chlorotrimethylsilane in DMF gave an epimer **56b**. The attempts to isomerize ethers **56a,b** into isomer **57** have failed. The product of hydrolysis has represented a

mixture of 4α- and 4β-acetyl-2-carenes **23, 53** (ratio 5:95). Ozonolysis of the ether **56a** in the mixture of CH_2Cl_2/MeOH followed by the decomposition of peroxides with Me_2S proceeds with the formation of well-known [135-138] car-2-en-4-one **7c**. As far as the stability of ethers **56a,b** towards isomerization is concerned, it is most probable that the rearrangement of intermediary products occurs during ozonization. The acid **57a** has been synthesized from the ketone **23** in the condition of hypobromide oxidation as well as by ozonolysis of the ether **56a** [139,140]. The ester **57b** or the ketone **23** could react with MeMgBr to give the alcohol **58**. Crystalline epimer **59a** is easily separated from the oil-like alcohol **59b** by the crystallization from hexane [141-143].

To develop new efficient routes to functionalized pyridines, amide **61** was tested as starting chirone [144].

***Scheme* 25**

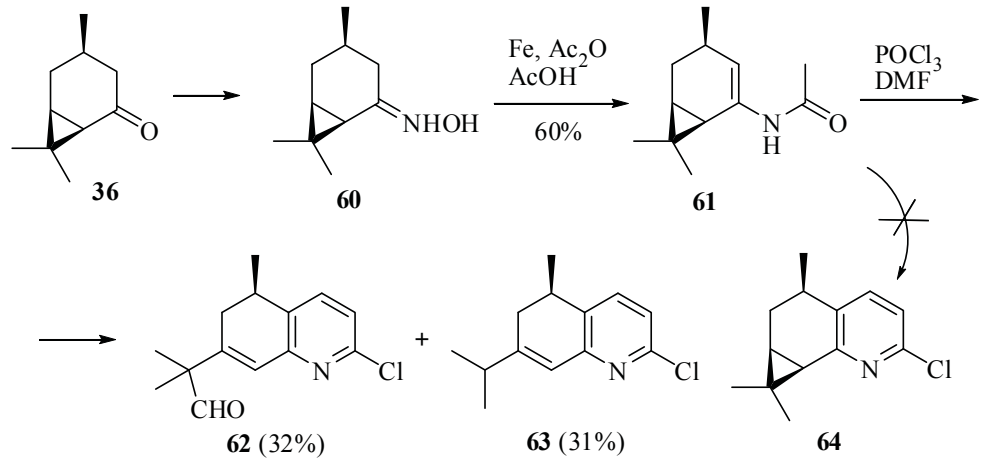

However, the heterocyclisation step leads to the cyclopropane ring opening reaction with the formation of two types of pyridines **62, 63** without target **64**. This problem was solved by replacing direct heterocyclisation step with a Krohnke annulation. The *exo*-methylene functionality was prepared via Claisen condensation followed by transaldolization. The reaction of enone **65** with Krohnke salt afforded pyridone **66**. The treatment of the latter derivative with $POCl_3$ produced the target chloride **67a** in a modest yield. By contrast, the conversion into the triflate **67b** occurred almost quantitatively. The triflate **67b** was then coupled using the Ni/Zn to afford the required bis-pyridine **68**.

***Scheme* 26**

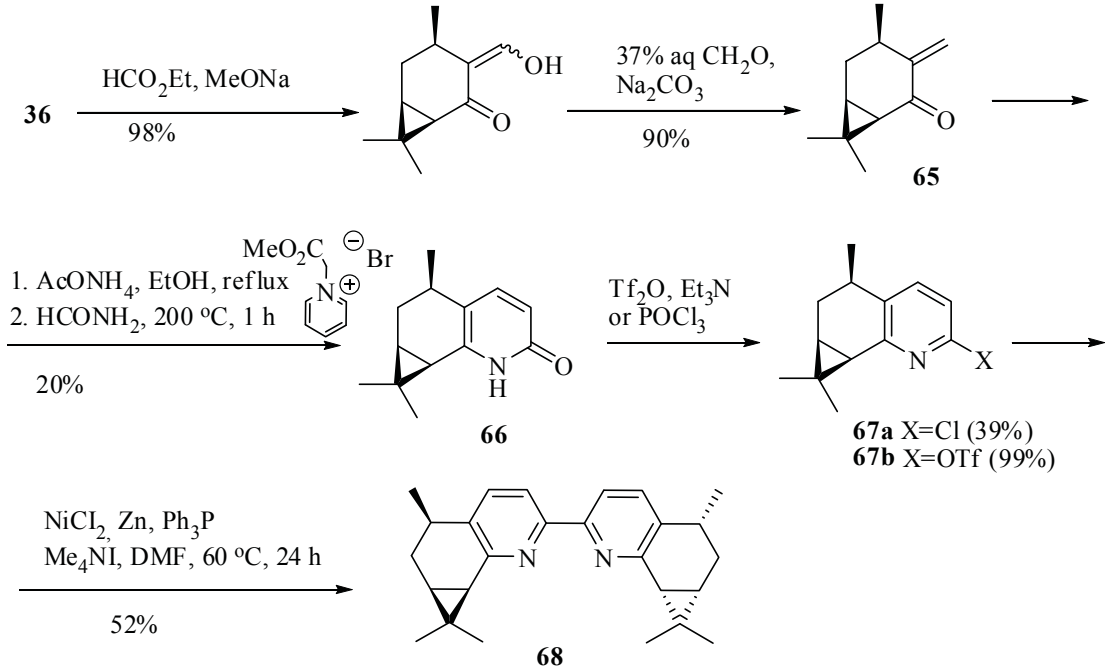

A moderate yield of asymmetric allylic oxidation of cycloalkenes catalyzed by Cu-complexes of chiral ligand **57** was observed.

The synthesis of more functionalized bis-pyridine **69, 70** was realized from the enone **65** [145,146]. The reactions carried out successfully are detailed in scheme 27.

***Scheme* 27**

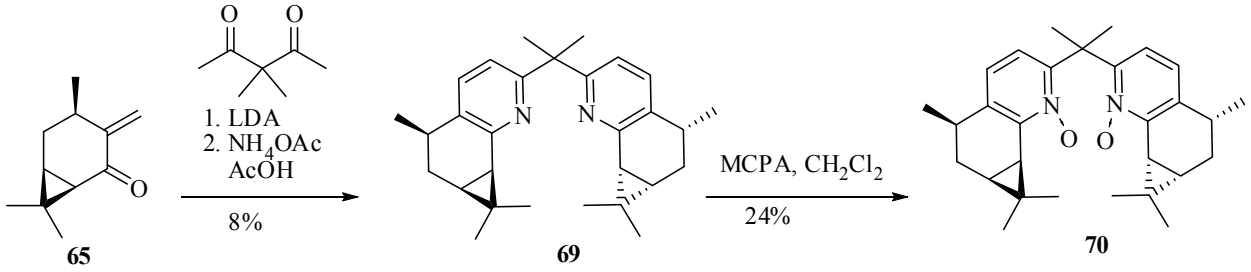

The allylation of aldehydes with allyltrichlorosilane promoted by new chiral dipyridylmethane N-oxides **70** was realized with moderate yield (58%) and good (83%) enantioselectivity.

Thus, it has been shown that the functionalization of carene's π-bond with subsequent conversions gives compounds with carane skeleton in the molecule.

3. Synthesis on the basis of 2-carenes with carane skeleton retention

As has been mentioned above, the 2-carene **1b** is a convenient initial compound for a purposeful synthesis. A heterogeneous catalyzed isomerization on inorganic materials (zeolites in the basic form, nickel catalysts on SiO_2) or via hydrogenation of (+)-3-carene **1a** was described [147-150]. In all cases the mixture of **1a,b** separated with a great difficulty was obtained.

The transformation of (+)-3-carene **1a** into mixture diethylboranes **72-74** and hydrolysis resulted in the mixture of carenes **1a** (yield 9%), **1b** (yield 9%) and **71** (yield 82%) (scheme 28) [151].

***Scheme* 28**

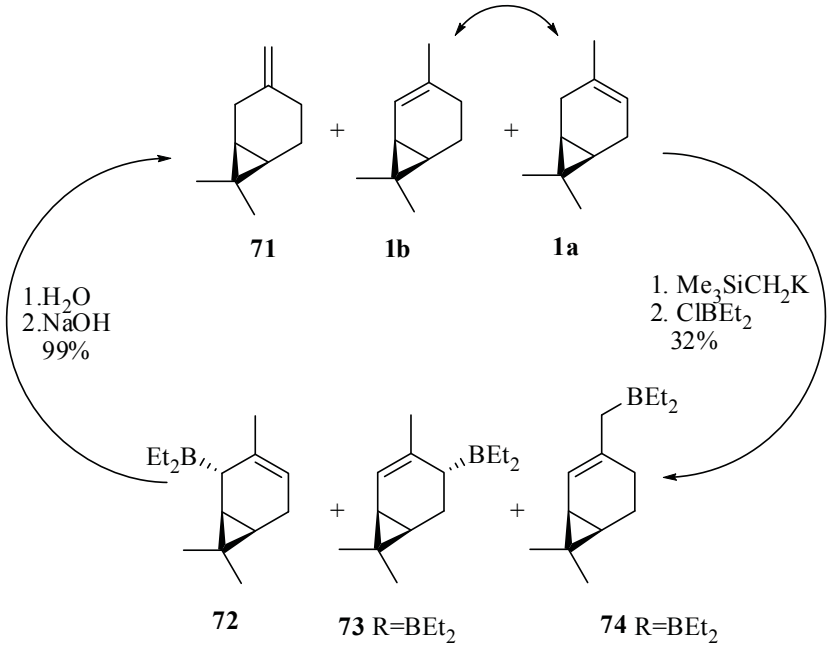

Amino homologues **75, 76** have been synthesized from 2-carene **1b** [152, 153].

The initially formed mixture of regioisomeric imides is subjected to [2,3]-sigmatropic rearrangement, and its subsequent hydrolysis leads to a pair of amines **75** (yield 11%), **76** (yield 5%).

***Scheme* 29**

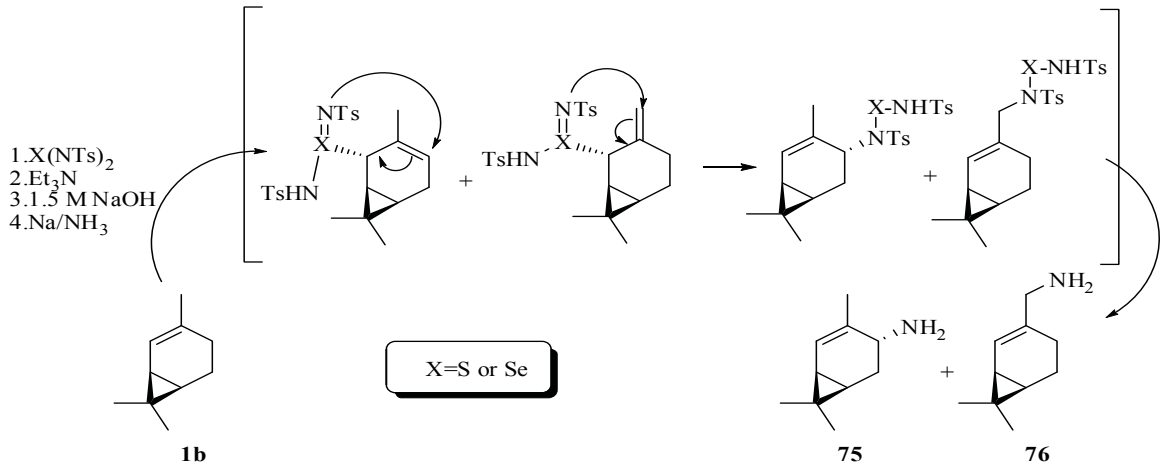

Brown and co-workers have proposed a stereocontrolled synthesis of caranol **77a** *via* hydroboration of (+)-2-carene **1b** [154].

***Scheme* 30**

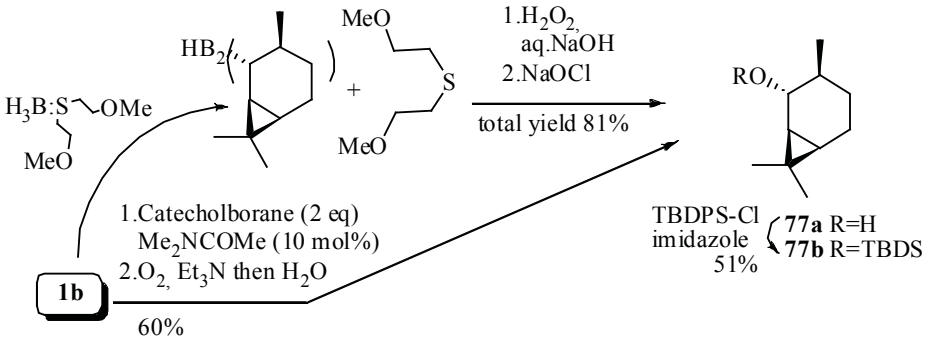

Another group has established that oxygen oxidizes the aryl(alkyl)boronates up to hydroxylated product **77a**, however this method is less selective [155]. The alcohol is characterized as ether **77b**.

A new and readily available modular phosphate ligand **79a** with P*-stereocentre has been prepared from caran-2,3-diols **78** [60]. The acetals **79b** were transformed into chiral intermediates **80a,b** and **81** (scheme 31) [156].

***Scheme* 31**

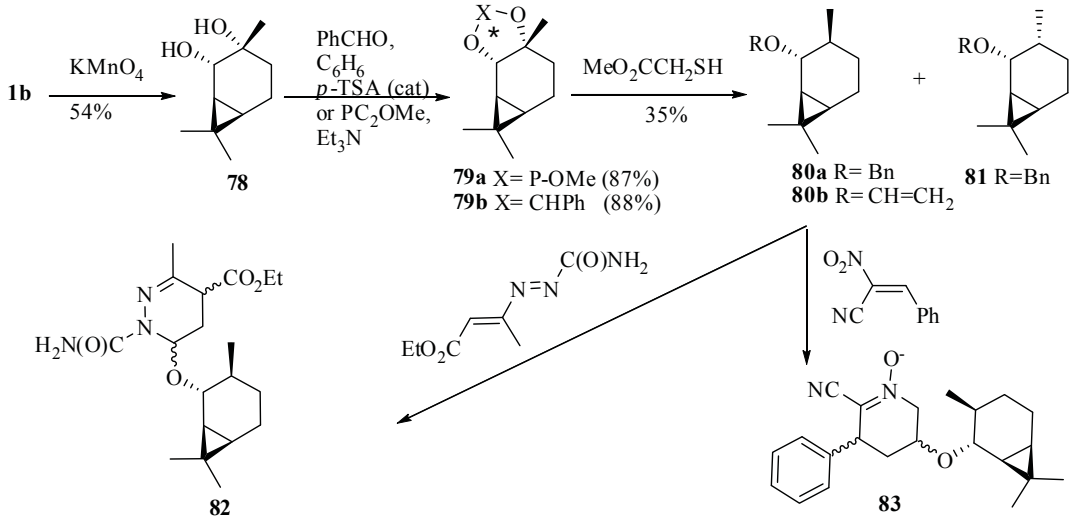

The synthesis of more functionalized ether **82, 83** via two different [4+2] cycloaddition reactions in aqueous medium is presented [157,158].

Bis-pyridine **85** was obtained *via* an initial transformation of (+)-2-carene **1b** into pyridone **84** [144]. The treatment of the latter compound with Tf_2O following the coupling affords the compound **85**. Asymmetric allylic oxidation of cyclic olefins with good conversion rates and acceptable enantioselectivity (67% ee) was registered by Cu-complexes of ligand **85.**

***Scheme* 32**

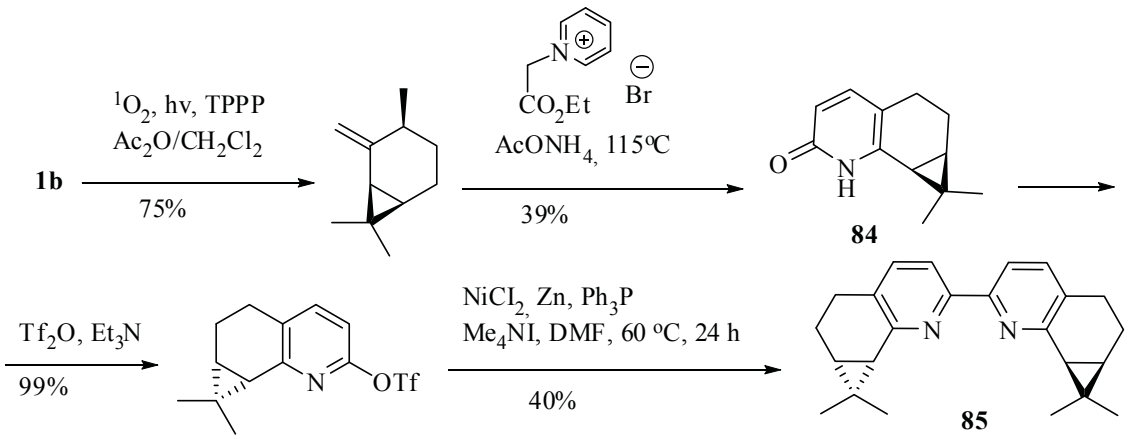

Mixtures of lactams **87**, **90** have been obtained by addition to monoterpene **1b** chlorosulfonyl isocyanate [159].

It was reported that isomers **87**, **90** could not be separated in a pure form and significant amounts. Analytically pure samples were isolated after fractional recrystallization from hexane.

In general, tricyclic compounds **87**, **90** gave a number of derivatives of β-amino acids **88**, **89**, **91a,b** and **92**. It is to be noted that, in contrast to amino ester **88** its region-isomer **91a** was readily hydrolyzed to the acid **91b** under the NaOMe catalyzed methanolysis as well as in the presence of even small amounts of water. The mixture of compounds **91a,b** can be reduced with a reasonable yield to amino alcohol **92** with $LiAlH_4$.

***Scheme* 33**

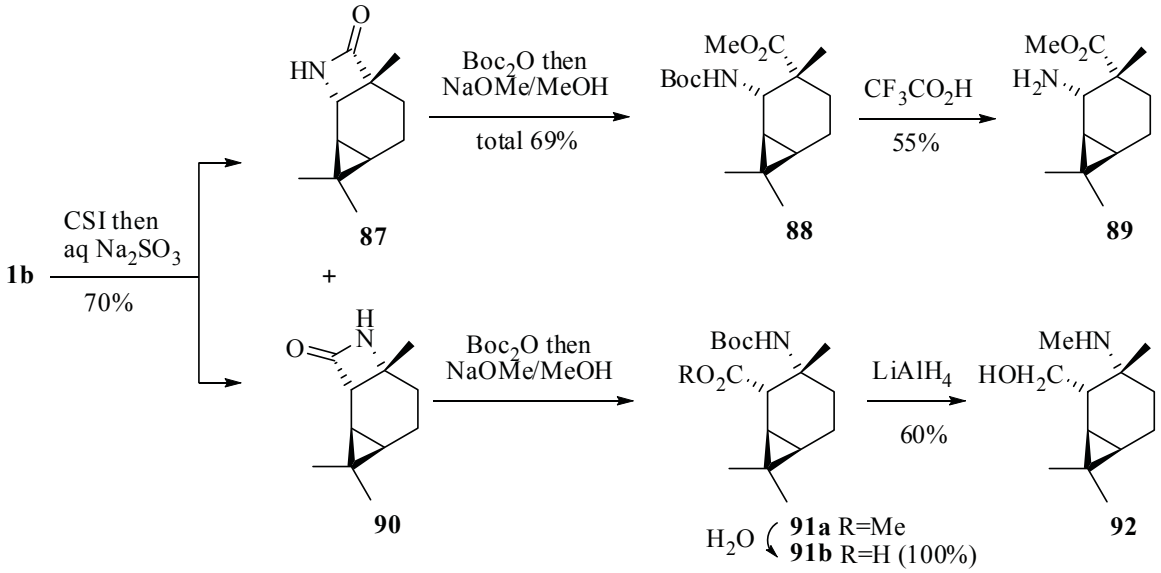

4. Conclusion

It is clear from the above relative reactivity data of monoterpenes (+)-2- and (+)-3-carenes that there are good posibilities of establishing objective or sets criteria which help decide whether electrophilic addition or dipolar cycloadditions to carbon-carbon double bonds involve the synthesis with the retention of the bicyclic framework. Although the coupling reactions should be optimised and the cyclisation of such compounds has not been attempted, one can rely on the results obtained with the polycyclic compounds. The synthesized compounds can be further converted

into the substances of known pharmaceutical interest and the obtained molecules can also display interesting biological properties.

In conclusion, it might be stated that the actual details of the transformation of bicyclic monoterpenes employing a stereoselective functionalized of the cyclohexene rings are yet to be clarified on the basis of more definitive studies.

5. Acknowledgements

The authors gratefully acknowledge generous financial support from the ASM-MESU bilateral project 01/UA.

6. References

[1]. Ho, T.L. Enantioselective Synthesis Natural Products from Chiral Terpenes. NY, Chichester, Brisbane, Toronto, Singapore. John Wiley&Sons, Inc. 1992, 324 p.
[2]. Ho, T.L. Carbocycle Construction in Terpene Synthesis. Weinheim, NY, Basel, VCH. 1988, 768 p.
[3]. Arlt, D.; Jautelat, M.; Lantzsch, R. Angew. Chem. 1981, 93, 719-840.
[4]. Хусид, А.Х.; Нефедов, О.М. Ж.В.Х.О. 1988, 33, 653-661.
[5]. Фокин, А.А.; Баула, О.П.; Красуцкий, П.А.; Юрченко, А.Г. Укр. Хим. журнал. 1992, 58, 1127-1133.
[6]. Macaev, F.Z.; Malkov, A.V. Tetrahedron. 2006, 62, 9-26.
[7]. Macaev, F. Cercetări în domeniul chimiei; Î.E.P. Ştiinţa: Chişinău, 1999, 66-92.
[8]. Chuiko V.A., Vyglazov O.G. Russ. Chem. Rev., 2003, 72, 49-67.
[9]. Salakhutdinov, N.F.; Barkhash, V.A. Russ. Chem. Rev., 1997, 66, 343-362.
[10]. Родионов, В.Н.; Козликовский, Я.Б.; Андрущенко, В.А. Ж. Орг. химии. 1991, 27, 2627.
[11]. Половинка, М.П.; Корчагина, Д.В.; Гатилов, Ю.В.; Выглазов, О.Г.; Зенкович, Г.А.; Бархаш, В.А. Ж. Орг. химии. 1998, 34, 342-1349.
[12]. Чуйко, В.А.; Выглазов, О.Г.; Тычинская, Л.Ю. Ж. Орг. химии. 1998, 34, 1357-1362.
[13]. Ильина, И.В.; Волчо, К.П.; Корчагина, Д.В.; Салахутдинов, Н.Ф.; Бархаш, В.А. Ж. Орг. химии. 1999, 35, 699-710.
[14]. Халиулин, Р.Р.; Племенков, В.В. Ж.Общ. химии. 1993, 63, с. 874-879.
[15]. Федюнина, И.В.; Никитина, Л.Е.; Племенков, В.В. Химия природ. соедин. 1993, 5, 677-684.
[16]. Федюнина, И.В.; Племенков, В.В., Никитина, Л.Е.; Литвинов, И.А.; Катаева, О.Н. Химия природ. соедин. 1995, 4, 576-580.
[17]. Kluge, R.; Schulz, M.; Liebsch, S. Tetrahedron. 1996, 52, 2957-2976.
[18]. Khanra, A.S.; Chakravarti, R.K.; Mitra, R.B. Indian J. Chem.1975, 13, 314-317.
[19]. Mane, B.M.; Gore, K.G.; Kulkarni, G.H. Indian J. Chem.1980, 19B, 605-607.
[20]. Bach, R.D.; Klin, M.W.; Ryntz, R.A.; Holbuka, J.W. J. Org. Chem. 1979, 44, 2569-2571.
[21]. Mitra, R.B.; Mulyiami, Z.; Deshmukh, A.R.A.S.; Joshi, V.S.; Garde, S.A. Synth. Commun. 1984, 14, 101-112.
[22]. Punniyamurthy, T.; Velusamy, S.; Iqbal, J. Chem. Rev., 2005, 105, 2329-2363.
[23]. Grigoropoulou, G.; Clark, J.H. Tetrahedron Letters, 2006, 47, 4461-4463.
[24]. Santos, I.C.M.S.; Rebelo, S.L.H.; Balula, M.S.S.; Martins, R.R.L.; Pereira, M.M.M.S.; Simoes, M.M.Q.; Neves, M.G.P.M.S.; Cavaliero, J.A.S,; Cavaliero, A.M.V. Journal of Molecular Catalysis A: Chemical, 2005, 231, 35-45.
[25]. Bordoloi, A.; Lefebvre, F.; Halligudi, S.B. Journal of Molecular Catalysis A: Chemical, 2007, 270, 177-184.
[26]. Saladino, R.; Andreoni, A.; Neri, V.; Crestini, C. Tetrahedron, 2005, 61, 1069-1075.
[27]. Nardello, V.; Aubry, J.M.; De Vos, D.E.; Neumann, R.; Adam, W.; Zhang, R.; Ten Elshof, J.E.; Witte, P.T.; Alsters, P.L. Journal of Molecular Catalysis A: Chemical, 2006, 251, 185-193.
[28]. Rebelo, S.L.H.; Goncalves, A.R.; Pereira, M.M.; Simoes, M.M.Q.; Neves, M.G.P.M.S.; Cavaliero, J.A.S. Journal of Molecular Catalysis A: Chemical, 2006, 256, 321-323.
[29]. Santos I.C.M.S.; Simões, M.M.Q.; Pereira, M.M.M.S.; Martins, R.R.L.; Neves, M.G.P.M.S.; Cavaleiro, J.A.S., Cavaleiro, A.M. V. Journal of Molecular Catalysis A: Chemical, 2003, 195, 253-262.
[30]. Martins, R.R.L.; Neves, M.G.P.M.S.; Silvestre, A.J.D.; Simões, M.M.Q.; Silva, A.M.S.; Tomé, A.C.; Cavaleiro, J.A.S.; Tagliatesta, P.; Crestini, C. Journal of Molecular Catalysis A: Chemical. 2001, 172, 33-42.
[31]. Krishnaswamy, D.; Bhawal, B.M.; Deshmukh, A.R.A.S. Tetrahedron Lett., 2000, 41, 417-420.
[32]. Krishnaswamy, D.; Govande, V.V.; Gumaste, V.K.; Bhawal, B.M.; Deshmukh, A.R.A.S. Tetrahedron, 2002, 58, 2215-2225.
[33]. Asouti, A.; Hadjiarapoglou, L. Synlett, 2001, 12, 1847-1850.
[34]. Van Vliet, M.C.A.; Arends, I.W.C.E.; Sheldon, R.A. Synlett, 2001, 1305-1307.
[35]. Saladino, R.; Neri, V.; Pelliccia, A.R.; Mincione, E. Tetrahedron, 2003, 59, 2403-2407.
[36]. Shaha, S.C.; Joshi, G.D.; Pai, P.P.; Deshmukh, A.R.A.S.; Kulkarni, G.H. Chem. Ind. 1989, 17, 568.

[37]. Kauffman, G.S.; Harris, G.D.; Dorow, R.L.; Stone, B.R.P.; Parsons, R.L.; Pesti, J.A.; Magnus, N.A.; Fortunak, J.M.; Confalone, P.N.; Nugent, W.A. Org. Lett. 2000, 2, 3119-3122.
[38]. Santos, I.C.M.S.; Simoes, M.M.Q.; Pereira, M.M.M.S.; Martins, R.R.L.; Neves, M.G.P.M.S.; Cavaleiro, J.A.S.; Cavaliero, A.M.V. Journal of Molecular Catalysis A: Chemical. 2003, 195, 253-262.
[39]. Martins, R.R.L.; Neves, M.G.P.M.S.; Silvestre, A.J.D.; Simoes, M.M.Q.; Silvia, A.M.S.; Tome, A.C.; Cavaleiro, J.A.S.; Tagliatesta, P.; Crestini, C. Journal of Molecular Catalysis A: Chemical. 2001, 172, 33-42.
[40]. Mitra, R.B.; Muljiani, Z.; Deshmukh, V.S.; Joshi, V.S.; Gadre, S.R. Synth. Commun. 1984, 14, 101-112.
[41]. Krishnaswamy, D.; Bhawal, B.M.; Deshmukh, A.R.A.S. Tetrahedron Lett. 2000, 41, 417-420.
[42]. Krishnaswamy, D.; Govande, V.V.; Gumaste, V.K.; Bhawal, B.M.; Deshmukh, A.R.A.S. Tetrahedron. 2002, 58, 2215-2225.
[43]. Asouti, A.; Hadjiarapoglou, L. Synlett. 2001, 12, 1847-1850.
[44]. Kluge, R.; Schulz, M.; Liebsch, S. Tetrahedron. 1996, 52, 2957-2976.
[45]. Reddy, M.M.; Punniyamurhty, T.; Iqbal, J. Tetrahedron Lett. 1995, 36, 159-162.
[46]. Kende, A.S.; Delair, P.; Blass, B.E. Tetrahedron Lett. 1994, 35, 8123-8126.
[47]. Kolehmainen, E.; Laihia, K.; Heinänen, M.; Rissanen, K.; Frönlich, R.; Korvola, J.; Mänttäri, P.; Kauppinen, R. J. Chem. Soc., Perkin Trans. 2. 1993, 641-648.
[48]. Van Vliet, M.C.A.; Arends, I.W.C.E.; Sheldon, R.A. Synlett. 2001, 1305-1307.
[49]. Saladino, R.; Neri, V.; Pelliccia, A.R.; Mincione, E. Tetrahedron. 2003, V. 59, № 14, p. 2403-2407.
[50]. Nardello, V.; Aubry, J.M.; De Vos, D.E.; Neumann, R.; Adam, W.; Zhang, R.; Ten Elshof, J.E.; Witte, P.T.; Alsters, P.L. Journal of Molecular Catalysis A: Chemical. 2006, 251, 185-193.
[51]. Rajan, V.P.; Bannore, S.V.; Subbarao, H.N.; Dev, S. Tetrahedron. 1984, 40, 983-990.
[52]. Cocker, W.; Grayson, D.H. Tetrahedron Lett. 1969, 10, 4451-4452.
[53]. Никитина, Л.Е.; Старцева, В.А.; Дорофеева, Л.Ю.; Артемова, Н.П.; Кузнецов, И.В.; Лисовская, С.А.; Глушко, Н.П. Химия природ. соедин., 2010, 1, 17-30.
[54]. Артемова, Н.П.; Бикбулатова, Г.Ш.; Племенков, В.В.; Ефремов, Ю.Я. Ж. Общ. химии.1991, 61, 1484-1485.
[55]. Артемова, Н.П.; Бикбулатова, Г.Ш.; Племенков, В.В.; Наумов, В.А.; Катаева, О.Н. Химия природ. соед. 1991, 2, 193-198.
[56]. Hendrich, A.; Piatkowski, K. Polish Journal of Chemistry. 1984, 58, 73-84.
[57]. Gomes, M.; Antunes, O.A.C. Catalysis Commun. 2001, 2, 225-227.
[58]. Волчо, К.П.; Татарова, Л.Е.; Корчагина, Д.В.; Салахутдинов, Н.Ф.; Бархаш, В.А. Ж. Орг. химии. 2000, 36, 41-48.
[59]. Gavrilov, K.N.; Benetsky, E.B.; Grishina, T.B.; Zheglov, S.V.; Rastorguev, E.A.; Petrovskii, P.V.; Macaev, F.Z.; Davankov, V.A. Tetrahedron: Asymmetry. 2007, 18, 2557-2564.
[60]. Benetsky, E.B.; Zheglov, S.V.; Grishina, T.B.; Macaev, F.Z.; Bet, L.P.; Davankov, V.A.; Gavrilov, K.N. Tetrahedron Lett. 2007, 48, 8326-8330.
[61]. Joshi, S.N.; Malhotra, S.V. Tetrahedron: Asymmetry, 2003, 14, 1763-1766.
[62]. Kauffman, G.S.; Harris, G.D.; Dorow, R.L.; Stone, B.R.P.; Parsons, R.L.; Pesti, J.A.; Magnus, N.A.; Fortunak, J.M.; Confalone, P.N.; Nugent, W.A. Organic Lett., 2000, 2, 3119-3121.
[63]. Parsons, R.L.; Fortunak, J.M.; Dorow, R.L.; Harris, G.D.; Kauffman, G.S.; Nugent, W.A. J. Am. Chem. Soc., 2001, 123, 9135-9143.
[64]. Fedunina, I.V.; Plemenkov, V.V.; Bikbulatova, G.Sh.; Nikitina, L. E.; Litvinov, I. A.; Kataeva, O.N. Chem. Natur. Compds. 1992, 2, 203-208.
[65]. Isaeva, Z.G.; Bakaleinik, G.A. Izvestia Akademii Nauk SSSR. Seriya Khimicheskaya. 1985, 3, 648-653.
[66]. Kazakova, E.Kh.; Davletshina, G.R.; Bakaleinik, G.A.; Vereshagin, A.N. Izvestia Akademii Nauk SSSR. Seriya Khim. 1986, 4, 842-846.
[67]. Исаева, З.Г.; Андреева, И.С. Докл. АН СССР. 1963, 152, 106-109.
[68]. Satoh Tsuyoshi; Okuda Teruyoshi; Kaneko Youhei. Chem. Pharm. Bull. 1984, 32, 1401-1410.
[69]. Shagidullin, R.R.; Isaeva, Z.G.; Povodyreva, I.P.; D'yakonova, R.R. Doklady Akademii Nauk. 1972, 202, 1349-1351.
[70]. Krasutskii, P.A.; Fokin, A.A.; Gulevich, A.V.; Yurchenko, A.G.; Promonenkov, V.K. Russ. J. Org. Chem. 1992, 28, 1098-1099.
[71]. Kazakova, E.Kh.; Davletshina. G.R.; Vereshagin, A.N. Izvestia Akademii Nauk SSSR. Seriya Khim. 1986, V. 4, p. 842-846.
[72]. Arbuzov, B.A.; Ibragimova, N.D.; Povodyreva, I.P. Izvestia Akademii Nauk SSSR. Seriya Khim. 1980, 1052-1054.
[73]. Isaeva, Z.G.; Bikbulatova, G.Sh.; Podvodyreva, I.P. Izvestia Akademii Nauk SSSR. Seriya Khimicheskaya. 1979, 5, 1107-1110.

[74]. Sonawane, H.R.; Nanjundiah, B.S.; Purohit, P.C. Tetrahedron Lett., 1983, 24, 3917-3918.
[75]. Carson, M.S.; Cocker, W.; Grayson, D.H.; Shannon, P.V.R. J. Chem. Soc. C. 1969, 2220-2228.
[76]. Kropp, P.J. J. Am. Chem. Soc. 1966, 88, 4926-4934.
[77]. Chabudzinski, Z.; Kuczynski, H. Roczniki chimii. Ann.Soc.Chim. Polonorum. 1962, 36, 1173-1181.
[78]. Толстиков, Г.А.; Галин, Ф.З.; Игнатюк, В.К.; Кашина, Ю.А.; Галкин, Е.Г. Журн. орг. химии. 1995, 31, 1149-1151.
[79]. Tolstikov, G.A.; Galin, F.Z.; Ignatyuk, V.K.; Kashina, Yu.A.; Zelenova, L.M. Chemistry of Natural Compounds. 1992, 22, 295-297.
[80]. Reddy, M.M.; Punniyamurthy, T.; Iqbal, J. Tetrahedron Lett., 1995, 36, 159-162.
[81]. Ohloff, G. Scent and fragrances. The fascination of odors and their chemical perspectivies. Berlin, Heidelberg, NY, London, Paris, Tokyo, Hong Kong, Barselona, Budapest. Springer-Verlag. 1994, 240 p.
[82]. Muller, P.M.; Lamparsky, D. Perfumes. Art, Science and Technology. London, Glasgow, NY, Tokyo, Melbourne, Madras. Blackie Academic&Professional. 1991, 661 p.
[83]. Шулов Л.М., Хейфиц Л.А. Душистые вещества и полупродукты парфюмерно-косметического производства. Москва, Агропромиздат. 1990, 208 с.
[84]. Хейфиц Л.А., Дашунин В.М. Душистые вещества и другие продукты парфюмерии. Москва, Химия. 1994, 256 с.
[85]. Silva, J.G.; Barros, H.J.V.; Balanta, A.; Bolaños, A.; Novoa, M.L.; Reyes, M.; Contreras, R.; Bayón, J.C.; Gusevskaya, E.V.; Santos, E.N. Applied Catalysis A: General. 2007, 326, 219-226.
[86]. Narasimhan, S.; Ramesha, A.R. Indian Journal of Chemistry, 1992, 31B, 645-647.
[87]. Hendrich, A.; Piatkowski, K.; Gora, J. Perfumer&Flavorist. 1986, 11, 85-88.
[88]. Арбузов, Б.А.; Исаева, З.Г.; Поводырева, И.П.; Ратнер, В.В. Изв. АН СССР. Сер. Хим. 1979, 10, 2231-2234.
[89]. Арбузов, Б.А.; Ратнер, В.В.; Исаева, З.Г.; Гудова, В.Н., Рубинова, Н.Р.; Беляева, М.Г. Изв. АН СССР. Сер. Хим. 1979, 6, 1294-1298.
[90]. Lochynski, S.; Kowalska, K.; Wawrzenczyk, C. Flavour and Fragrance Journal. 2002, 17, 181-190.
[91]. Lochynski, S.; Frackowiak, B.; Olejniczak, T.; Ciunik, Z.; Wawrzenczyk, C. Tetrahedron: Asymmetry. 2002, 13, 1761-1767.
[92]. Sekine, A.; Kumagai, N.; Uotsu, K.; Ohshima, T.; Shibasaki, M. Tetrahedron Lett. 2000, 41, 509-513.
[93]. Mühlstädt, M.; Richter, P. Chem. Ber. 1967, Bd 100, 1892-1897.
[94]. Gollnick, K.; Schade, G.Tetrahedron. 1966, 22, 133-137.
[95]. Borowiecki, L.; Zacharewicz. Rocziki Chem. 1963, 37, 1143-1149.
[96]. Brown, H.C.; Garg, C.P. J.Am.Chem.Soc. 1961, 83, 2952-2953.
[97]. Lajuenen, M. Tetrahedron. 1994, 50, 13181-13198.
[98]. Фокин, А.А.; Бутова, Е.Д.; Коломицин, И.В.; Гагаева, Е.А.; Гогоман, И.В.; Корнилов, А.М.; Сорочинский, А.Е.; Юрченко, А.Г.; Красуцкий, П.А. Орг. химии. 1994, 30, 669-679.
[99]. Fletcher, R.J.; Motherwell, W.B.; Popkin, M.E. Chem. Commun. 1998, 20, 2191-2192.
[100]. Krepinsky, J.; Jommi, G.; Samek, Z.; Sorm, F. Coll. Čzech. Chem. Commun. 1970, 35, 745-748.
[101]. Barlow, F. Pest. Sci. 1971, 2, 115-118.
[102]. Мельников, Н.Н. Пестициды. 1987, Москва, Химия, 712 с.
[103]. Elliot, M. Nature. 1973, 244, 546-547.
[104]. Motherwell, W.B.; Bégis, G.; Cladingboel, D.E.; Jerome, L.; Sheppard, T.D. Tetrahedron, 2007, 63, 6462-6476.
[105]. Fletcher, R.J.; Motherwell, W.B.; Popkin, M.E. Chem. Commun., 1998, 20, 2191-2192.
[106]. Motherwell, W.B.; Roberts, L.R. Tetrahedron Lett., 1995, 36, 1121-1124.
[107]. Makaev, F. Z.; Vlad, L. A.; Bets, L. P.; Malinovskii, S. T.; Gavrilov, K. N.; Gdanets, M. Chemistry of Natural Compounds, 2010, 46, 528-533.
[108]. Gyonfalvi, S.; Szakonyi, Z.; Fulop, F..Tetrahedron: Asymmetry. 2003, 14, 3965-3972.
[109]. Srirajan, V.; Deshmukh, A.R.A.S.; Bhawal, B.M. Tetrahedron. 1996, 52, 5585-5590.
[110]. Joshi, S.N.; Deshmukh, A.R.A.S.; Bhawal, M.B. Tetrahedron: Asymmetry. 2000, 11, 1477-1485.
[111]. Joshi, S.N.; Puranik, V.G.; Deshmukh, A.R.A.S.; Bhawal, B.M.. Tetrahedron: Asymmetry. 2001, 12, 3073-3076.
[112]. Irako, N.; Hamada, Y.; Shioiri, T. Tetrahedron. 1995, 51, 12731-12744.
[113]. Malkov, A.V.; Bella, M.; Stara, I.G.; Kocovsky, P. Tetrahedron Lett. 2001, 42, 3045-3048.
[114]. Kawai, T.; Ooi, T.; Kusumi, T. Chem. Pharm. Bull. 2003, 51, 291-294.
[115]. Malkov, A.V.; Pernazza, D.; Bell, M.; Bella, M.; Massa, A.; Teply, F.; Meghani, P.; Kocovsky, P. J. Org. Chem. 2003, 68, 4727-4742.
[116]. Petukhov, P.; Tkachev, A. Tetrahedron. 1997, 53, 9761-9768.

[117]. Tkachev, A.V.; Petukhov, P.A.; Konchenko, S.N.; Korenev, S.V.; Fedotov, M.A.; Gatilov, Y.V.; Rybalova, T.V.; Kholdeeva, O.A. Tetrahedron: Asymmetry. 1995, 6, 115-122.
[118]. Lochynski, S.; Kuldo, J.; Frackowiak, B.; Holband, J.; Wojcik, G. Tetrahedron: Asymmetry. 2000, 11, 1295-1302.
[119]. Muljiani, Z.; Deshmukh, A.R.A.S.; Garde, S.R.; Joshi, V. Synth. Commun. 1987, 17, 25-32.
[120]. Petukhov, P.A.; Tkachev, A.V. Mendeleev Commun. 1996, 2, 64-66.
[121]. Roy, C. D.; Brown, H.C. Tetrahedron: Asymmetry, 2006, 17, 1931-1936.
[122]. Scianowski, J.; Rafinski, Z.; Wojtczak, A.; Burczynski, K. Tetrahedron: Asymmetry, 2009, 20, 2871-2879.
[123]. Tiecco, M.; Testaferri, L.; Santi, C.; Tomassini, C.; Santoro, S.; Marini, F.; Bagnoli, L.; Temperini, A. Tetrahedron, 2007, 63, 12374-12378.
[124]. Laczkowski, K.Z.; Kmieciak, A.; Kozakiewicz, A. Tetrahedron: Asymmetry, 2009, 20, 1487-1492.
[125]. Macaev, F.; Munteanu, V.; Styngach, E.; Barba, A.; Pogrebnoi, S. Chem. J. Mold., 2007, 2, 119-122.
[126]. Şargorovschi, V.; Styngach, E.; Chem. J. Mold., 2008, 3, 95-97.
[127]. Sargorovschi V., Sucman N., Iudin T., Duca D., Stingaci E., Prodius D., Pogrebnoi S., Macaev F.. Chem. J. Mold., 2010, 5, 36-56.
[128]. Sargorovschi, V.; Sucman, N.; Iudin, T.; Stingaci, E.; Macaev, F. Chem. J. Mold., 2010, 5, 109-117.
[129]. Macaev, F.; Gavrilov, K.; Munteanu, V.; Stingaci, E.; Vlad, L.; Bet, L.; Pogrebnoi, S.; Barba, A. Chem. Nat. Comp. 2007, 43, 136-139.
[130]. Brownbridge, P. Synthesis. 1983, № 1, p. 1-28.
[131]. Brownbridge, P. Synthesis. 1983, № 2, p. 85-104.
[132]. House, H.O.; Czuba, L.G.; Call, M.; Olmstead, H.D. J.Org.Chem. 1969, 34, 2324-2336.
[133]. Макаев, Ф.З.; Галин, Ф.З.; Толстиков, Г.А. Известия РАН, Сер. хим., 1995, 2, 305-309.
[134]. Макаев, Ф.З. Известия РАН, Сер. хим. 2000, 8, 1480-1481.
[135]. Newman, A.A. Chemistry of Terpenes and Terpenoids. London, NY, Academic Press, **1972**, 450 p.
[136]. Shastri, M.H.; Patil, D.G.; Patil, V.D.; Dev, S. Tetrahedron. 1985, 41, 3083-3090.
[137]. Jochynski, S.; Jarosz, P.; Wolkowiez, M.; Piatkovski, K. J. Pract. Chimie. 1988, 330, 284-288.
[138]. Khaura, A.S.; Mitra, R.B. Indian J.Chem. 1976, 14B, 716-718.
[139]. Галин, Ф.З.; Макаев, Ф.З.; Толстиков, Г.А. Конференция посвященной 70-летию со дня рождения академика В.А. Коптюга “Современные проблемы органической химии”. Новосибирск, 2001, 51.
[140]. Bet, L.; Vlad, L.; Pogrebnoi, S.; Barba, A.; Macaev, F. The 1st International Conference of the Moldavian Chemical Society. Chisinau, Moldova. 2003, 153.
[141]. Макаев, Ф.З.; Бец, Л.; Влад, Л.; Погребной, С.И.; Галин, Ф.З.; Касрадзе, В. Материалы Российской конференции «Химия и медицина» В книге «Проблемы создания новых лекарственных средств». Гилем, Уфа, Россия, 2003, 72.
[142]. Бец, Л. Cercetări în domeniul chimiei Realizări şi perspective. Chişinău, Î.E.P. Ştiinţa. 2003, II, 93-95.
[143]. Макаев, Ф.; Бец, Л.; Влад, Л.; Погребной, С.; Барба, А.; Бесолов, А.; Малиновский, В.; Любодарский, Р. Ж. Орг. химии. 2006, 42, 872-876.
[144]. Malkov, A. V.; Pernazza, D.; Bell, M.; Bella, M.; Massa, A.; Teply, F.; Meghani, P.; Kocovsky, P. J. Org. Chem., 2003, 68, 4727-4742.
[145]. Chelucci, G.; Baldino, S.; Pinna, G. A.; Benaglia, M.; Buffa, L., Guizzetti S. Tetrahedron, 2008, 64, 7574-7582.
[146]. Chelucci, G.; Chelucci, G.; Belmonte, N.; Benaglia, M.; Pignataro, L. Tetrahedron Letters, 2007, 48, 4037-4041.
[147]. Ohloff, G.; Schulte-Elte, K.H.; Giersch, W. Helv. Chim. Acta. 1965, 48, 1665-1668.
[148]. Cocker, W.; Shannon, P.V.R.; Staniland, P.A. J. Chem. Soc. 1966, № 1, p. 41-47.
[149]. Meyer, U.; Hoelderich, W.F.; Journal of Molecular Catalysis A: Chemical. 1999, 142, 213-222.
[150]. Lesage, P.; Candy, J.P.; Hirigoyen, C.; Humblot, F.; Loconte, M.; Basset, J.M. Journal of Molecular Catalysis A: Chemical. 1996, 112, 303-309.
[151]. Zaidlewicz, M.; Giminska, M. Tetrahedron: Asymmetry. 1997, 8, 3847-3850.
[152]. Wyzlic, I.; Uzarewicz, A. Polish J.Chem. 1991, 65, 1999-2004.
[153]. Uzarewicz, A.; Scianowski J. Polish J.Chem., 1997, 71, 48-58.
[154]. Zaidlewicz, M.; Kanth, J.V.B.; Brown, H.C. J.Org.Chem. 2000, 65, 6697-6702.
[155]. Cadot, C.; Dalko, P.; Cossy, J.; Olliver, C.; Chuard, R.; Renaud, P. J.Org.Chem. 2002, 67, 7193-7202.
[156]. Dang, H.S.; Roberts, B.P.; Tocher, D.A. Organic & Biomolecular Chemistry. 2000, 31, 4073-4084.
[157]. Fringuelli, F.; Matteucci, M.; Piermatti, O.; Pizzo, F.; Burla, M.C. J. Org. Chem. 2001, 66, 4661-4666.
[158]. Attanasi, O.A.; De Crescentini, L.; Flippone, P.; Fringuelli, F.; Mantellini, F.; Matteucci, M.; Piermatti, O.; Pizzo, F. Helv. Chim. Acta. 2001, 84, 513-525.
[159]. Koneva, E.A.; Volcho, K.P.; Gatilov, Y.V.; Korchagina, D.V.; Salnikov, G.E.; Salakhutdinov, N.F. Helvetica Chimica Acta, 2008, 91, 1849-1856.

CATALYTIC WAVE OF CHLORATE IONS IN THE PREZENCE OF THE MOLYBDENUM (VI) - 2,3-DIHYDROXYBENZALDEHYDE COMPLEX

Ludmila Kiriyak[a], Tatiana Cazac[a], M. Revenco[b], and I. Povar[a*]

[a] *Institute of Chemistry, Academy of Sciences of Moldova, 3 Academiei str., Chisinau MD-2028, Republic of Moldova*
[b] *State University of Moldova, 60 A. Mateevici str., Chisinau MD-2009, Republic of Moldova*

Abstract: The polarographic catalytic current in acid solutions of Mo(VI), 2,3-dihydroxybenzaldehyde (2,3-DHBA) and chlorate ions has been investigated. The scheme of reactions taking place in the solutions and on the electrode has been elaborated. The increase of the catalytic current is explained by the formation of the active intermediate complex [Mo(V)·2,3-DHBA (ClO_3^-)]. The rate constant of formation for the active intermediate complex $K = 2.5 \cdot 10^6$ $mol^{-1} \cdot dm^3 \cdot s^{-1}$, the activation energy of reaction E_a=14.0 kcal·mol^{-1} and the activation entropy $\Delta S_a^{\neq}$= -28.3 e.u. have also been determined.

Keywords: Voltammetry, catalytic current, molybdenum, 2,3-dihydroxybenzaldehyde, potassium chlorate.

Introduction

The addition of organic compounds into the polyvalent metal - oxidant system exerts various influences on the catalytic current magnitude. It has been proved that some oxy-acids, catechol and mandelic acid, increase greatly the catalytic activity of Mo(VI) and W(VI) while ClO_3^- or BrO_3^- ions are used as oxidants [1-4]. The catalytic currents of chlorate and bromate ions have been used to determine several elements (Mo, Ti, and Cr) in a range of objects [5 – 10]. In the review [11] the authors discussed comprehensively the investigations concerning the determination of molybdenum in the presence of such oxidants as NO_3^-, ClO_4^-, ClO_3^- , BrO_3^-, as well as papers with the preliminary concentration of molybdenum complex compounds with several organic reagents. The authors [12] have shown that complexes V(V) and Mo(VI) with 2,5-dyhydroxy-1,4- benzoquinone in solutions of such an oxidant as ClO_4^- display a great surface activity, thus allows to use this catalytic system for the adsorptive voltammetric determination Mo(VI) and other metal ions [13].

This paper is dedicated to the investigation of the polarographic current nature in solutions of Mo(VI), chlorate ions and 2,3-DHBA. The main attention is focused on the impact of 2,3-DHBA under the catalytic current in the system Mo(VI) - ClO_3^-, as well as on the choice of optimal conditions for determining molybdenum by the value of the catalytic current.

Experimental

Polarographic measurements were carried out on polarograph PU-1 (Russia) in the thermostated (25±0.1°C) three-electrode cell. The working electrode was the mercury drop electrode (MDE, 2.45 $mg^{2/3} \cdot s^{-1/2}$), the reference electrode – the saturated calomel (SCE) one and a platinum wire as an auxiliary electrode. The drop-time curves were obtained by measuring drop-time in the three-electrode cell with a slowly dropping capillary (12 s). The solution acidity was verified by the universal pH-meter OP-104/1 (Hungary). The oxygen was removed from the solution by the electrolytic hydrogen blowing.

The standard solution of molybdenum (VI) was prepared by dilution of the exact weighted amount of the chemically pure $Na_2MoO_4 \cdot 2H_2O$. The purity for other reagents was at least of analytical grade.

Solutions $Na_2SO_4 + H_2SO_4$ (pH 2.0 – 2.5) served as a supporting electrolyte. Solutions of a smaller concentration were prepared by subsequent dilution of the initial ones.

The standard solution of $1 \cdot 10^{-3}$M 2,3-DHBA was prepared as follows: the exact weighted portion of 2,3-DHBA was placed in a 100 cm^3 volumetric flask; 1.0 – 1.5 cm^3 of ethanol was added and filled up to the mark by means of bidistilled water.

The working solutions were prepared in the following order: 2,3-DHBA was added to the neutral molybdate solution, then the supporting electrolyte and oxidant (potassium chlorate) were added and the necessary pH value was established.

Results and discussion

Fig. 1 shows the polarograms of solutions containing $1 \cdot 10^{-5}$ M Mo(VI) (curve 2), $5 \cdot 10^{-7}$ M Mo(VI) (curve 3)and $1 \cdot 10^{-4}$ M Mo(VI) (curve 4) on sulphuric supporting electrolyte (curve 1) in the presence of 0.2 M $KClO_3$ with $2 \cdot 10^{-5}$ M 2,3-DHBA (curve 3) and without it (curve 2). In the absence of 2,3-DHBA two catalytic waves responding to the reduction of Mo(VI) to Mo(V) and of Mo(V) to Mo(III) are registered on polarograms, while in the presence of 2,3-

DHBA, there was observed a great maximum in the area of first peak potentials. At low concentrations of Mo(VI) in solution, only this maximum is registered on polarograms (curve 3).

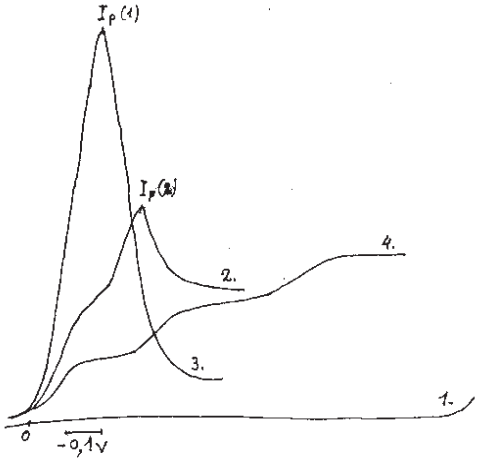

Fig. 1. Polarograms:

1. 0.1 M H_2SO_4 + 0.2M Na_2SO_4, pH 2.3;
2. 1 + $1\cdot10^{-5}$ M Mo(VI) + 0.2 M $KClO_3$;
3. 1 + $1\cdot10^{-7}$ M Mo(VI) + $2\cdot10^{-5}$ M 2,3-DHBA + 0.2 M $KClO_3$;
4. 1 + $1\cdot10^{-4}$ M Mo(VI);

In order to identity the nature of this maximum, we have studied the influence of the mercury column height above the capillary (h_{Hg}), temperature, pH values, as well as the 2,3-DHBA, Mo(VI) and ClO_3^- concentrations on the maximum current value (I_p).

The change of the mercury column height within 45-25 cm is shown in Fig. 2.

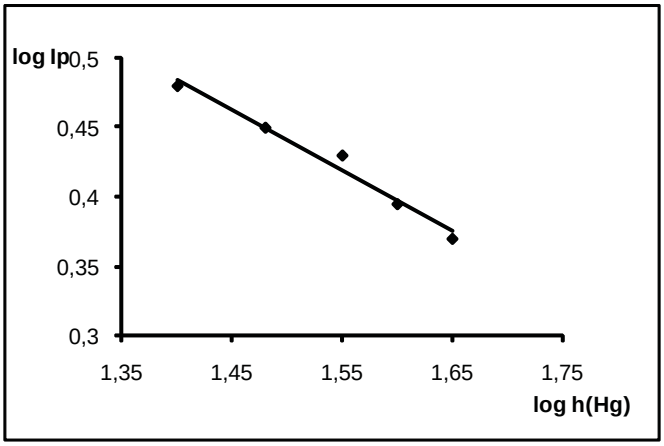

Fig. 2. Dependence of I_p on h_{Hg} for the solution that contains $5\cdot10^{-7}$ M Mo(VI), $2\cdot10^{-5}$ M 2,3-DHBA and 0.2 M $KClO_3$ at pH = 2.3.

As one can see from Fig. 2, the I_p value increases when the height of the mercury column above the capillary decreases. Such dependence is characteristic for electrode processes complicated by reacting substances adsorption on the electrode. The average value of the temperature coefficient in the temperature interval (20 – 40)°C is 7% /degree which points out to the catalytic nature of the current.

Dependence of the I_p value on the concentration of oxidant (ClO_3^-) in the form of a curve with a bend and a saturation section (Fig. 3., curve 1) proves the formation of a polarographically active complex that is characteristic for catalytic currents.

The curve showing the dependence of I_p on the ligand concentration passes through the maximum. The ligand activated action increases with the concentration growth (at its low concentrations), then it decreases.

The ligand (activator) availability in the catalyst coordination sphere contributes to the acceleration of the reaction of polarographically active mixed complex formation if in the catalyst coordination sphere there is enough space for the substrate (oxidant) entry, consequently the catalytic current increases. If in the catalyst – activator – substrate (Mo(VI) - 2,3-DHBA-ClO_3^-) system there are conditions when the ligand blocks all the catalyst coordination places, then the

catalytic activity decreases and the current drops. The maximum value of the current is observed when the concentration of 2,3-DHBA is equal to $2 \cdot 10^{-5}$ M.

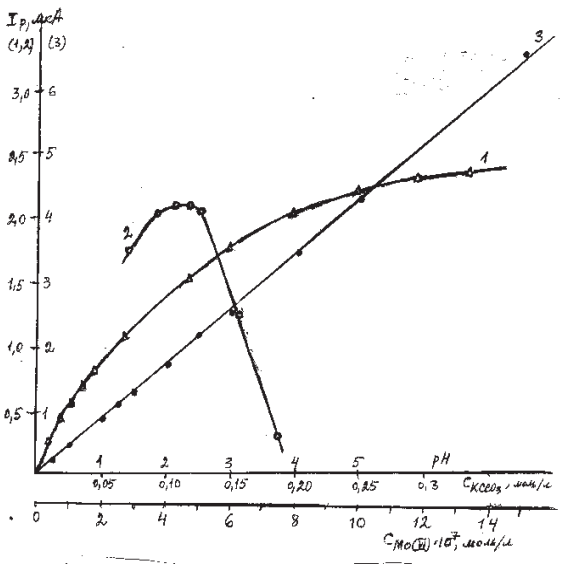

Fig. 3. Dependence of I_p on the concentration of $KClO_3$ (1), pH (2) and the Mo(VI) concentration (3):
1. $5 \cdot 10^{-7}$ M Mo(VI), $2 \cdot 10^{-5}$ M 2,3-DHBA and pH 2.3;
2. $5 \cdot 10^{-7}$ M Mo(VI), $2 \cdot 10^{-5}$ M 2,3-DHBA and 0.2 M $KClO_3$;
3. $2 \cdot 10^{-5}$ M 2,3-DHBA, 0,2 M $KClO_3$ and pH 2.3.

The influence of pH on I_p (Fig. 3, curve 2), as for other ligands, is manifested through the influence of pH on the complexing organic ligand dissociation or its protonization, as well as on the molybdenum active particles concentration in solution. Besides, the hydrogen ions participate in the oxidation – reduction process leading to the depolarizer regeneration. While the pH value increases, the potential of the maximum peak shifts towards more negative values.

The catalytic wave unusual shape in the form of a high maximum in solutions containing molybdenum (VI), ClO_3^- and the organic ligand can be explained by adsorption of all the components of the catalytic system on the electrode, this being shown by the dependence of drop – time of the capillary upon the electrode potential (Fig.4), but mainly by the higher rate of the chemical reaction running at the mercury - solution interface and determining the catalytic process rate on the whole.

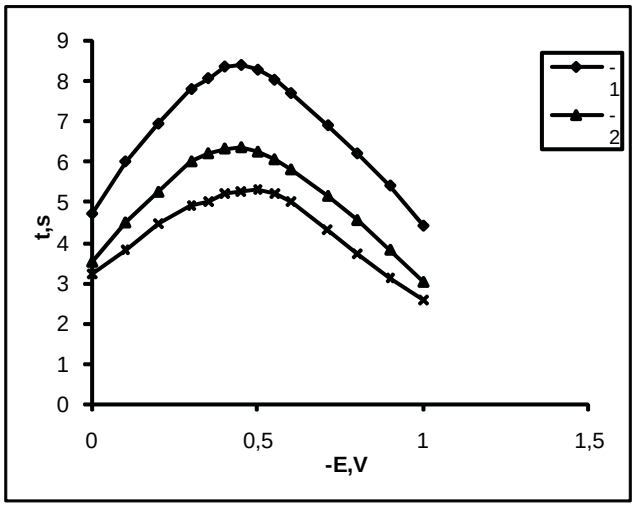

Fig. 4. Drop – time curves:
1. 0.2M Na_2SO_4, pH 2.3;
2. 1 + $2 \cdot 10^{-7}$ M Mo(VI), $2 \cdot 10^{-5}$ M 2,3-DHBA and pH 2.3;
3. 2 + 0.2 M $KClO_3$ and pH 2.3.

The analysis of experimental dependences of the catalytic current from the solution acidity and the concentration of catalytic system components (e.g. the catalyst, organic ligand and oxidant) has allowed representing the catalytic process by a scheme of subsequent chemical and electrochemical stages:

1. The complex formation of Mo(VI) with the organic ligand (L) in solution (the charges of complex species are dropped)

$$Mo(VI) + L \leftrightarrow [\ Mo(VI)\ L] + H^+$$

2. The catalyst formation

$$[Mo(VI)\ L] + e \rightarrow [Mo(V)\ L]$$

3. The formation of the intermediate active complex with an oxidant

$$[Mo(V)\ L] + ClO_3^- \leftrightarrow [Mo(V)\ L(ClO_3^-)] \leftrightarrow [Mo(V)\ L(ClO_3^-)]_{ads} \quad (3)$$

4. The catalyst redox – regeneration.

As it has been shown by the authors [14] on the example of the Mo(VI) + $H_2C_2O_4$ + ClO_3^- catalytic system, the catalyst redox – regeneration can proceed in two ways:

a) In the polarographically active complex $[Mo(V)\ L(ClO_3^-)]$ the electronic charge transfer on the substrate (ClO_3^-), followed by the catalyst in the highest oxidation degree intra – complex oxidation and regeneration, take place.

$$[Mo(V)\ L(ClO_3^-)]_{ads} + 2H^+ \rightarrow [Mo(VI)\ L] + ClO_2^- + H_2O \quad (4)$$

b) The electronic density shift from the substrate (ClO_3^-) to the catalyst in the polarographically active complex occurs. As a result, the catalyst catalytically active form is regenerated in the lowest oxidation degree.

$$[Mo(V)\ L(ClO_3^-)]_{ads} + e + 2H^+ \rightarrow [Mo(V)\ L] + ClO_2^- + H_2O \quad (5)$$

The obtained polarographic data do not allow making a conclusion concerning the catalyst regeneration in any form. Nevertheless, it is necessary to emphasize that at ligand low concentrations ($< 3 \cdot 10^{-5}$M) one high sharp maximum with a peak potential corresponding to the first wave of complex Mo(VI) reduction into Mo(V) is registered on polarograms, so the preference should be given to the first mechanism. With the increase of ligand concentration ($> 5 \cdot 10^{-5}$M) the peak bifurcates and, at the further increase of ligand concentration ($1 \cdot 10^{-4}$ M) the second maximum becomes slightly higher than the first one. It is quite possible that this phenomenon can be also explained by the catalyst regeneration in the lowest oxidation degree. Additionally, the authors [12] noted that at the (2,5-dichloro-3,6-dihydroxy-1,4-benzoquinone) ligand concentration of $5 \cdot 10^{-5}$ M, one maximum is registered while at the ligand concentration growth the peak decreases and its potential changes. Also, for the Mo(VI) – catechol – ClO_3^- system, it was pointed out that the catalytic current in the form of a peak was observed in the case of ligand small concentrations (Fig. 1, curve 3) [1]. At the $5 \cdot 10^{-2}$ M catechol concentration, the peak becomes wide without a clearly expressed peak and the current decrease is observed at more negative potentials (Fig. 1, curve 4 [1]). It is quite possible that in this case the catalyst regeneration occurs according to the abovementioned mechanisms. The maximum shape change, generated by the ligand concentration growth, can also be connected with a smaller deficit in the ligand molecule layer close to the electrode-solution interface necessary for the intermediate active complex formation. It may also be due to a stronger influence of the ligand and Mo(VI) complex electrode surface adsorption on the electrochemical depolarizer reduction (Fig. 4, curves 2 and 3).

The rate constant of the $[Mo(V)\ L\ (ClO_3^-)]$ intermediate active complex formation has been calculated by Koutetski's equation $I_k/I_d = 0{,}81\sqrt{nKC_st}$ in solutions with $2 \cdot 10^{-5}$ M concentration of 2,3-DHBA in the linear I_p - $C^{1/2}(ClO_3^-)$ dependence area (where I_k is the catalytic current equal to $I_p - I_d$; I_d – diffusion reduction current of the process $[Mo(VI)\ L] + e \rightarrow [Mo(V)\ L]$, recalculated for the $5 \cdot 10^{-7}$ M concentration of Mo(VI) and *t* is dropping time, 3.6s) (Fig. 5, Table 1).

Table 1

Rate constants of complex $[Mo(V)\ L(ClO_3^-)]$ formation

$C^{1/2}(KClO_3)$, M	I_p, mkA	I_p / I_d	$K \cdot 10^6$, $mol^{-1} \cdot dm^3 \cdot c^{-1}$
0.22	1.02	509	2.2
0.26	1.28	639	2.5
0.30	1.44	719	2.4
0.39	1.85	924	2.4
0.44	2.30	1149	2.8

$K_{av} = 2.5 \cdot 10^6$, $mol^{-1} \cdot dm^3 \cdot c^{-1}$

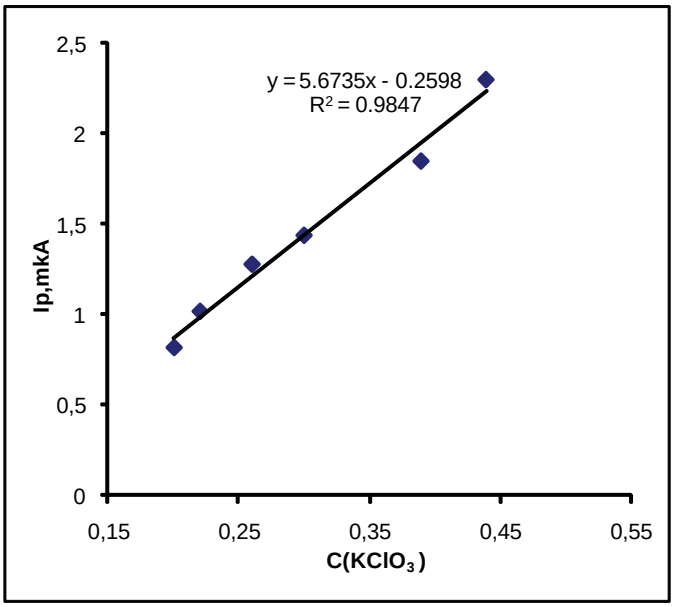

Fig. 5. Dependence of I_p on $C^{1/2}(KClO_3)$ for the solutions with $5 \cdot 10^{-7}$ M Mo(VI), $2 \cdot 10^{-5}$ M 2,3-DHBA and pH 2.3.

The activation energy and entropy of the catalytic process (Table 2) have been determined from the log K - 1/T dependence [15] for the 20 – 40°C temperature interval (Fig. 6).

Table 2

Kinetic and thermodynamic characteristics of the catalytic processes in the solutions of *Mo(VI)* with *2,3-DHBA Catechol* , *H_2Glucar* or *HMandel* complexes

Ligand - activator	$K \cdot 10^6$, $mol^{-1} \cdot dm^3 \cdot s^{-1}$	E, kcal/mol	ΔS_a^*, e.u.	References
2,3-DHBA	2.5	14.0	-28.3	-
Catechol	8.2	16.6	-26.0	[1]
H_2Glucar	7.6	9.3	-27.4	[1]
HMandel	220	14.3	-20.4	[3]

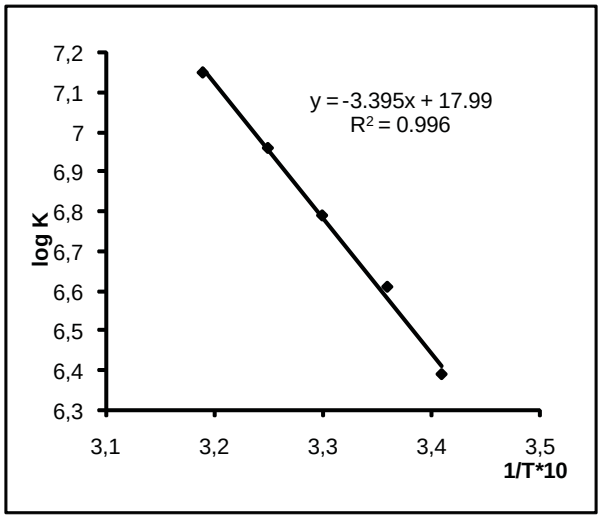

Fig. 6. Dependence of log K on 1/T for the solution of $5 \cdot 10^{-7}$ M Mo(VI), $2 \cdot 10^{-5}$ M 2.3-DHBA, 0.2 M $KClO_3$ and pH 2.3.

The calculated rate constant of intermediate active complex formation, activation energy and entropy demonstrate the high catalytic activity of the studied system. The activation influence of 2,3-DHBA slightly differs from catechol and

glucaric acid due to the addition of ethyl alcohol for a better solubility of 2,3-DHBA, being considerably smaller than for mandelic acid (Table 2). The large negative activation entropy values indicate on the spatial difficulties that occur when ClO_3^- ions are introduced into the Mo(V) complex coordination sphere. As one can see from the entropy activation $\Delta S_a^{\neq}$ values, the introduction of ClO_3^- ions into the coordination sphere of Mo(V) complexes with mandelic acid is the easiest, so the influence of the *HMandel* activation is higher than for other ligands [1-3].

The catalytic reaction in the Mo(VI) - 2,3-DHBA - ClO_3^- system is quite selective and may serve for the metal – catalyst micro-quantities determination. The optimal conditions of this determination are: $2 \cdot 10^{-5}$ M 2,3-DHBA, 0.2 M ClO_3, 0.2M Na_2SO_4 and pH 2 – 2,3. The dependence of I_p on the Mo(VI) concentration in the solution within $(1 – 15) \cdot 10^{-7}$ M is shown in Fig. 3 (curve 3).

Conclusions

This study describes the polarographic catalytic current behavior in acid solutions containing Mo(VI), 2,3-dihydroxybenzaldehyde (2,3-DHBA) and chlorate – ions. From the results of the measurements the scheme of reactions occurring in the solution and on the electrode has been elaborated. The catalytic current increase in the presence of 2,3-DHBA is explained by the formation of the active intermediate complex [Mo(V) · 2,3-DHBA (ClO_3^-)]. The rate constant of the intermediate active complex reaction formation $K = 2.5 \cdot 10^6$ mol^{-1} · dm^3 ·s^{-1}, as well as the reaction activation energy E_a = 14.0 kcal · mol^{-1} and the activation entropy $\Delta S_a^{\neq}$ =-28.3 e.u. have been determined. Further research will focus on the established possibility of the Mo(VI) small quantities determination.

Acknowledgments

This work was done under the support of the SCOPES 2009-2012 joint research grant.

References

[1]. CHIKRYZOVA, E.G.; KIRIYAK, L.G., Zh. Anal. Khim. 1974, **29**, 2420 – 2426.
[2]. CHIKRYZOVA, E.G.; KIRIYAK, L.G., Zh. Anal. Khim. 1980, **35**, 492-499.
[3]. BARDINA, S.M.; CHIKRYZOVA, E.G., Zh. Anal. Khim. 1978, **32**, 358.
[4]. TOROPOVA, V.F.; KOPYLOVA, O.V., Zh. Anal. Khim. 1977, **32**, 1159.
[5]. SAFARI, A.; SHARNS, E., Anal. Chem. Acta. 1999, **396**, 215 – 220.
[6]. YOKOIL, K.; VAN DEN BERG, C.M.G., Anal. Chem. Acta. 1992, **257**, 293 – 299.
[7]. KOCHELAEVA, G.A.; IVANOV, V.M.; PROKHOROVA, G.V., Zh. Anal. Khim. 2001, **56**, 860 – 866.
[8]. TOROPOVA, V.F.; POLYAKOVA, IU.N.; MALTSEVA, I.I., MIKRUKOVA, E. IU., Zh. Anal. Khim. 1999, **45,** 272 – 279.
[9]. BOBROWSKI, A.; BAS, B.; DOMINIK, J., NIEWIARA, E. ; SZALINSKA, E.; VIGANDI, Z; ZAREBSKI, J., Talanta. 2004, **63,** 1003 – 1012.
[10]. FITSEV, I. M.; TOROPOVA, V. F.; ROMADANSKAYA, E.V., ANISIMOVA, L.A., Zh. Anal. Khim. 1999, **54,** 510 – 512.
[11]. IVANOV, V.M.; KOCHELAEVA, G.A.; PROKHOROVA, G.V., Zh. Anal. Khim. 2002, **57,** 902 – 917.
[12]. NOVOTNY, L.; NAVRATIL, T,; SANDER, S.; BASOVA, P., Electroanalysis, 2002, **14,** 1105 – 1109.
[13]. SANDER, S., Anal. Chim. Acta., 1999, **394,** 81 -89.
[14]. BERSUKER, I.B.; BARDINA, S.M., Theor. Exp. Chim., 1978, **13,** 455 – 463.
[15]. KOLDIN, E., Quick reactions in the solutions. M.: Mir, 1966, p. 285.

THE STUDY OF THE BUFFERING CAPACITY OF SEVERAL WATER OBJECTS IN THE REPUBLIC OF MOLDOVA

Angela Lis[a*], Gheorghe Duca,[b] Elena Bunduchi[a], Viorica Gladchi[a], Nelli Goreaceva[a]

[a] *Moldova State University, 60 A. Mateevici str. MD 2010, Moldova*
[b] *Academy of Sciences of Moldova, Ştefan cel Mare 1, Moldova*
**E-mail: angelalis85@yahoo.com*

Abstract: The Republic of Moldova is situated among countries with relatively poor water resources, therefore their protection and rational use remains a national problem. Due to its geographic position, the Republic of Moldova is subjected to transboundary pollution. The current work represents the estimation of the buffering capacity on the Dniester River waters and its tributaries between November 2008 and October 2009. Decrease of the buffering capacity in water basins leads to disruption of the normal activity of aquatic biota, by increasing the toxicity in their living environment. On the basis of the results of measurements, suggestions for the improvement of the situation will be made and for enhancing public awareness and public authorities involvement.

Keywords: buffering capacity, acid-base balance, carbon system, humic system, stability to acidification.

Introduction

The Dniester River represents an important aquatic artery for the Republic of Moldova at the same time being a source of drinking water and fishery products and playing the role of a valuable recreation zone. Monitoring of the Dniester water quality has always been a priority for investigations in the Republic of Moldova. Decrease of the buffering capacity in water basins leads to disruption of the normal activity of aquatic biota, by increasing the toxicity in their living environment. On the basis of the results of measurements, suggestions for the improvement of the situation will be made and for enhancing public awareness and public authorities involvement.

Buffering capacity is water's property to oppose to the change of its chemical reaction (pH) more than is typical (6,5-8,5). Buffering capacity of waters can be defined as the maximum quantity of acid or base, which reaches the aquatic environment and without changing the background pH value.

As criterions of water bodies withstanding to acidification the following parameters can be used: pH, alkalinity, acids neutralizing capacity (ANC), the ratio of molar concentrations of anions HCO_3^-/SO_4^{2-} and buffering capacity of waters [1].

A more appropriate criterion to determine the stability of water bodies to acidification is the buffering capacity (power), which shows how the water pH changes when strong acids are added to it [2].

In the natural waters the buffer capacity is due to the presence of two systems: carbonic and humic. Buffer capacity of the carbonic system is caused by the HCO_3^- and CO_2 excess, but the humic system - by the quantity of organic acids, primarily by the humic and fulvic acids and their salts [3].

To determine the buffering capacity of natural waters the following linear dependence is used [3]:

$$[H^+]/m = f([H^+])$$

$$\frac{[H^+]}{m} = \frac{k}{C_t} + \frac{[H^+]}{C_t};$$

where $[H^+]$ – equilibrium concentration of hydrogen ions after adding acid; m – the content of weak acids (CO_2 and humic) ; C_t – total concentration of acids and salts, mmol-equiv/L; k – the dissociation constant of the weak acid.

Buffering capacity and pH of the aquatic environment depend on the ratio of the soluble forms of the carbonic acid concentrations and acid-base equilibrium constants.

The acid-base balance in the aquatic environment, which is determined by the carbonic system, may be disturbed only if a quantity of acids and bases in concentrations equal to that of carbonic acid arrive in water. The presence of metal ions in water, which form carbonic soluble complex, also can lead to the decrease of the buffering capacity. Besides the carbonic acid and its derivatives, the carbonic system is directly linked to hydrogen and calcium ions and indirectly with all dissolved substances. The total equilibrium may be represented by the following scheme:

$$\begin{array}{l} \mathbf{pCO_{2atm}} \\ \uparrow\downarrow \\ \mathbf{pCO_{2aq} \leftrightarrow H_2CO_3 \leftrightarrow HCO_3^- + H^+ \leftrightarrow CO_3^{2-} + 2H^+ \leftrightarrow CO_3^{2-} + Ca^{2+} \leftrightarrow CaCO_{3sol.}} \\ \qquad\qquad\qquad\qquad\qquad\qquad\qquad\qquad\qquad\qquad\qquad\qquad\qquad\qquad\qquad\qquad \uparrow\downarrow \\ \qquad\qquad\qquad\qquad\qquad\qquad\qquad\qquad\qquad\qquad\qquad\qquad\qquad\qquad\qquad\qquad \mathbf{CaCO_{3prec}} \end{array}$$

Buffering capacity of water bodies towards anthropogenic acidulation depends on a number of factors bound among them. The most important of them are the natural water, aquatic biota, and bottom deposition, hydrodynamic and meteorological factors [3]. An important role in decreasing of hydrogen ion concentration during anthropogenic acidulation is played by contained in natural water substances, many of them having the property to bind hydrogen ions. For example, weak anions of the inorganic acids (carbonates, phosphates, silicates, sulphites, etc.) and organic (carbonyl) also humic and fulvic acids, and polyphenols as a result of interaction with hydrogen ions will transform them into bind form or into salts of alkaline or alkaline earth metals.

Aquatic biota, such as phytoplankton or higher vegetation, in the process of photosynthesis or other biochemical processes increase pH values, thus preventing anthropogenic acidulation [5].

It should be noted that the buffering capacity of water bodies is not a constant value, but varies widely due to individual characteristics of different water basins, and also depends on the region of the water basin and on the season.

One of the anthropogenic factors that negatively influence water systems is their acidulation, mainly due to the penetration of acid rain waters. The property of withstanding the acidulation of the water basins is determined by hydrological and geochemical factors [4].

Decreased pH values in the water basins not only disturb normal activity of aquatic biota, but also lead to increased toxicity of other pollutants in the basin or their solubilization from suspensions [6].

Results

This paper presents the estimation of the stability towards acidulation of the Dniester river waters and its tributaries during the period November 2008 – October 2009, monitoring the buffering capacity indicator. Measurements were taken along a 310 km river segment. Samples were selected in the following sections: Naslavcea village (200 m around the Naslavcea barrage), Cosautsi village, Boshernitsa village, the Dubasari water reservoir upstream the barrage, 100 m downstream the Dubasari barrage. To determine the impact of the tributaries on the Dniester waters, were collected samples upstream and downstream of the mouth of the following rivers: r. Raut, r. Ichel, r. Botna and r. Bic.

Estimation of the buffering capacity

Titrations were carried out with 0.025 N HCl solution, for one volume of 50 ml of natural water. To determine the equilibrium concentration of hydrogen ions in the titration process the pH value was measured [7]. The graph $[H^+]/m = f([H^+])$ was plotted, where $[H^+]$ is equilibrium concentration of hydrogen ions after adding acid; m – the content of weak acids (CO_2 and humic);

$$m = \text{initial aidity} + b - [H^+]; \quad b = C \cdot V/V_s$$

where C – concentration of added acid, V - volume of added acid, b – amount of strong acid added, mmol-equiv/L, $V_{s.}$ - volume of analyzed sample.

From the obtained graph, the slope is determined: $tg\ \alpha = 1/C_t$, where: $C_t = 1/tg\ \alpha$, and the intersection of the graph with the Oy axis gives the ratio k/C_t and thus the value of the constant k can be calculated [8].

To determine the buffering capacity of natural waters with pH within limits 6.5 to 8.5 the formula of Van Slaik for weak acids and its salts is used [9]:

$$\beta = 2{,}3 \frac{C_t \cdot 10^{pk-\,pH}}{(1 + 10^{pk-pH})^2}$$

Example of buffering capacity calculation for water sample taken from the Dniester river in the point of capture Naslavcea on December 9, 2008.

$$\text{Acid.} = \frac{V \cdot C}{V_{s.}} \cdot 1000, \text{ mmol-equiv/L, where}$$

V – volume of NaOH consumed for titration, C - concentration of NaOH solution, V_s - volume of analyzed sample.

$$\text{Acid.} = \frac{0{,}2 * 0{,}1}{50} * 1000 = 0{,}4 \text{ mmol-equiv/l},$$

$$\text{Alcal.} = \frac{V \cdot C}{V_{s.}} \cdot 1000, \text{ mmol-equiv/l, where}$$

V – volume of HCl consumed for titration, C - concentration of HCl solution, $V_{s.}$ - volume of analyzed sample.

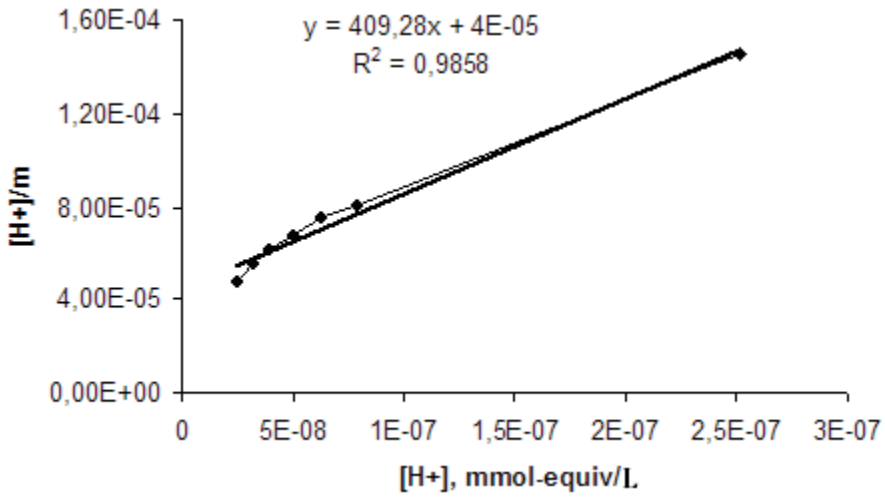

Fig. 1. Dependence $[H^+]/m$ according to $[H^+]$ for Dniester river water (Naslavcea).

$$\text{Alcal.} = \frac{3{,}2 \cdot 0{,}05}{50} \cdot 1000 = 3{,}2 \text{ mmol-equiv/l}$$

$b = C \cdot V/V_{s.}$, where: C- concentration of HCl solution, V – volume of HCl consumed for titration, $V_{s.}$- volume of analyzed sample.

$b = 0{,}024 \cdot 0{,}25/50 \cdot 1000 = 0{,}12$ mmol-equiv/L
$m = Acid_{init.} + b - [H^+]$; where $[H^+]$ – equilibrium concentration of hydrogen ions after adding acid;
$pH = -\lg[H^+]$, $[H^+] = 10^{-pH}$; $[H^+] = 10^{-7,6} = 2{,}5 \cdot 10^{-8}$ mol/L
$m = (0{,}4 + 0{,}12) \cdot 10^{-3}$ mol-equiv/L – $2{,}5 \cdot 10^{-8}$ mol-equiv/L = $52{,}25 \cdot 10^{-5}$ mol-equiv/L;
$[H^+]/m = 2{,}5 \cdot 10^{-8}$ mol-equiv/L / $52{,}25 \cdot 10^{-5}$ mol-equiv/L = $4{,}8 \cdot 10^{-5}$;
The dependence $[H^+]/m = f([H^+])$ is plotted, fig.1.

From this dependence tg α is calculated: $tg\ \alpha = 1/C_t$, where: $C_t = 1/tg\ \alpha$,
$C_{tot} = 1/409{,}3 = 2{,}44 \cdot 10^{-3}$ M or 2,44 mmol-equiv/L
the intersection of the graph with the Oy axis gives the ratio k/C_t and thus the value of the constant k can be calculated
$k/C_{tot} = 4{,}4724 \cdot 10^{-5}$, $K = 4{,}4724 \cdot 10^{-5} \cdot 2{,}44 \cdot 10^{-3} = 10{,}93 \cdot 10^{-8}$
$pk = -\lg k$; $pk = -\lg 10{,}93 \cdot 10^{-8}$; $pk = 8 - \lg 10{,}93$; $pk = 6{,}96$

Buffering capacity is calculated from the relationship:

$$\beta = 2{,}3 \frac{C_{tot} \cdot 10^{pk-pH}}{(1 + 10^{pk-pH})^2}$$

$$\beta = 2{,}3 \frac{2{,}44 \cdot 10^{6{,}96 - 8{,}1}}{(1 + 10^{6{,}96 - 8{,}1})^2} = 0{,}35 \text{ mmol-equiv/L.}$$

Water samples were collected from surface layer (h = 0.5 m) and the following parameters were determined: pH, alkalinity, acidity, COD_{Mn}, buffering capacity, acid-base constant (tab. 1, 2).

A set of abiotic and biotic factors contribute to the formation of buffering capacity of natural waters.

The group of abiotic factors comprises: the chemical composition of water (ions HCO_3^-, CO_3^{2-}, humic substances, carbonyl and oxicarbonyl acids, HPO_4^{2-}, $HSiO_3^-$, $H_3BO_3^{2-}$, polyphenols), bottom deposition, rainfall, food sources, nature of the rocks and the location of the basin.

The second group is formed from aquatic biota. It influences the buffering capacity by using carbon dioxide in the process of photosynthesis, and by eliminating metabolic products such as nitrogen compounds (amino acids, proteins, polypeptides, etc.).

As the result of processing the curves of potentiometric titration and those calculations, were determined the values of buffering capacity of the Dniester river waters.

Table 1. Quality indicators of r. Dniester in p.c. Cosauti, Naslavcea, Boshernitsa, upstream and downstream of Dubasari in November 2008 - July 2009

Date of capture	Place of capture	pH init.	HCO_3^-	Acid	Alk.	β	pK	K* 10^7	COD_{Mn} mgO/L	CO_2 mg/L
			mmol-equiv/L							
04.11.08	r.Dniester (Naslavcea)	7,6	2,3	0,32	2,3	0,54	6,9	1,9	8,16	-
04.11.08	r.Dniester (Cosautsi)	7,5	2,3	0,30	2,3	0.38	6,3	4,5	7,52	-
04.11.08	r.Dniester (Boshernitsa)	7,9	2,4	0,32	2,4	0,49	6.9	1,2	6,08	-
04.11.08	r.Dniester (Dub. upst.)	8,1	2,4	0,32	2,4	0,41	6.8	1,6	6,08	-
04.11.08	r.Dniester (Dubasari downst.)	8,1	2,4	0,32	2,4	0,41	6.8	1,5	5,76	-
09.12.08	r. Dniester (Naslavcea)	8,1	3,2	0,40	3,2	0,35	6.9	1.1	5,44	-
09.12.08	r.Dniester (Cosautsi)	8,1	3,1	0,44	3,1	0,35	6.9	1.3	5,44	-
09.12.08	r.Dniester (Boshernitsa)	-	-	-	-	-	-	-	-	-
09.12.08	r.Dniester (Dub. upst)	8,0	3,3	0,18	3,3	0,34	6.8	1,5	5,12	-
09.12.08	r.Dniester (Dubasari downst.)	-	-	-	-	-	-		-	-
14.03.09	r. Dniester (Naslavcea)	8.1	3.3	0.39	3.3	0.35	6.8	1,5	2.48	3.1
14.03.09	r. Dniester (Cosautsi)	8.1	3.6	0.37	3.6	0.34	6.8	1.5	4.40	3.3
23.03.09	r.Dniester (Boshernitsa)	8.1	3.3	0.39	3.3	0.30	7.2	0.7	3.12	1.3
14.03.09	r. Dniester (Dub.upst.)	8.1	3.5	0.62	3.5	0.49	7.1	0,8	2.24	1.4
28.02.09	r. Dniester (Dubasari downst.)	8.4	3.2	0.31	3.2	0.29	7.3	0,5	3.26	1.7
11.04.09	r. Dniester (Naslavcea)	8.2	3.3	0.21	3.3	0.32	6.8	1,5	2.88	2.4
11.04.09	r. Dniester (Cosautsi)	8.2	3.3	0.41	3.3	0.35	6.9	1,2	2.72	1.7
12.04.09	r.Dniester (Boshernitsa)	8.4	3.6	0.31	3.6	0.34	7.1	0,8	3.20	1.2
21.04.09	r. Dniester (Dubasari downst.)	8.1	3.0	0.19	3.0	0.17	6.6	2,1	3.04	1.3
21.04.09	r. Dniester (Dub.upst.)	8.0	3.0	0.21	3.0	0.18	6.7	2,5	3.20	1.9
7.07.09	r. Dniester (Naslavcea)	7.9	2.7	0.19	2.7	0.28	6.6	2.6	2.79	3.0
7.07.09	r. Dniester (Cosautsi)	8.2	3.0	0.19	3.0	0.25	6.8	1.5	2.09	0.6
8.07.09	r.Dniester (Boshernitsa)	8.1	3.0	0.08	3.0	0.14	6.3	5,2	2.93	2.6
14.07.09	r.Dniester (Dub.upst.)	8.1	3.0	0.08	3.0	0.19	6.5	3.0	2.50	1.5
14.07.09	r.Dniester (Dubasari downst.)	8.1	2.8	0.06	2.8	0.13	6.6	2.2	2.10	1.8

The results obtained show that the collection points of the Dniester river may be placed in the following order, regarding their stability to acidulation: Cosautsi > Naslavcea > Boshernitsa > Dubasari upstream > Dubasari downstream.

In the collection point Cosautsi waters are characterized by constant values of buffering capacity between 0.34 and 0.38 mmol-equiv/L. A sharper decline of buffering capacity in this point of capture is observed in July 2009 (0.25 mmol-equiv/L). In p.c. Boshernitsa and Naslavcea, the recorded values for the buffering capacity of the Dniester waters were of 0.31 to 0.35 mmol-equiv/L, except for November 2008. The buffering capacity of water in the reservoir Dubasari both upstream and downstream, included a much wider range of values compared with other collection points, from 0.17 to 0.50 mmol-equiv/L. In July there was a sharp decrease in values of the buffering capacity at all points of capture.

Among the factors that determine the buffering capacity, the contribution of biotic factors can be neglected, because the activity of biota during the monitored period was reduced or even stopped due to low temperatures.

Among abiotic factors which influence values of the buffering capacity, was determined the content of HCO_3^- ions and humic substances (COD_{Mn}) (tab.1).

Comparing the content of HCO_3^- ions with total alkalinity leads to the conclusion that these values are practically equal, so alkalinity value mainly consists of the hydrocarbonate ions. But, comparing the alkalinity with the values of buffering capacity doesn't lead to the conclusion that buffering capacity increases with the increase of alkalinity. Therefore, estimation of the buffering capacity only using alkalinity values is not complete. Other substances are also present in natural waters, which may contribute to decreased values of the buffering capacity. Thus metabolites of the aquatic biota, especially compounds containing nitrogen (amino acids, proteins, polypeptides etc.) can interact with hydrogen ions, leading to increasing buffering capacity.

The data presented above show that there is a poly-component buffering system in the Dniester waters. In the capture points Boshernitsa, Dubasari upstream and downstream Dubasari was registered a direct correlation between buffering capacity and alkalinity, which makes these waters unstable to acidulation. Such a direct dependency between buffering capacity and alkalinity wasn't found in the collection points Naslavcea and Cosautsi, but however, values of the buffering capacity didn't vary considerably. Here buffering capacity is probably influenced by other components, such as the nature of the rocks. In c.p. Cosauti are present limestone and dolomite rocks, which ensures the maintenance of constant values of the buffering capacity.

Results showed that there is no strict law to describe the increase of buffering capacity with increasing content of humic substance in the r. Dniester waters, as determined by the indicator COD_{Mn} (Tab.1).

Table 2. Quality indicators of r. Raut, r. Ichel, r. Botna and Bic waters in February-October 2009

Date of capture	Place of capture	pH init.	HCO_3^-	Acid	Alk.	β	pK	K* 10^7	COD_{Mn} mgO/L	CO_2 mg/L
			mmol-equiv/L							
28.02.09	r. Raut	8.3	8.6	0.94	8.6	0.56	8.6	0.02	5.12	5.3
28.02.09	r. Dniester, upstream Raut	8.4	3.2	0.31	3.2	0.22	8.4	0.03	3.26	1.7
28.02.09	r. Dniester, down. Raut	8.4	4.6	0.62	4.6	0.31	8.9	0.01	3.68	2.5
28.02.09	r. Ichel	8.3	7.6	0.52	7.6	0.39	8.3	0.05	3.76	4.6
28.02.09	r. Dniester, upstream Ichel	8.5	3.6	0.42	3.6	0.19	8.9	0.01	3.36	1.7
28.02.09	r. Dniester, down. Ichel	8.5	3.6	0.21	3.6	0.15	8.2	0.06	3.44	1.5
14.03.09	r. Botna	8.4	8.5	0.62	8.5	0.46	8.1	0.07	6.96	4.2
14.03.09	r. Dniester, upstream Botna	8.3	3.8	0.25	3.8	0.16	7.9	0.11	3.00	2.2
14.03.09	r.Dniester, down. Botna	8.3	3.7	0.29	3.7	0.22	8.2	0.08	2.72	2.5
14.03.09	r. Bic	8.1	7.4	1.14	7.4	0.78	7.9	0.11	6.24	7.1
21.04.09	r. Raut	8.4	7.9	0.42	7.9	0.31	8.3	0.05	5.52	2.0
21.04.09	r. Dniester, upstream Raut	8.1	3.0	0.19	3.0	0.14	7.9	0.12	3.04	1.3
21.04.09	r. Dniester, down. Raut	8.2	3.7	0.17	3.7	0.12	8.1	0.08	2.76	1.3
21.04.09	r. Ichel	8.3	7.1	0.21	7.1	0.16	8.0	0.09	6.00	1.7
21.04.09	r. Dniester, upstream Ichel	8.2	3.2	0.23	3.2	0.16	8.2	0.07	3.12	1.3
21.04.09	r. Dniester, down. Ichel	8.2	3.2	0.15	3.2	0.11	8.0	0.10	2.80	1.3
21.04.09	r. Botna	8.2	3.3	0.15	3.3	0.11	7.9	0.13	2.56	1.1
21.04.09	r. Dniester, upstream Botna	8.2	3.3	0.10	3.3	0.08	7.8	0.17	1.52	1.5
21.04.09	r. Dniester, down. Botna	8.2	3.2	0.15	3.2	0.11	7.9	0.13	2.72	1.9
21.04.09	r. Bic	8.1	7.1	0.52	7.1	0.39	7.9	0.14	12.32	4.9
21.04.09	r. Dniester, upstr. Bic	8.3	3.2	0.12	3.2	0.09	8.0	0.10	2.56	1.5
19.05.09	r. Raut	8.2	8.5	0.17	8.5	0.42	6.9	0.03	3.90	1.6
19.05.09	r. Dniester, upstream Raut	8.3	2.8	0.06	2.8	0.25	8.5	1.89	4.40	1.5
19.05.09	r. Dniester, down. Raut	8.4	3.9	0.12	3.9	0.22	6.7	0.92	4.80	1.5
19.05.09	r. Ichel	8.4	9.0	0.37	9.0	0.57	7.0	1.31	4.30	3.5
19.05.09	r. Dniester, upstream Ichel	8.3	2.8	0.15	2.8	0.19	6.9	1.26	4.80	0.9
19.05.09	r. Dniester, down. Ichel	8.3	2.9	0.15	2.9	0.19	6.9	1.95	4.10	1.2
18.05.09	r. Botna	8.2	7.1	0.39	7.1	0.53	6.7	1.23	6.30	5.1
23.06.09	r. Raut	8.9	8.3	0	8.3	0.28	7,6	2.32	3,63	1.3
23.06.09	r. Dniester, upstream Raut	8.6	3.0	0	3.0	0.11	6,6	2.65	2,23	1.4
23.06.09	r. Dniester, down. Raut	8.4	3.9	0.15	3.9	0.18	6,9	1.12	2,02	1.4
23.06.09	r. Ichel	8.4	9.1	0.33	9.1	0.59	7,0	0.99	6,41	6.3
23.06.09	r. Dniester, upstream Ichel	8.3	3.1	0.17	3.1	0.23	6,9	1.24	1,71	1.5
23.06.09	r. Dniester, down. Ichel	8.3	3.1	0.15	3.1	0.17	6,9	1.29	2,09	1.7

22.06.09	r. Botna	8.8	6.3	0	6.3	0.28	7,8	0.17	9,12	0.7
22.06.09	r. Dniester, upstream Botna	8.2	3.1	0.17	3.1	0.19	6,7	1.85	2,23	0.9
22.06.09	r. Dniester, down. Botna	8.2	3.2	0,17	3.2	0.19	6,8	1.49	1,85	1.2
22.06.09	r. Bic	7.9	7.2	0.49	7.2	0.74	6,7	1.76	9,2	7.2
22.06.09	r. Dniester, upstr. Bic	8.2	3.1	0.16	3.1	0.22	6,8	1.41	1,67	1.7
22.06.09	r. Dniester, down. Bic	8.1	3.3	0.21	3.3	0.23	6,6	2.23	2,09	2.7
14.07.09	r. Raut	8.4	8.6	0	8.6	0.37	7.1	0.77	6.5	3.0
14.07.09	r. Dniester, upstream Raut	8.1	2.8	0.06	2.8	0.13	6.6	2.23	2.1	1.8
14.07.09	r. Dniester, down. Raut	8.3	4.1	0	4.1	0.14	6.8	1.62	4.5	1.7
14.07.09	r. Ichel	8.0	5.2	0.04	5.2	0.33	6.5	3.41	16.49	4.1
14.07.09	r. Dniester, upstream Ichel	8.1	2.9	0.08	2.9	0.15	6.5	2.84	1.8	1.6
14.07.09	r. Dniester, down. Ichel	8.0	2.9	0.12	2.9	0.19	6.5	3.00	1.8	1.7
13.07.09	r. Botna	8.8	5.7	0	5.7	0.22	7.7	0.21	8.84	0.6
13.07.09	r. Dniester, upstream Botna	8.1	2.9	0.1	2.9	0.19	6.7	1.92	2.09	1.8
13.07.09	r. Dniester, down. Botna	8.1	2.9	0.1	2.9	0.17	6.6	2.56	2.44	2.3
13.07.09	r. Bic	7.8	6.7	0.41	6.7	0.62	6.6	2.47	8.15	9.1
13.07.09	r. Dniester, upstr. Bic	8.2	3.0	0.31	3.0	0.29	7.0	0.92	2.16	1.4
13.07.09	r. Dniester, down. Bic	8.1	3.2	0.23	3.2	0.25	6.9	1.29	2.5	1.8
8.10.09	r. Dniester, upstream Raut	8.1	3.1	0.07	3.1	0.18	6.6	2.48	1.50	5.0
8.10.09	r. Raut	8.5	10.0	0	10.0	0.30	6.6	2.32	7.55	3.5
8.10.09	r. Dniester, down. Raut	8.3	4.6	0	4.6	0.18	6.2	5.99	2.58	4.2
8.10.09	r. Dniester, upstream Ichel	8.2	3.2	0.09	3.2	0.23	6.7	2.03	1.79	2.8
8.10.09	r. Ichel	8.4	8.4	0	8.4	0.37	6.6	2.20	7.26	4.5
8.10.09	r. Dniester, down. Ichel	8.3	3.2	0	3.2	0.19	6.6	2.29	1.57	4.2
8.10.09	r. Dniester, upstream Botna	8.2	3.3	0	3.3	0.21	6.7	2.01	2.15	2.3
8.10.09	r. Botna	8.8	7.7	0	7.7	0.33	7.3	0.45	10.62	1.2
8.10.09	r. Dniester, down. Botna	8.3	3.1	0	3.1	0.20	6.6	2.31	2.37	1.8
8.10.09	r. Dniester, upstr. Bic	8.3	3.2	0	3.2	0.12	6.4	4.07	1.65	2.4
8.10.09	r. Bic	7.8	8.3	0.30	8.3	1.31	6.6	2.38	15.23	11.9
8.10.09	r. Dniester, down. Bic	7.9	3.9	0.15	3.9	0.30	6.5	2.80	3.59	3.4

To elucidate the tributaries impact on the Dniester waters, the same indicators were determined for the following rivers: Raut, Ichel, Botna and Bic (Tab.2).

According to data presented in Tab. 2, the waters of monitored rivers have maximum values of the buffering capacity in March (from 0.7 - up to 1.2 mmol-equiv/L), except for r. Bic for which maximum values were registered in October (1.3 mmol-equiv/L). This development was due to high HCO_3^- ion content (7.1-8.6 mmol-equiv/L) in mentioned period. In April was noticed a sudden fall in values of the buffering capacity of rivers (down to 0.2 and 0.5 mmol-equiv/L). Also in this month there have been low HCO_3 ion concentrations (3.3 to 7.1 mmol-equiv/L). In May it was noticed a slight increase in values of the buffering capacity of the monitored rivers (r. Ichel - 0.57 mmol-equiv/L, r. Botna - 0.53 mmol-equiv/L) except for r. Raut, in which case the value slightly decreased (from 0.5 - to 0.42 mmol-equiv/L). In June values of the buffering capacity were reduced almost 2 times for r. Raut (from 0.416 - till 0.282 mmol-equiv/L) and r. Botna (from 0.533 - till 0.285 mmol-equiv/L), but there was a slight increase in these values for r. Ichel (from 0.567 - till 0.598 mmol-equiv/L) and r. Bic (from 0.595 - till 0.738 mmol-equiv/L).

The obtained results show that the monitored rivers are placed in the following order, regarding the stability to acidulation: Ichel > Bîc > Răut > Botna.

Lower values of buffering capacity were found upstream and downstream rivers Ichel, Bîc, Răut and Botna (0.17 to 0.35 mmol-equiv/L) compared with those rivers. Was confirmed that small rivers have a positive impact on water quality of r. Dniester. Buffering capacity values downstream of the mouth are higher than the buffering capacity of the upstream values.

The data presented in Tab. 2 show that unlike the Dniester river waters, in the waters of small rivers, a direct dependence between the buffering capacity and HCO_3^- ions content is observed. I.e. the buffering capacity increases with

increasing of HCO_3^- ions content, and respectively, it decreases with the reduction of HCO_3^- ions content. Exceptions were values from April 2009, for r. Botna, when the buffering capacity was influenced by other factors.

The results presented in Tab. 2 show that COD_{Mn}, just like the alkalinity, affects the buffering capacity of small rivers. It was established that increasing of COD_{Mn} values lead to the increase of the buffering capacity and vice versa, decreasing of COD_{Mn} values lead to the diminishing of the buffering capacity. Exceptions were r. Raut and Ichel in May, which demonstrates that in these rivers the buffering capacity is particularly influenced by the carbon system. For river Botna waters in April was registered a greater influence of the humic system on the buffer. The buffering capacity values did not show a direct dependence on the HCO_3 ions content for this river, but was observed a direct dependence on the CCO_{Mn} values.

So, unlike large rivers, the buffer system of small rivers in the monitored period is influenced particularly by the carbon system, less by the humic system and very little by other components such as aquatic biota, bottom deposits, etc.

Conclusions

From the above data we conclude that the buffering capacity of aquatic objects is not a constant value but it varies in time and space. Depending on the season the buffering capacity values are characterized by small variations. There is a complex buffer system in natural waters, consisting of biotic and abiotic factors. The results obtained show that the collection points of the Dniester river may be placed in the following order, regarding the stability to acidulation: Cosautsi > Naslavcea > Boshernitsa > Dubasari upstream > Dubasari downstream. The Cosauti capture point is the most stable to acidulation, due to river basin rocks forming in this point, namely the presence of limestones and dolomites that contribute to increasing buffering capacity of waters. The results obtained show that the monitored rivers may be placed in the following order, regarding the stability to acidulation: Ichel > Bîc > Răut > Botna. It was demonstrated that monitored rivers have a positively influence on the Dniester river waters, because they lead to the increase of the buffering capacity downstream of the river mouth. During low photosynthetic activity of the year the waters vulnerability to anthropogenic factors increases, which may lead to lower buffering capacity of natural waters.

In order to prevent the phenomenon of waters acidification and to identify sources of pollution, we recommend expanding the National Standards with the indicator of the buffering capacity. Also, we recommend authorized bodies to inform the parties responsible for the impact of emissions on the national aquatic ecosystems, and to require these parties to take measures to decrease the impact.

References

[1]. Горячева, Н. В.; Дука, Г. Г. Гидрохимия малых рек Республики Молдова - Chişinău. - 2004 - p. 91-101.
[2]. Lei, D.; Jiming, H. Critical loads of acidity for surface waters in China / The Science of the Total Environment. *PR* China. - 2000 – p. 1-10.
[3]. Никаноров, А. М.; Лапин, И. А. Оценка буферной ёмкости. // Доклады Академии наук – 1990.- том 314.- № 6 – с. 1507-1510.
[4]. Дворак, Н. А.; Потапова, И. Ю.; Лозовик, П. А. Устойчивость озера Пряжинское к закислению. // Материалы карельского государственого университета. - 2007 – с. 71-73.
[5]. Chris, J. C.; Ivan, B.; Lluis, C. Acidification in European mountain lake districts: A regional assessment of critical load exceedance / Aquatic Sciences. Dübendorf. - 2005 – p. 237-251.
[6]. Curtis, C. J.; Barbieri, A.; Camarero, L. Application of static critical load models for acidity to high mountain lakes in Europe / Water, Air, and Soil Pollution: Focus. - 2002 – p. 115-126.
[7]. Rapp, L. Critical Loads of Acid Deposition for Surface Water-Exploring existing models and a potential alternative for Sweden. Doctor's dissertation. Uppsaia, 2001 – 35 p.
[8]. Потапова, И. Ю.; Лозовик, П. А. Оценка устойчивости водных объектов Карелии к закислению по буферной ёмкости и кислотонейтрализующей способности. // Матер. Института водных проблем Севера Карелии. – 2007. – с. 93-98.
[9]. Лозовик, П. А. Устойчивость водных объектов к закислению в зависимости от удельного водосбора на примере озёр и рек. // Водные ресурсы Т. 33.- 2006 – с. 15-19.

CATALYTIC OXIDATION OF METHYLENE BLUE

T. Lupaşcu*, M. Ciobanu, V. Boţan, A. Nistor

Institute of Chemistry of ASM, 3 Academy str., Chisinau, MD-2028, Republic of Moldova
Email: lupascut@gmail.com

Abstract: The intact activated carbon CAN-8, obtained from nutshells by activation with water vapors, in the presence of oxygen and at relatively low temperatures, possesses catalytic activity, caused by the presence of alkaline functional groups on its surface, as well as by the formation, in these experimental conditions, of the $OH^{\bullet}$ radical, which has a high oxidation potential. After 25 cycles of the process of methylene blue oxidation, the data of chromatographic analyses indicate the presence of three organic components in the solution.

Keywords: catalytic oxidation, methylene blue, activated carbon.

Introduction

Waste waters generated by coloring pans are toxic and non-biodegradable substances. The presence of these substances in surface waters leads to the intoxication of aquatic flora and fauna. Modern technologies of waste waters purification from colorants are known, which comprise procedures of sorption of these toxicants on mineral and/or carbonic adsorbents [1].

The utilization of solid catalysts and first of all, of those on the basis of activated carbons, for the oxidation of organic compounds in aqueous media, represents an original solution of significant promise.

The procedure of waste waters purification from methylene blue in the presence of the catalyst obtained on the basis of manganese oxide nanoparticles and hydrogen peroxide is known [2]. Also, was described the procedure of catalytic oxidation of methylene blue at various temperatures (50°C, 65°C, 80°C) and oxygen purging, in the presence of activated carbons obtained from olive stones by activation with water vapors and subsequent impregnation with copper(II) oxide [3].

The elimination of organic substances from waste waters, using the method of adsorption on porous adsorbents, is widely used in various technologies.

Oxidative treatment leads to the destruction of organic compounds with the formation of non-toxic products. The choice of alternative technologies depends on the content and stability towards oxidation of organic pollutants. In this sense, hydrogen peroxide is the proper agent for waste waters that contain relatively small quantities of organic pollutants.

Synthesis of new catalysts which would oxidize organic pollutants in waters, in order to obtain non-toxic products at low temperatures represents an important objective for industrial applications.

Although methylene blue has antimicrobial and antifungal actions, it also exhibits a negative influence on plants and therefore it has to be eliminated from waste waters.

Results and discussions

Samples of 50 mg of activated carbon CAN-8 (the 0,06 – 0,08 mm fraction) and volumes of 100 mL of methylene blue solution (C=20 mg/L) were introduced in two reactors with magnetic stirrers and water cloaks. Reactors' content was heated up to 50°C. Nitrogen was bubbled trough the solution with the adsorbent from the first reactor, and oxygen – in the second reactor, at a pressure of 2 atm. After ~ 10 min the quantity of methylene blue drastically reduced. The colorless solution from the second reactor was transferred into a 100 mL calibrated flask, and demineralized water was added to the mark. A new portion of methylene blue, of the same volume and concentration, was added to the reactor where the activated carbon remained, and the oxidation procedure was repeated for another 10 min. Thus, 25 cycles were performed. The solution through which nitrogen was purged remained colored, i.e. the oxidation process of methylene blue did not occur. Only the adsorption process took place.

It is known that functional alkaline groups on the activated carbon surface possess catalytic activity [3]. The concentration of the functional alkaline and acid groups on the surface of the activated carbon CAN-8 is presented in Table 1.

Table 1

Ionic exchange capacity of the activated carbon CAN-8 and the pH values of the water extract

Nr.	Type of AC	Cs / alkaline mg- equiv/g	Cs / acid mg -equiv/g	pH
1	CAN-8. (nutshells)	0.555	0.139	7.0

The data in Table 1 clearly point out the predominance of alkaline groups on the surface of the intact activated carbon CAN-8.

It is mentioned in [3] that the formation of alkaline oxides is accompanied by the formation of hydrogen peroxide.

Table 2 shows the data regarding the structural parameters of the activated carbon CAN-8 (the specific surface S_{BET}, the surface of mesopores S_{Me}, the volume of the micropores W_0, the characteristic energy E_0, the semi-width of crevice-shaped micropores X_0).

Table 2

Structural parameters of the activated carbon CAN-8.

Nr.	Type of AC	S_{BET} m^2/g	S_{Me}, m^2/g	W_0, cm^3/g	E_0, kJ/mol	X_0, nm
1	CAN-8.(nutshells)	708	166	0,35	22,41	0,45

The data shown in Tab. 2 indicate a high value for the surface of the mesopores of the activated carbon CAN-8, which is very important in the case of potential utilization of such an adsorbent in catalytic processes.

Table 3 shows the quality indices of the studied adsorbent, obtained from the adsorption isotherm of methylene blue, iodine and benzene vapors.

Table 3

Indices of quality of the activated carbon CAN-8, obtained from the adsorption isotherm of methylene blue, iodine and benzene vapors.

Nr.	Type of AC	Indices		Vs (the exicator method) cm^3/g
		I_2(mg I_2/g)	AM (mg /g)	
1	CAN-8.(nutshells)	1095,6	300,33	0,62

The data presented in Tab. 3 show a high adsorption capacity of the investigated activated carbon.

Fig.1. shows the UV/Vis spectrum of the initial methylene blue and of that subjected to catalytic oxidation, in the presence of the intact activated carbon CAN-8 and oxygen at 50°C.

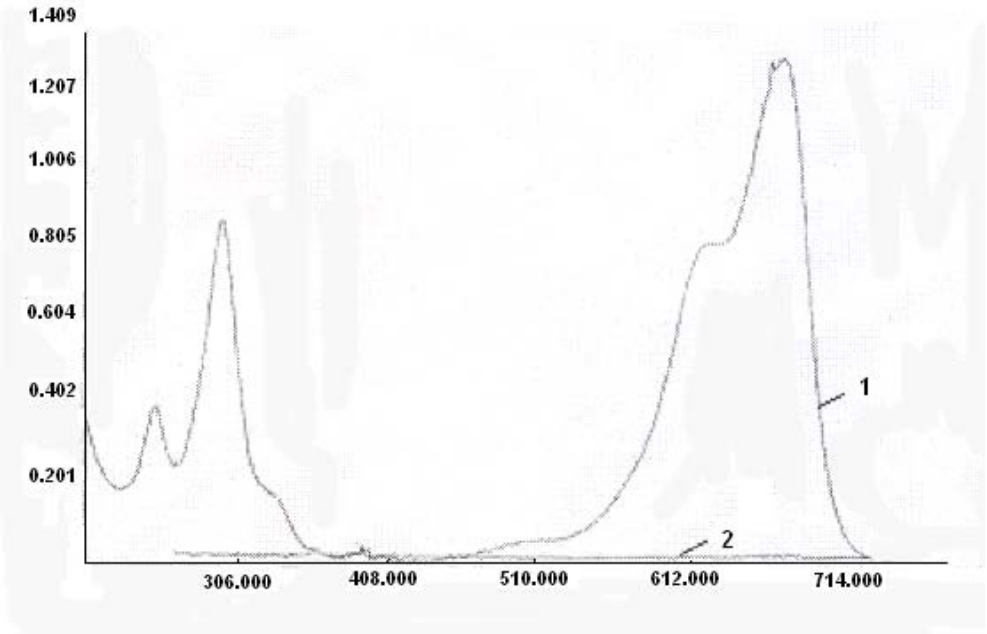

Fig.1. UV/Vis spectrum of methylene blue: (1) initial 20mg/L solution and (2) after the oxidation process.

Figure 1 points out the result of the complete catalytic oxidation of methylene blue. The band at 290 cm^{-1} completely disappeared, as well as all other bands in the visible region. As a result of purging oxygen through the solution containing methylene blue, the intact activated carbon CAN-8, the methylene blue is adsorbed on the surface of the adsorbent, just as the oxygen, which leads to the appearance of a potential jump at the adsorbent-solution frontier. This is due to the oxygen electrode on the surface of the activated carbon, which confers it properties of an oxidation catalyst [4]. As a result, the activated carbon acquires a positive charge and thus, the accumulation of hydrogen peroxide, as an intermediary product, at the contact surface activated carbon-solution, becomes possible [5]:

$$O_2(ads) + 2H_2O + 2e \rightarrow H_2O_2 + 2OH^- \quad (1)$$

$$H_2O_2 \rightarrow 2OH^{\cdot} \quad (2)$$

$$2OH^{\cdot} + 2e \rightarrow 2OH^- \quad (3)$$

It is well known that hydroxyl radicals $OH^{\cdot}$ easily attack organic compounds, due to their high reactivity, and transform it into simple compounds which, eventually, may be mineralized to CO_2, H_2O and mineral species [6]. Generally, due to the fast reaction of the hydroxyl-radical in oxidizing processes, the advanced oxidation technology is characterized by an increased reaction rate and a reduced treatment time.

It is possible that the $OH^{\cdot}$ radical, along with functional alkaline groups on the surface of the intact activated carbon CAN-8, plays a role in the process of oxidation of methylene blue. In any case, after 25 cycles of methylene blue oxidation, the number (concentration) of alkaline functional groups on the surface of the intact activated carbon CAN-8 decreased from 0.55 mg-equiv/g to 0.05 mg-equiv/g, and the duration of the oxidation process was ~ 10 min for each cycle. Authors mention in [7] the possibility of formation of various forms of adsorbed oxygen during its transformation from mobile forms, obtained in the first stage of the adsorption process, into strictly fixed forms which appear during longer interactions, or somewhat higher temperatures.

It should be mentioned that the $OH^{\cdot}$ radical, having an oxidation potential of 2.8 V, which is higher than the oxidation potential of ozone (2.07 V), may oxidize sodium dodecylsulfate to CO_2 and H_2O [8].

Fig. 2 presents the NMR spectrum (400 megacycles) of methylene blue oxidized with intact activated carbon CAN-8 in the presence of oxygen at 2 atmospheres, for 2 hours, at 50^0 C. The NMR spectrum of intact methylene blue is shown in Fig. 3.

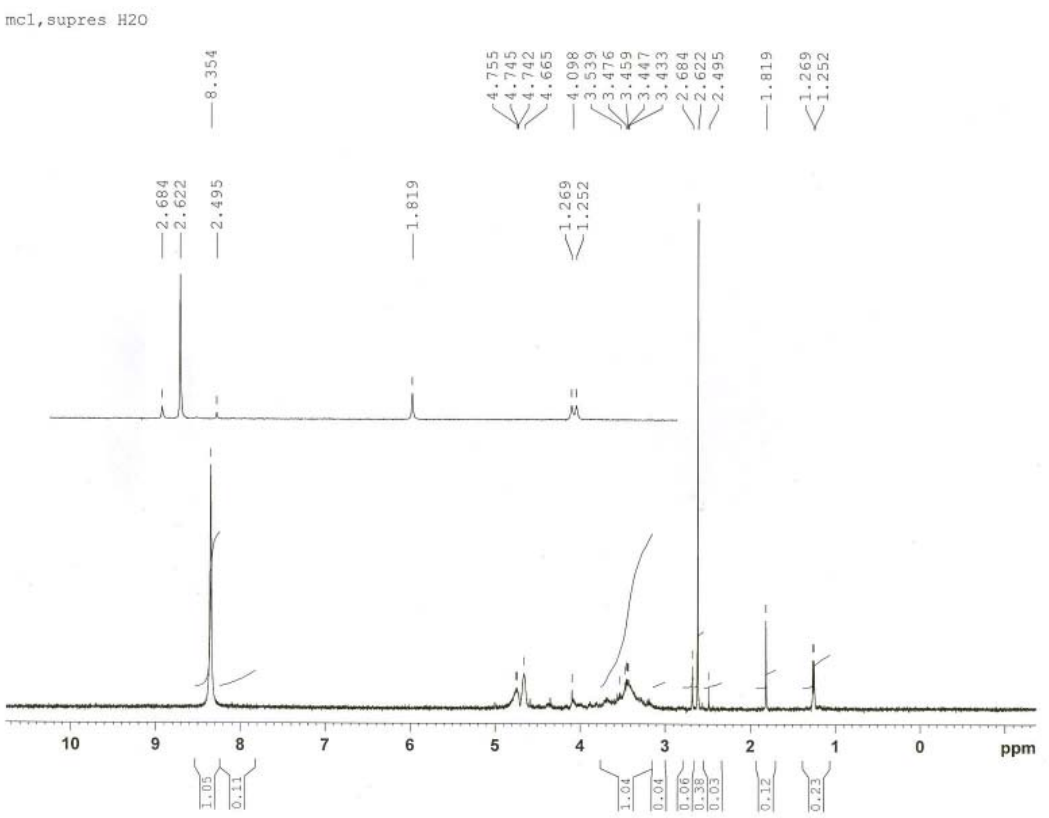

Fig.2. NMR spectrum of oxidation products of methylene blue in the presence of intact activated carbon and oxygen purging (pressure of 2 atmospheres) at 50^0 C.

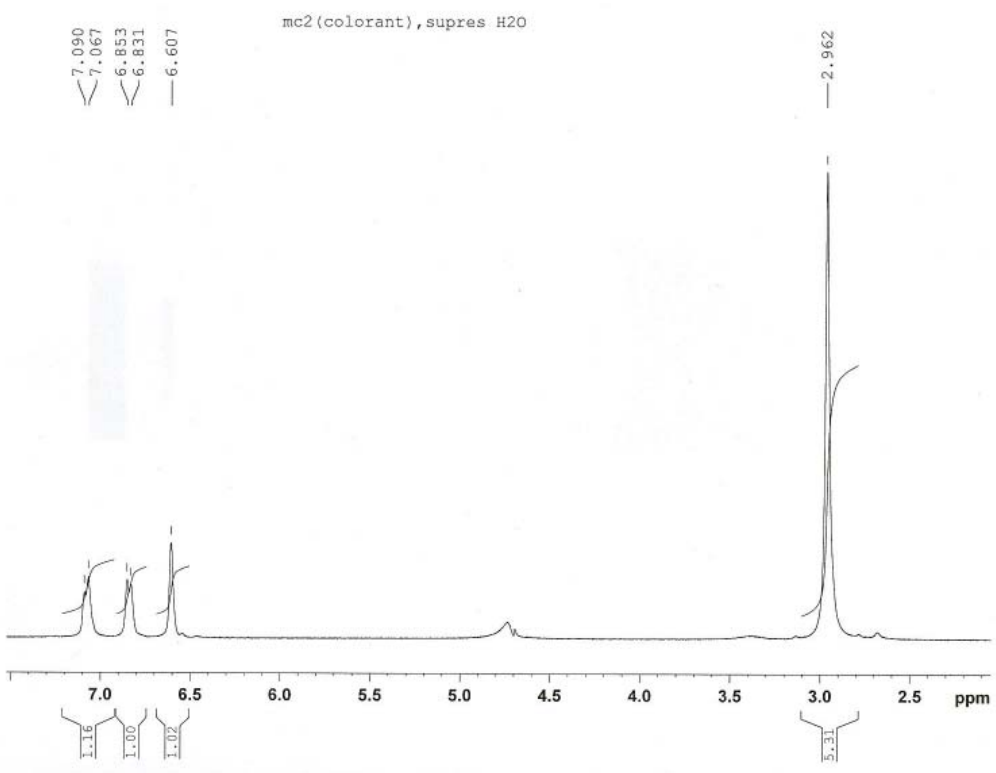

Fig. 3. NMR spectrum of methylene blue.

Figures 2 and 3 clearly indicate that as a result of the catalytic oxidation of methylene blue, the substance undergoes transformations and several organic structures remain in the solution.

Conclusions

1. The intact activated carbon CAN-8, obtained from nutshells using the physico-chemical method under experimental conditions, possesses catalytic activity, which is due to the presence on the intact activated carbon of functional alkaline groups, as well as to the formation of the $OH^{\cdot}$ radical at the interface, which has a high oxidation potential.
2. Catalytic performance of the intact activated carbon CAN-8 in the process of methylene blue oxidation was displayed during 25 cycles, and it was acknowledged that the content of alkaline groups on the surface of the activated carbon diminished significantly after the last cycle – from 0.55 mg-equiv/g to 0.05 mg-equiv/g, without significant decrease of its catalytic activity.
3. As a result of the process of methylene blue oxidation, fragments are obtained from the initially studied organic substance.

References

[1]. Zhang Weixin Yang. Process for treating waste water of metylene blue dye and process for preparing catalyst. C02F 1/72; B01J 23/34; C01G 45/02; (+5). CN 1792866 (A) – 2006 – 06-28.
[2]. H.S.Silva, N.D.Martinez, A.C.Deiana, J.E. Gonzalez. Catalytic oxidation of methylene blue in aqueous solutions. – 2nd Mercosur Congress on Chemical Engineering. 2005. p. 1-8.
[3]. Roop Chand Bansal, Jean-Baptiste Donnet, Fritz Stoeckli. Active Carbon. Marcel Dekker, INC. New York and Basel. 1988. p.107.
[4]. В.В.Стрелко, Н.Т.Картель, Л.А.Клименко, К.А. Каздобин. Электрохимические свойства углеродных гемосорбентов. – ЖПХ, №6, 1987. с.1257-1260.
[5]. А.И.Анурова, В.С. Даниель-Бек, А.Л.Ротинян. – Электрохимия, 1968, т.4, №7, с.815-821.
[6]. Rein Munter. Advanced oxidation processes – current status and prospects – Proc. Estonian Acad.Sci.Chem., 2001, 50, 2, 59-80.
[7]. А.Н.Фрумкин. Адсорбция и окислительные процессы. - Успехи химии. 1949. т.18,вып.1, с. 9 – 21.
[8]. Н.М.Панич, А.Ф.Селиверстов, Б.Г.Ершов. Фотоокислительное разложение додецилсульфата натрия в водных растворов. – Ж.П.Х., 2008, т.81, вып.12. с. 1991-1995.

THE POLLUTION SPECTRUM OF OLD PESTICIDES STORAGES IN MOLDOVA

Duca Gh., Bogdevich O.*, Cadocinicov O., Porubin D.

Academy of Science of Moldova, 1 Stefan cel Mare str., Chisinau, Moldova
**Email: bogdevicholeg@yahoo.com*

Abstract. The old pesticide storages in Moldova showed a large quantity of polluted sites. The inventory of POPs polluted sites showed a huge number of extra high polluted sites (more 50,0 mg/kg) which need the first place a remediation or other action to eliminate direct contact with people and animals. The pollution spectrum of POPs is a complex and consists of five groups: DDTs isomers, HCHs isomers, Toxaphene mixture, Chlordane and Heptachlor. The principal groups among these substances are DDTs and HCHs isomers.

Keywords: soil pollution, POPs, PAHs, pesticides

Introduction

The inventory of old pesticide storages in Moldova executed by Ministry of Environment and World Bank showed a large quantity of polluted sites (near 1500) remains after the repacking and evacuation project [1,2]. This work was made first of all for Persistent Organic Pollutants (POPs). More that 15 % sites were determined as extra high polluted territory with the POPs concentration in soil more 50,0 mg/kg. They include some of the world's most harmful chemicals including highly toxic pesticides such as HCH, DDT; industrial chemicals such as PCBs. The management of domestic and hazardous wastes is considered as one of the most urgent environmental problems in Moldova. Old pesticide storages are in different conditions and can be classify as important pollution sources for environment. Other toxic substances were detected also in soils which are in list of monitoring substances of Water Framework Directive: PAHs, trifluralin, triazines and others. They are synthetic chemical substances with high toxic characteristics to wildlife and humans. However the information about the actual status and complete pollution spectrum is not sufficient at present. This investigation is important also for the assessment what remediation technologies can be used for the future soil detoxication.

The aim of the study was an assessment of the pollution spectrum in soil at obsolete pesticide storages. This objective was realized by the determination of different type of pollutant in Gas Chromatographs equipped with μECD and mass selective detectors.

Analytical procedure

Sampling

Samples will be collected according to the Standard Guide for Composite Sampling and Field Sub-sampling for Environmental Waste Management Activities, EPA's Guidance for Choosing a Sampling Design for Environmental Data Collection, EPA QA/G-5S (USEPA 2000c), and other standardized procedures [3-8].

Extraction and clean up.

The extraction and analytical procedures were made by appropriate normative documents [9-13]. Prior to the extraction, the soil samples (1 g) were spiked with 1 ml of the solution of two internal standards (PCB29 and DCB) of appropriate concentration in the final solution. Extraction was carried out by Microwave Extraction System in the mixture of hexane-acetone (proportion 1:2, 20 ml) three times. After cooling down, the extracts were collected in the glass condenser and concentrated in n-hexane to a volume of 1 ml. The extracts were cleaned up on adsorption chromatography columns filled up with 1 g of activated silica gel (activated at a temperature of 135^0 C for 16 hours. The column was conditioned with 5 ml of hexane. Interested substances (PAHs and POPs) were eluted from column with 5 ml of n-hexane, followed by 5 ml of n-hexane/dichloromethane mixture (1:1). Final elutes were evaporated in argon flow to 1 ml. Sulfur interference was removed by Cupper powder activated in nitric acid.

Analytical determination.

All reagents (solvents, standard solutions, anhydrous sodium sulfate, and pure gases) were of the pesticide grade purchased from Supelco-Aldrich. Agilent 6890 gas chromatograph equipped with 63Ni μECD detector, split–splitless injector, and capillary column HP5 were used for the pesticide analysis. PAHs and trizines analysis were performed on an Agilent 6890 gas chromatograph equipped with Agilent 5973 Mass Spectrometer (CG/MS 6890/5973) based on the

selected ion monitoring system (SIM) of molecular ion peaks and associated characteristic fragment ion peaks. Method conditions are presented in tables (1-4).

Instrument calibration parameters included calculation of the sensitivity (I-SE) as the slope of calibration curve at P-value < 0,05, linearity (I-LI) as a correlation coefficient for the calibration regression line and the instrument detection limit (IDL) corresponding to 3SD (standard deviation) of five replication of the lowest standard solution.

Table 1.

Experimental Conditions for pesticide determination in GC 6890

System elements	Method parameters
Injection ports	Split/splitless inlet; injection – Split 5:1, 2 µl, inlet temperature of 300°C
Column	HP-5: 30 m Length, 320 µm I.D., 0,25 µm Film, max 325^0 C
Carrier gas	He, 1,4 ml min^{-1} or Average Velocity 30 cm/sec, Constant Flow
Oven	First ramp: 100°C (hold 1 min) to 200°C at 20°C min^{-1} hold 2 min; Second ramp: 200°C to 280°C at 10°C/min, hold time 2 min.
Detector	63Ni µECD, 320^0 C, N2 makeup gas, 60 ml min^{-1}
Data collection	ChemStation

Table 2.

Experimental Conditions for PAHs and triazines determination in CG/MS 6890/5973

System elements	Method parameters
Injection	Autosampler Agilent 7683 B
Injection ports	Split/splitless inlet; injection – Splitless (keeping the split closed for 1.0 min), 1 µl, inlet temperature of 300°C
Column	HP-5MS: 30 m Length, 320 µm I.D., 0,25 µm Film, max 325^0 C.
Carrier gas	He, 1,5 ml min^{-1} or Average Velocity 46 cm/sec, Constant Flow
Oven	First ramp: 120°C (hold 1 min) to 200°C at 20°C min^{-1}; Second ramp: 220°C (hold 1 min) to 290°C at 5°C/min, hold time 2 min.
Detector	Mass detector, EI 70 eV, quadropole 150^0 C, SIM
Data collection	ChemStation

Results

Five POPs compound groups namely ∑ DDT, ∑ HCH, Chlordane, Heptachlor and Toxaphene have been found in soil samples taken at investigated sites, in concentrations exceeding the national standard for organochlorinated substances in soil (0.1 mg/kg). Six DDTs isomers, three HCHs isomers, and Toxaphene as a mixture of approximately 200 organic compounds were analyzed in soil and waste samples. The pollution of POPs sites with DDT (88,2%) and – to lesser extent – with HCH (74,9%) can be defined as widespread. The share of sites contaminated with Chlordane (31%) and Heptachlor (22,7%) is also significant. The less number of sites are polluted by Toxaphene mixture (10,2%), but this pollution is characterized usually by high level. Aldrine, Dieldrine, Endrine, HCB and Mirex were not detected in the investigated samples. The acquired data showed a severe level of soil contamination with DDTs and HCHs at some sites, in the order of hundreds and even thousands of mg/kg.

Table 3

GC/MS calibration parameters for PAHs and triazines determination

Nr	Name	Mass ion	ISE	ILI	IDL ng/ml
		PAHs			
1	Naphtalene	128	2.71	0.999	4.0
2	Acenaphtylene	152	3.01	0.999	1.2
3	Acenaphtene	152	2.57	0.999	0.5
4	Fluorene	166	2.15	0.999	0.5
5	Phenanthrene	178	3.03	0.999	0.4
6	Antracene	178	3.05	0.999	1.0
7	Fluoranthene	202	3.41	0.999	2.5
8	Pyrene	202	3.49	0.999	2.1
9	Chrysene	228	3.28	0.999	2.0
10	Benz[a]anthracene	228	3.22	0.999	2.1
11	Benzo[b]fluoranthene	252	3.51	0.999	3.5
12	Benzo[k]fluoranthene	252	3.86	0.999	2.2
13	Benz[a]pyrene	252	3.33	0.999	2.0

14	Benz[ghi]perylene	276	3.26	0.999	2.2
15	Dibenz[ah]anthracene	276	4.14	0.999	2.5
16	Indeno[1,2,3-cd]pyrene	276	3.7	0.999	2.5
Triazines					
1	Ametryn	227	3.15	0.996	3.4
2	Atrazine	215	4.15	0.998	2.5
3	Prometon	225	3.25	0.995	4.1
4	Prometryn	241	3.42	0.995	3.2
5	Propazine	229	3.54	0.997	3.5
6	Simazine	201	4.25	0.998	2.5
7	Terbutryn	241	3.64	0.996	3.8

Table 4

GC calibration parameters for organochlorine pesticides determination

Nr	Name	Range of standards, μg/ml	ISE	ILI	IDL ng/ml
1	Trifluralin	0.20 – 2.00	0.40	0.999	2.0
2	a_BHC	0.05 – 0.50	2.16	0.998	1.6
3	b_BHC	0.20 – 2.00	0.38	0.998	1.5
4	g_HCH	0.05 – 0.50	1.76	0.998	1.2
5	Heptachlor	0.15 – 1.50	0.36	0.995	2.5
6	Aldrine	0.10 – 1.00	2.14	0.998	1.8
7	Chlordane	0.20 – 2.00	0.52	0.998	2.9
8	o-p-DDE	0.20 – 2.00	1.34	0.999	3.5
9	p,p-DDE	0.20 – 2.00	1.38	0.998	3.6
10	Dieldrine	0.23 – 2.30	1.68	0.998	3.2
11	o,p-DDD	0.38 – 3.80	0.74	0.996	4.5
12	Endrine	0.40 – 4.00	1.20	0.996	4.0
13	p,p-DDD	0.40 – 4.00	0.67	0.996	3.5
14	o,p-DDT	0.50 – 5.00	0.75	0.996	4.2
15	p,p-DDT	0.40 – 4.00	1.09	0.997	4.5
16	Mirex	0.20 – 2.00	0.91	0.999	3.5

Some part of site is polluted by several groups of compounds. The toxicology impact on these sites is higher in the case of synergism of different toxicants. The distribution of high polluted sites (more 50,0 mg/kg) by POPs compounds are following: 144 sites are polluted by one substance; 48 sites – by two substances; 9 sites – by three substances, and 3 sites – by four POPs. Actually there are 252 POPs polluted sites with the concentration more that 50.0 mg/kg (15,9 % of total 1589 sites).

Sites with high POPs concentration (more 50,0 mg/kg) have a additional complex pollution by Trifluraline (85%) triazines (64%) and PAHs (33%). Some sites with relative low POPs pollution have high concentration of these substances. Near 10% of investigated site have high pollution (more 50,0 mg/kg) by other toxic substances which are not included in the inventory program. From other site determined pollutants also have high toxicity and should be monitored.

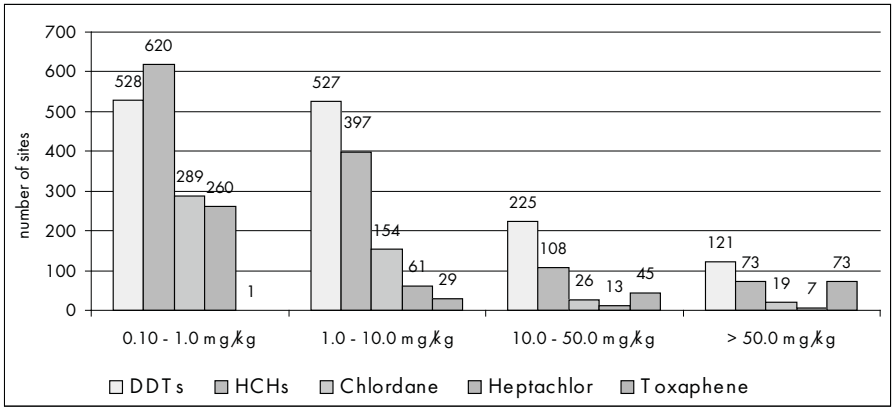

Figure 1. Distribution of POPs polluted sites by pollution clusters

The interpretation of this large set of analytical results and wide interval of concentration may become easier by showing their distribution (assuming distribution is lognormal) in a few clusters: 0.10 – 1.0 mg/kg; 1.0 – 10.0 mg/kg; 10.0 – 50.0 mg/kg; and > 50.0 mg/kg. The distribution of five investigated groups by pollution clusters gives a better understanding of the extent and severity of contamination (Fig. 1 and 2).

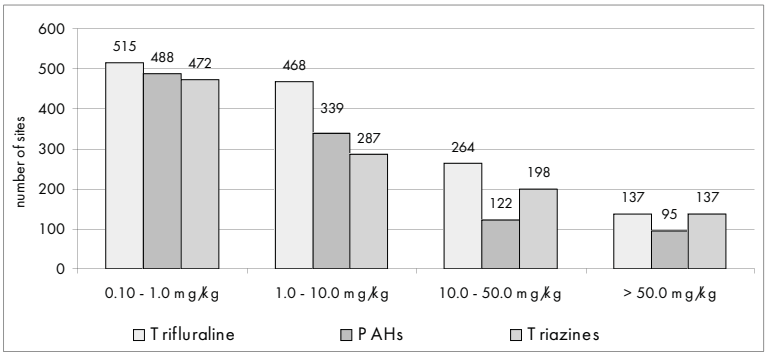

Figure 2. Distribution of polluted sites with other toxic substances by clusters

The spatial distribution of old deposits ranges with the different pollution level in soil is presented on figure 3. This map is illustrated total POPs concentration in complex soil samples. The density of high polluted sites is higher for raions with more intensive fruit production. 18 raions have more that 15% of extra high pollution sites (figure 4).

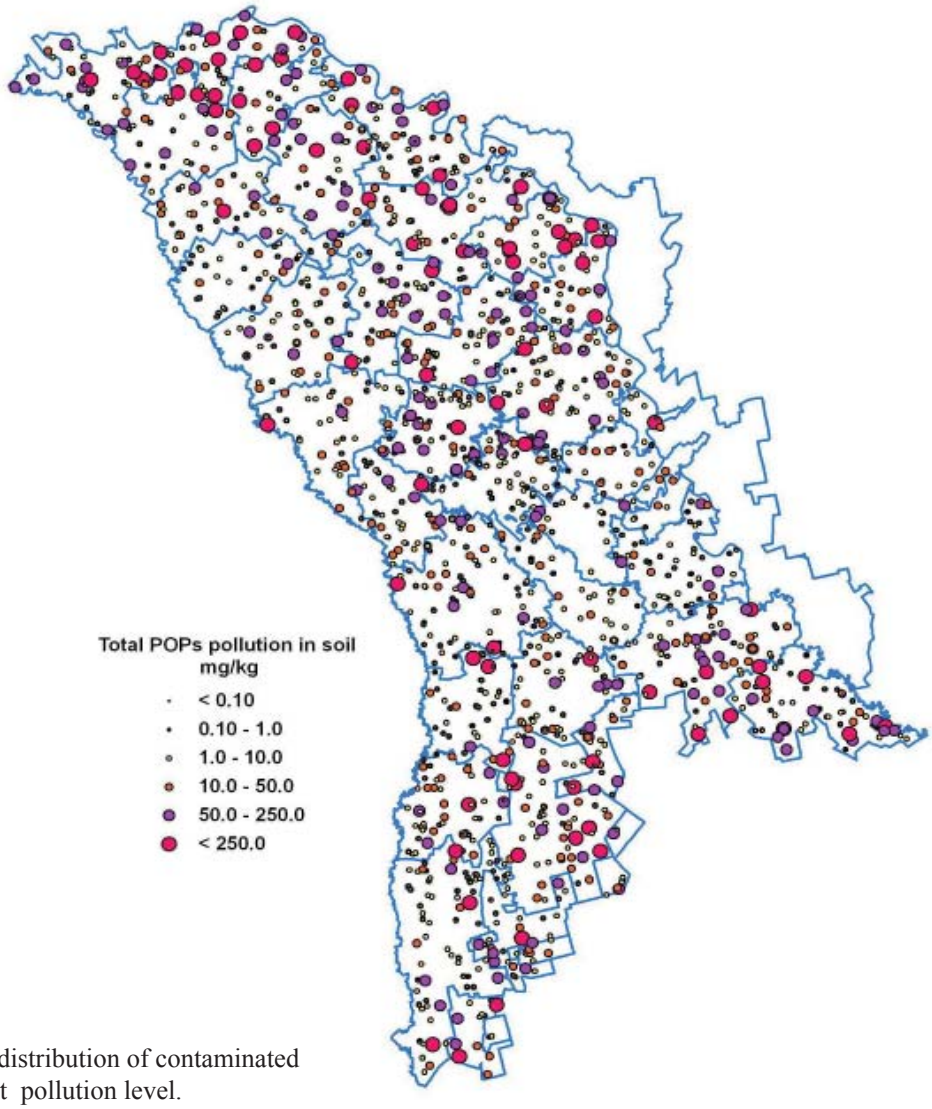

Figure 3. Spatial distribution of contaminated sites with different pollution level.

The polluted soil with concentration more 50,0 mg/kg can be classify as hazardous waste. This fact means these sites should to be protected first from the population access and recommended for the remediation to minimize direct contact with animals and people. The sampling of these sites confirmed indirectly a relative big volume of the toxic waste residuals on old pesticide storages

Conclusions

1. The inventory of POPs polluted sites showed a huge number of extra high polluted sites (more 50,0 mg/kg) remained after repacking projects in Moldova which need the first place a remediation or other action to eliminate direct contact with people and animals.

2. The pollution spectrum of POPs is a complex and consists of five groups: DDTs isomers, HCHs isomers, Toxaphene mixture, Chlordane and Heptachlor. The principal groups among these substances are DDTs and HCHs isomers.

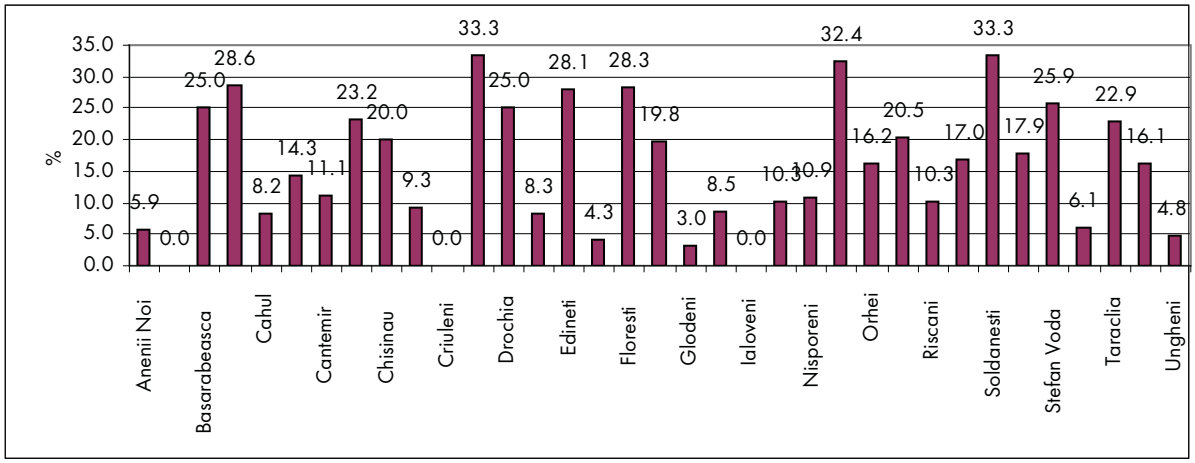

Figure 4. Distribution of high POPs polluted sites (> 50,0 mg/kg) by raions in Moldova.

3. The pollution spectrum is characterized also by other toxic substances as triazines, trifluraline, PAHs and others, which were not analyzed in this study. Determined pollutants are included in normative documents for the monitoring of water quality (Water Framework Directive of EU, etc).

4. The database of POPs polluted sites was created by inventory project in Moldova but this information needs in the development for other pollutants and classification for risk level for environment;

5. The character of pollution spectrum demonstrates a complex character of future remediation and other action by the elimination of negative impact from polluted sites to environmental and public health.

Acknowledgements. The research is made in the frameworks of the project "Creation of the Center for the control and water quality monitoring" of the State Program "Scientific and Management Researches of Water Quality" of the Academy of Sciences of Moldova.

References

[1]. National Implementation Plan for the Stockholm Convention on Persistent Organic Pollutants (2004) Ministry of Ecology and Natural Resources of the Republic of Moldova, 80 pp.

[2]. Environmental Impact Assessment And Environmental Management Plan (2005) Ministry of Ecology and Natural Resources of the Republic of Moldova, GEF PAD Grant for Preparation of Sustainable Persistent Organic Pollutants (POPs) Stockpiles Management Project, 179 pp.

[3]. Assessing Soil Contamination. Reference Manual (2000) FAO. United Nations 232 p.

[4]. Risk Assessment Guidance for Superfund. (2002) EPA/540/1-89/002 December 1989 Vol I, Human Health Evaluation Manual, 17 pp.

[5]. Guidance for Comparing Background and Chemical Concentrations in Soil for CERCLA Sites. (2002) EPA, 540-R-01-003

[6]. RCRA Waste Sampling Draft Technical Guidance Planning, Implementation, and Assessment. (2002) United States, Environmental Protection Agency, Solid Waste and Emergency Response (5305W), EPA530-D-02-002, Office of Solid Waste www.epa.gov/osw

[7]. Pre-Acquisition Environmental Site Assessment Guidance Manual (1999) National Park Service, Washington, DC 20013
[8]. Environmental Risk Assessment Manual (2008) Scottish Environment Protection Agency Issue 10.1, 94 pp.
[9]. EPA Method 3500B: Organic Extraction and Sample Preparation
[10]. EPA Method 8081A (1996) Organochlorine Pesticides by Gas Chromatography, 44 pp.
[11]. SMV ISO 10382: 2002 Soil quality. Determination of organichlorine pesticides and polychlorinated biphenyls. Gas-chromatographic method with electron captures detection.
[12]. ISO 18287:2006 Soil quality -- Determination of polycyclic aromatic hydrocarbons (PAH). Gas chromatographic method with mass spectrometric detection (GC-MS).
[13]. SM GOST R 51209: 2006 Вода питьевая. Метод определения содержания хлорорганических пестицидов газожидкостной хроматографией.

MODIFIED SCREEN-PRINTED CARBON ELECTRODES WITH TYROSINASE FOR DETERMINATION OF PHENOLIC COMPOUNDS IN SMOKED FOOD

V. Dragancea[1]*, R. Sturza[1], M. Boujtita[2]

[1]*Technical University of Moldova, MD 2004, 168, Stefan cel Mare, Chisinau, Moldova*
tel: (3732-2) 31-90-82, Email: veronicadragancea@yahoo.fr
[2]*CEISAM, Université de Nantes, CNRS, 2 rue de la Houssinière, B.P. 92208, 44322, Nantes, FRANCE*

Abstract: A screen-printed carbon electrode modified with tyrosinase (SPCE-Tyr/Paa/Glut) has been developed for the determination of phenol concentration in real samples. The resulting SPCE-Tyr/Paa/Glut was prepared in a one-step procedure, and was then optimized as an amperometric biosensor operating at 0 mV versus Ag/AgCl for phenol determination in flow injection mode. Phenol detection was realized by electrochemical reduction of quinone produced by tyrosinase activity. The possibility of using the developed biosensor to determine phenol concentrations in various smoked products (bacon, ham, chicken and salmon) was also evaluated.
Gas chromatography (GC) method was used for result validation obtained in flow injection mode using amperometric biosensor. The result showed good correlation with those obtained by flow injection analysis (FIA).

Keywords: screen-printed carbon electrode SPCE; biosensor; phenol; tyrosinase; gas chromatography.

1. Introduction

Quality evaluation of smoked products is needed because of the wide range of quality of these products on the market. Several previous studies of smoke or smoked foods included estimates of total phenolic compounds [1]. Phenolic derivates are very important compounds in smoked products.

The determination of phenol and its derivative compounds are important for the environment because these substances are toxic and are a result of various industrial processes. They are present in any wastewater streams, resulting of the oil, paint, polymer and pharmaceutical processing industries [2]. Ingestion of phenol and cresol causes intense burning of mouth and throat, followed by marked abdominal pain and distress. Phenol is considered to be very toxic to humans through oral exposure; ingestion of 1g are reported to be lethal with symptoms including muscle weakness and tremors, loss of coordination, paralysis, convulsion, coma, and respiratory arrest [3].

The detection of mono- and polyphenols is usually carried out by HPLC and/or spectrometry methods [4]. However, these methods are used with sample pretreatment and unsuitable for “in situ” monitoring. Many efforts have been made for simple and effective determination of phenol to solve these problems. Electrochemical methods have been widely used for measuring these compounds due to their advantages such as good selectivity in presence of phenol oxidizes, relatively low-cost of realization and storage and the potential for miniaturization and automation [5-7].

Enzymatic biosensors arrays represent promising prescreening method for rapid and simple measurements and express analysis of many pollutant phenols derivatives. Biosensors based on tyrosinase have proved to be sensitive and convenient tools for this purpose.

Various methods have been reported for the immobilization of tyrosinase on different suitable substrates. These reports have employed conventional electrode materials as substrates, such as glassy carbon [8-9], graphite-epoxy resin [10], gold [11] and other materials [12-14], etc. However, tyrosinase-based electrochemical biosensors on some substrates suffer from low stability and significant inhibition of enzyme by reaction products; both these factors deteriorate electrode characteristics in phenolic compounds determination [15]. One of the major causes of poor stability is desorption of enzyme from electrode materials. Therefore, the search for reliable methods or electrode substrates that would be a strong and efficient bonding of tyrosinase is still interesting. The aim of this study is to apply an analytical technique for determination of volatile phenolic derivatives in traditional smoked meat.

2. Results and discussion

2.1. Optimization of Membrane

The starting point for the tyrosinase biosensor development was the study of its electrochemical behaviour in the cyclic voltammetry. The electroenzymatic effect of the modified electrode was examined in the presence and absence of the phenol in the buffer phosphate solution. In figure 1 there are represented three voltammograms: the voltammogram 1

represents the behaviour of a bare screen-printed electrode in the presence of phenol solution and voltammograms 2 and 3 show the behaviour of a screen-printed electrode modified by tyrosinase in the absence (2) or presence (3) of phenol. Adding the phenol in the solution leads to a change in the shape of the voltammogram.

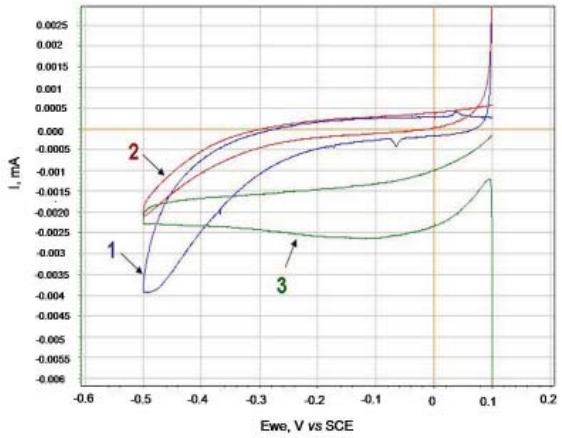

Fig. 1. The Voltammograms were performed on a bare screen-printed electrode (1) and modified by tyrosinase (2 and 3) in the absence (2) and presence of phenol (1 and 3). The scan rate of 5 mV/s, Phosphate Buffer (0.1 mol / L, pH = 6.0 + KCl 0.1 mol / L). C (Phenol) = 1 mmol / L

In the initial potential (0.1 V) there is a reduction current which shows the formation of quinone as a result of phenol oxidation by tyrosinase.

In order to find an optimal composition of the used membrane and to increase the analytical performance of the biosensor in terms of sensitivity and operational stability, a range of experiments were used. For the choice of parameters (factors) to study, it was decided to vary the tyrosinase, the PAA and the Glut that seemed to be able to affect the response of the biosensor. The effect of these three factors and their interactions were assessed at two levels denoted minimum (low) '− 1' and maximum (high) '+1'. These levels were selected to build this plan of experiments that are based on various preliminary work and the results obtained previously for electrodes already tested in the laboratory. The code and levels fixed for each factor are displayed in Table 1.

Table 1

Factor and Levels Used in the Factorial Design for Biosensor Optimization

	Variable	Low level (- 1)	High level (+1)
1	Tyrosinase (Tyr), mg/ml	2,5	5,0
2	Polyallylamine (Paa),%	0,025	0,05
3	Glutaraldehyde (Glut), %	0,0125	0,025

The organization of the needed achieved manipulations for a comprehensive plan 2^3 is summarized in Table 2.

Table 2

Design Matrix and Responses for Biosensor Optimization

Experiment	Factor 1	Factor 2	Factor 3	Response
1	-	-	-	y_1
2	+	-	-	y_2
3	-	+	-	y_3
4	+	+	-	y_4
5	-	-	+	y_5
6	+	-	+	y_6
7	-	+	+	y_7
8	+	+	+	y_8
Effect	$\mathbf{E_1}$	$\mathbf{E_2}$	$\mathbf{E_3}$	

To solve the plan of experiments we proceed and calculate the effects of each factor and the interactions on each response (sensitivity, operational stability). The value of effects is obtained by calculation in three steps:

Step 1: Multiplying each response by the sign of the corresponding column of the matrix effects;

Step 2: multiplying the obtained results;

Step 3: dividing by the number of experiments (8).

If the calculated effect (or interaction) is the same order of magnitude as the error, it may or may not influence the response. The significance of effects has been evaluated using Student-test in which *t* values are calculated by dividing the effect values E_i by the standard error σ_E which has been evaluated using the standard error σ_k on the response obtained for each run ($k \in [1,8]$) according to the following equation :

$$\sigma_E = \frac{\sigma_y}{\sqrt{16}} \quad \text{avec} \quad \sigma_y = \sqrt{\frac{1}{8}\sum_k \sigma_k^2}$$

In this way, eight types of electrodes are provided.

In conclusion, the effects of the three parameters studied on the electrode performance can be presented as follows:

- Increasing the amount of used tyrosinase influences significantly the sensitivity of the electrode;
- Increasing the rate of Paa in the membrane induces an increase in the operational stability of the biosensor;
- The simultaneous increase of Paa and that of tyrosinase improves measurement repeatability;
- The decrease in Glut improves the linearity of the modified electrode and operational stability.

Table 3

Principal and Interactions effect values for 2^3 factorial

Effects and Interactions on the Sensitivity

	Average	38,47
E_1=1	1 (Tyr.)	10,63
E_2=2	2 (Paa)	-1,23
E_3=3	3 (Glut.)	2,94
E_{12}=12	12	-2,62
E_{13}=13	13	4,67
E_{23}=23	23	2,57
E_{123}=123	123	0,58
		Erreur-type on the effect : 0,5905

Effects and Interaction on the operational stability of Electrodes

	Average	3,0250
E_1=1	1 (Tyr.)	**0,6425**
E_2=2	2 (Paa)	**-0,5625**
E_3=3	3 (Glut.)	-0,2138
E_{12}=12	12	**-0,4425**
E_{13}=13	13	-0,0013
E_{23}=23	23	-0,2163
E_{123}=123	123	-0,2113
		Erreur-type on the effect : 0,2675

Given the results of experimental sessions, it was chosen to modify the electrodes from the mixture with test 4 in the matrix of experimental design.

- Tyrosinase 5mg/ml (equivalent of 16 unities)
- Paa - poly (allylamine), 0,05%;
- Glutaraldehyde (Glut), 0,0125%.

This composition gives a better compromise between sensitivity and operational stability. The modified electrodes are prepared by putting manually on the working electrode a solution composed of these three compounds mixed in equal volumes (50μL)

2.2. Influence of Applied Potential

The use of the modified electrode with tyrosinase for the detection of phenol in flow injection analysis necessitated the search for optimum conditions of analysis. We studied the potential, the pH and the organic solvent influences on the biosensor response.

In order to determine the choice of potential, the current response of the biosensor for a phenol concentration of 0,050 mmol/L was measured in the comprised potential range between -0.3 and + 0.3V/Ag/AgC1, a throughput and a constant injection volume.

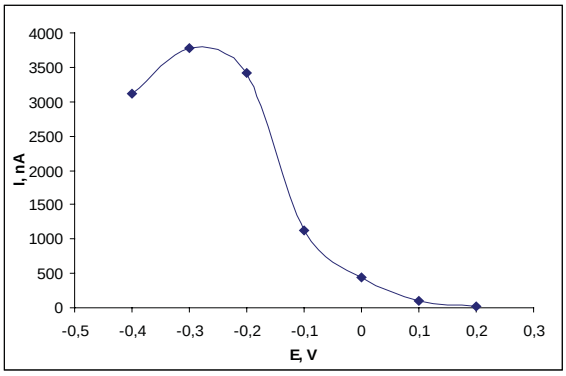

Fig. 2. Influence of applied potential on amperometric response of the SPCE-Tyr/Paa/Glut in the Flow injection analysis. Phosphate buffer (0.1 mol/ L, pH=6)

It was found that the maximum reduction current is at a potential of E =- 0.3V (Figure 2). Furthermore, it was found out that although the biosensor sensitivity has a maximum potential of -0.3 V versus Ag/AgC1, however this has some potential drawbacks such as the time required to stabilize the baseline. Approximately two hours are needed for the baseline to stabilize when the working potential is set at - 0.3 V and about 1 hour at a potential of -0.1 V. This relatively long, waiting time to obtain a stable baseline is incompatible with a rapid method. In order to obtain a potential value of 0 V, it has been determined that only 5 to 7 minutes are required to obtain a stable baseline with very low background noise. Also, it must be noted that at 0 V, the reactions of electrochemical reduction of oxygen are minimized. For further experiments and to minimize the base current, it was chosen to conduct a study to a potential value of 0V / Ag / AgCl.

2.3. pH-dependence

The kinetics of an enzymatic reaction is always dependent on the pH value in the enzyme environment. For this reason, we examined the influence of this parameter on the response of amperometric biosensor.

The isoelectric point of tyrosinase is located around pHi = 4.7 - 5, it was chosen to conduct the study between pH values of 4 and 8, for a 0,050 mmol/L phenol concentration. The figure 3 shows the variation of the current function in comparison with the environment reaction's pH. The dependence presents a bell–characteristic shape with a maximum response for pH values between 5.5 and 6.5. An optimal amperometric response at pH 6.0 was obtained. Then for the tyrosinase electrode, a pH value of 6 for the analysis was chosen.

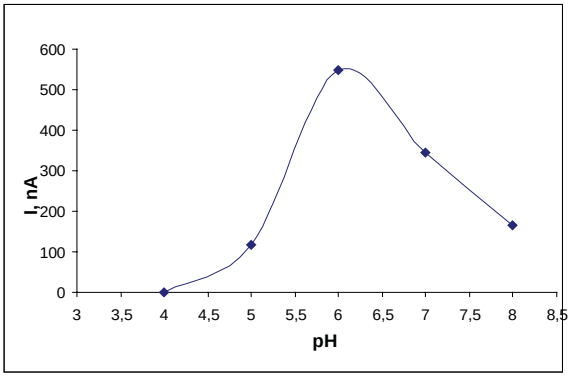

Fig. 3. pH effect on response of the SPCE-Tyr/Paa/Glut in the Flow injection analysis. Phosphate buffer (0.1 mol/ L, pH=6). For 0,050 mmol/L phenol. Operating potential 0 mV vs. SCE

2.4. Linearity and limit of detection

The optimal conditions for using the modified electrodes with tyrosinase in order to detect the phenol were determined and furthermore the electrode calibration was performed (Figure 4).

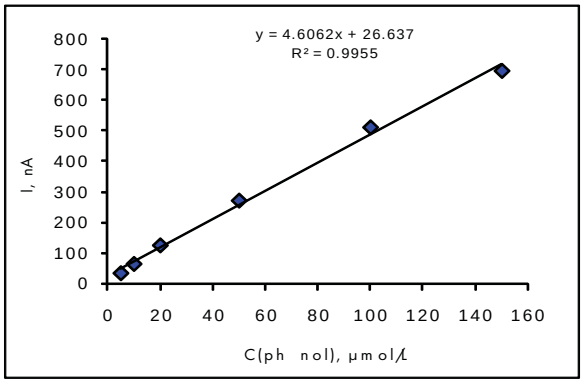

Fig. 4. FIA calibration curves for phenol using SPCE– Tyr/Paa/Glut. Phosphate buffer (0.1 mol/ L, pH = 6,0 + KCl 0,1 mol/L) Operating potential 0mV vs. Ag/AgClspce. Flow rate: 0.7mL/min.

The curve l-intensity resulting from the phenol concentration I=f([phenol]) is linear between 5 and 150µmol/L, the sensibility is of 4,7 nA.cm-1/µM.

2.5. Applications to Standard and Real Samples

In the study the focus was set on ten major phenolic compounds contained in smoked products. According to T. Serot and his collaborators these are: Phenol, o-Cresol, p-Cresol, Guaiacol, 4-Methylguaiacol, 4-Ethylguaiacol, Syringol, Eugenol, 4-Propylguaiacol and Isoeugenol. One eleventh compound was also studied, m-cresol, which is present in smoked bacon, according to Chi-Kuen and his collaborators.

Only phenol, m- and p-cresol gave a significant response. Therefore it was decided to carry out the calibration of the electrode with different standard solutions of phenol, p-cresol and m-cresol to determine the linear range. The obtained results show that the best sensitivity of the biosensor is obtained with p-cresol, while the linearity range is broader for phenol. The phenol was chosen as a standard for calibration of tyrosinase electrodes during the dosage of real samples. At the same time the dosage of standard solutions of phenolic compounds was carried out in gas chromatography. The dosage of real samples was effectuated using the method "additions and assayed" using an internal standard 2.4-dichlorophenol.

In order to validate the measurement results obtained for the determination of phenolic compounds in smoked products with the biosensor, a comparison with gas chromatography was made (Table 4). The following results are averages of the three successive determinations.

Table 4

Concentrations (µmol/ L) of phenol, p-cresol in various smoked products determined using Flow Injection Analysis (FIA) and gas chromatography (CG) methods

ANALYZED PRODUCTS	FIA, C, Mmol/ L	CG C, Mmol/ L
Smoked ham	Phenol + p-cresol : **44.44 ± 1.09**	Phenol : 40.23 ± 1.38 p-cresol : 2.92 ± 0.42 Total : **45.10 ± 1.54**
Smoked bacon	Phenol + p-cresol : **39.10 ± 0.99**	Phenol : 36.68 ± 7.31 p-cresol : 2.32 ± 0.39 **total : 39.00 ±7.70**
Smoked chicken	Phenol + p-cresol : **41.40 ± 2.35**	Phenol : 35.13 ± 1.12 p-cresol : 17.21 ± 1.73 **total : 52.34 ± 2.85**
Smoked salmon	Phenol + p-cresol : **37.07 ± 1.86**	Phenol : 30.76 ±0.86 p-cresol : 7.5 ± 1.34 **total : 38.26 ± 2.20**

In the case of phenolic derivates content determination in smoked products, a good degree of correlation was found between the results obtained in CPG and the ones obtained by biosensor.

3. Conclusions

This research has demonstrated the feasibility of preparing a phenol SPCE based on one-step screen-printing procedure.

A simple to be implemented biosensor for the phenol detection was developed. The biosensor was used in scanning mode by flow injection. Thus, the electrode composition was optimized in order to improve the analytical performance parameters such as the sensitivity and operational stability.

The modified electrode was used in order to determine the low concentration of phenol in real samples of smoked food such as smoked ham, bacon, chicken and salmon. The results obtained when using the biosensor in the FIA have a good correlation with results obtained by CPG.

4. Experimental

4.1. Reagents

Phenol and glutaraldehyde were bought from SIGMA. P-cresol, m-cresol, guiacol, creosol, eugenol, 4-ethylguaicol were bought from ACROS, syringol, o-cresol were purchased from ALDRICH, isoeugenol from LANCASTER, 4-propylguiacol for SΛFC, dichlorophenol, tyrosinase (E.C. 1.14.18.1, approximately 3216 U/mg) were obtained from FLUKA, poly(allylamine hydrochloride) for ALFA ACSAR. Stock standard solutions of phenolic compounds were prepared by dissolution in HPLC grade methanol from PROLABO. All solutions were stored in brown glass bottles at -20 ^{0}C.

The used commercial products such as smoked bacon, ham, chicken and salmon were purchased from the local market (Nantes, France).

4.2. Screen-Printed Electrodes Preparation

DEK Albany model 245 screen printer machine and stainless screens with a 200 mesh and variable thickness (13, 23 or 36μm) have been used to prepare the three electrodes system in four printing steps: (a) printing of Ag/AgCl electrode (13μm) using the commercially available ink Ag/AgCl (GEM-Gwent), the resulted printed Ag/AgCl electrode presents a stable half-cell potential (0.276V versus NHE), (b) printing of both the counter electrode and the conducting tracks of working electrode using graphite – CA ink, (c) printing of the activated surface using the graphite-binder (CA) ink (the diameter of the work surface is 2 mm) (d) printing of nonconductive dielectric layer to define the working surface area. For each printing step a group of four electrodes was simultaneously printed on alumina ceramic substrate (1.5 cm×1.5 cm). All printed layers were cured at room temperature overnight.

4.3. Tyrosinase Biosensor: Preparation and Analytical Performances

The modified electrodes were prepared by the deposition of the worked electrodes in a three compounds mixture: tyrosinase (Tyr), the Paa – poly(allylamine) 0.05% and Glutaraldehyde (Glut) 0.0125%.

The modification of electrodes was made manually by deposing on the working electrode 3μL of mixture. The electrodes were then left to dry for 1 hour.

4.4. Sample Preparation

The extraction of phenolic compounds from smoked products was realized using methanol because it permitted the dilution of samples using aqueous solution of electrolytes. The extraction of phenolic real samples was carried out in several stages. First of all, phenolic compounds were extracted from smoked products then they were filtered and finally concentrated.

4.5. Appliances and Procedures

Flow Injection Analysis (FIA) measurements were performed using a three-electrode flow-through amperometric homemade cell of wall-jet type adapted to the screen-printed configuration. The cell was connected to a potentiostat (BAS model Small Ampere CV-1B). A strip chart recorder (Linseis model L200E) was used to follow the electrode response. The flow-injection system consisted of a flow carrier and sample pump (Ismatec) and an electrical six way-valve (Rheodyne) for sample injections by means of 100 μl injection loop. The flow carrier, 0.1 mol/L phosphate buffer (pH 6.0) with 0.1 mol/L KCl added, was pumped at a flow rate of 0.7ml·min^{-1}. All presented results were the mean of at least three similar electrodes.

Flow Injection Analysis (FIA) technique was used to characterize the amperometric response of the biosensor in terms of sensitivity, repeatability and linear range. In the second part of this work, it was investigated the possibility to

use the proposed biosensor in flow injection analysis mode in order to determine the phenol concentration in various real samples such as smoked products. The obtained results were compared with those obtained using the gas chromatography method.

• GC-analysis

Gas chromatography analysis was carried out using a HP-6890 Gas chromatograph equipped with a split / splitless injector and FID detector. A capillary column (Agilent 19091J-413 HP5; 30 m × 0.25 mm I.D. fused-silica column coated with a 0.25-μm layer of poly (5% phenyl: 95% methylsiloxane) was used to separate phenolic compounds.

Injector temperatures were of 270 °C, the flow rate of carrier gas (helium) was 1.4 ml/min, and oven temperature was programmed from 80 °C (1.5 min) to 290 °C at 50 °C/min, and the final temperature (290°C) was maintained for 10 min finally). The split mode (split ratio: 10:1 was used in all cases. The flame ionisation detector (FID) used in the chromatographic analysis was set at 260 °C throughout the experiment. Chromatographic data acquisition and processing were carried out using HP ChemStations system.

Compounds were identified by matching their GC retention times with those obtained from authentic standards analysed under the same experimental conditions.

References

[1]. Kornreich M. R.; Issenberg P., Determination of Phenolic Wood Smoke Components as Trimethylsilyl Ethers, J. Agr. Food chem., 20, 6, 1972, 1109-1113.
[2]. Seyda Korkut; Bulent Keskinler; Elif Erhan , An amperometric biosensor based on multiwalled carbon nanotube-poly(pyrrole)-horseradish peroxidase nanobiocomposite film for determination of phenol derivatives, Talanta, 76, 2008, 1147–1152
[3]. Boatto G.; Nieddu M.; Carta A.; Pau A.; Lorenzoni S.; Manconi P.; Serra D., Determination of phenol and o-cresol by GC/MS in fatal poisoning case. Forensic Science International, 139, 2004, 191-194
[4]. Poerschmann J., Zhang Z.; Kopinke F-D.; Pawliszyn J., Solid phase microextraction for determining the distribution of chemicals in aqueous matrices. Anal Chem 69, 1997, 597-600.
[5]. Nistor C., Emneús J., Gorton L., A. Ciucu, Improved Stability and Altered Selectivity of Tyrosinase Based Graphite Electrodes for Detection of Phenolic Compounds, Anal. Chim. Acta 387, 1999, 309-326.
[6]. Puig D.; Ruzgas T.; Emnéus J.; Gorton L.; Marko-Varga G. and Barcelo D., Characterization of Tyrosinase-Graphite/Teflon Composite Electrodes for Determination of Catechol in Environmental Analysis, Electroanal., 8, 1996, 885-890.
[7]. Rijiravanich P.; Aoki K.; Chen J., Surareungchai W., Somasundrum M., Micro-cylinder biosensors for phenol and catechol based on layer-by-layer immobilization of tyrosinase on latex particles: Theory and experiment. Journal of Electroanalytical Chemistry 589, 2006, 249–258.
[8]. Dempsey E.; Diamond D.; Collier A., Development of a biosensor for endocrine disrupting compounds based on tyrosinase entrapped within a poly(thionine) film. Biosensors and Bioelectronics 20, 2006, 367-377.
[9]. Carralero Sanz V.; Mena M-L.; González-Cortés A.; Yáñez-Sedeño P.; Pingarrón J.M., Development of a tyrosinase biosensor based on gold nanoparticles-modified glassy carbon electrodes: Application to the measurement of a bioelectrochemical polyphenols index in wines. Analytica Chimica Acta 528, 2005, 1-8.
[10]. Wang J., Lu F., Lopez D., Tyrosinase-based ruthenium dispersed carbon paste biosensor for phenols. Biosensors and Bioelectronics 9, 1994, 9-15.
[11]. Campuzano S.; Serra B.; Pedrero M.; Villena FJ.; Pingarrón J.M., Amperometric flow-injection determination of phenolic compounds at self-assembled monolayer-based tyrosinase biosensors. Analytica Chimica Acta 494, 2003, 187-197.
[12]. Liu S.; Yu J.; Ju H., Renewable phenol biosensor based on a tyrosinase-colloidal gold modified carbon paste electrode. Journal of Electroanalytical Chemistry 540, 2003, 61-67.
[13]. Rogers K.R.; Becker J.Y.; Cembrano J., Improved selective electrocatalytic oxidation of phenols by tyrosinase-based carbon paste electrode biosensor. Electrochimica Acta 45, 2000, 4373-4379.
[14]. Serra B.; Jiménez S.; Mena M.L.; Reviejo A.J.; Pingarrón J.M., Composite electrochemical biosensors: a comparison of three different electrode matrices for the construction of amperometric tyrosinase biosensors. Biosensors and Bioelectronics 17, 2002, 217-226.
[15]. Zhou Y.L.; Tian R.H.; Zhi J.F., Amperometric biosensor based on tyrosinase immobilized on a boron-doped diamond electrode. Biosensors and Bioelectronics 22, 2007, 822-828.

STEROIDAL GLYCOSIDES FROM *VERONICA CHAMAEDRYS L.* PLANTS. THE STRUCTURES OF CHAMAEDROSIDES A, B, C AND E.

Alexandra Marchenko[1]*, Pavel Kintia[1] and Bożena Wyrzykiewicz[2]

[1]*Institute of Genetics and Physiology of Plants, Academy of Sciences of Moldova, Padurii 20, 2004, Chisinau, Moldova*
[2]*Adam Mickiewicz University in Poznan, Grunwaldzka 6, 60-780 Poznań, Poland*
** lexmarcenco@mail.ru, tel. 373 22 555259, fax 373 22 556180*

Abstract: Four steroidal glycosides, named by us chamaedrosides, where two are new steroidal glycosides, have been isolated from the plants of *Veronica chamaedrys L.* (*Scrophulariaceae*) for the first time and their structures have been elucidated. Complete assignments of the 1H and 13C NMR chemical shifts for these glycosides were achieved by means of one- and two-dimensional NMR techniques, including 1H-1H COSY, HSQC, HMBC and ROESY spectra.

Keywords: steroidal glycoside, NMR analysis, *Veronica chamaedrys L.*

Introduction

The genus *Veronica* (*Scrophulariaceae*), which is widely distributed in Europe and Asia, especially in the Mediterranean area, is represented by 32 species in Republic of Moldova [1, 2]. Several *Veronica* species are used for the treatment of cancer, influenza, hemoptysis, laryngopharyngitis, hernia, and against cough, respiratory diseases plus as an expectorant and antiscorbutic in different countries [3–5]. As it was reported earlier, *Veronica* species contain steroidal glycosides, phenylethanoid and iridoid glycosides [6–13].

In the course of our phytochemical studies on the plant *Veronica chamaedrys L.* we had previously reported phenylethanoid and iridoid glycosides [14]. This paper describes the structural elucidation of the steroidal glycosides isolated from *Veronica chamaedrys L.* plants on the basis of extensive spectral analysis, including 2D NMR spectral data and chemical evidences.

Results and Discussion

The water extract of plants of *Veronica chamaedrys L.* was successively subjected to Sephadex gel filtration and silica gel column chromatography to afford four steroidal glycosides, named by us chamaedroside A (**1**), chamaedroside B (**2**), chamaedroside C (**3**) and chamaedroside E (**4**). All isolated compounds gave positive Sannie test [15], and compound 2 and 4 – positive Ehrlich test [16]. All compounds have been isolated as amorphous powders. Their structures were determined by corresponding shifts of ^{1}H and ^{13}C NMR spectral data.

The ^{1}H NMR spectrum of **1** displayed signals due to four steroidal methyl groups at δ 0.89 (3H, s, H–18), 1.1 (3H, s, H–19), 1.5 (3H, d, J=6.7 Hz, H–21), 1.19 (3H, d, J=6.7 Hz, H–27), two methine proton signals at δ 4.30 (1H, m, H-3) and 4.98 (1H, m, H-16) indicative of secondary alcoholic functions, two methylene proton signals at δ 4.128 (1H, m, H-26b) and 3.48 (1H, m, H-26a), ascribable to a primary alcoholic function, and signals for the one anomeric at δ 4.98 (1H, d, J=7.07 Hz). ^{13}C-NMR signals due to a total of 27 carbon signals originating from the sapogenol were composed of four methyl groups at δ 16.5, 16.3, 23.9 and 17.3, one oxygen bearing methine carbon at δ 77.6 (C–3), three quaternary carbons at δ 35.9 (C–10), 110.5 (C–22) and 40.5 (C–13), six methine carbons at δ 35.4 (C–8), 36.6 (C–5), 40.4 (C–9), 56.3 (C–14), 81.1 (C–16), 63.7 (C–17), eleven methylene carbons at δ 21.3 (C–11), 30.5 (C–2), 37.0 (C–1), 32.4 (C–7), 27.1 (C–6), 34.9 (C–4), 40.2 (C–12), 32.3 (C–15), 36.6 (C–23), 28.3 (C–24), 65.4 (C–26). On the basis of the HSQC and HMBC correlations, the aglycone moiety of chamaedroside A was identified as (25S)-5β-spirostan-3β-ol (sarsasapogenin) [17]. The 25S stereochemistry was inferred by the resonance of H-27 methyl protons at δ 1.19, a few bigger than 1.00, and also by the resonance difference between equatorial proton signal (3.48, dd, J=6.5, 9.5 Hz) and axial proton signal (4.128, m) of H-26: 0.648 ppm, a few bigger than 0.57 ppm [18]. 5β configuration was deduced by HMBC correlation between the methyl signal at δ 1.1 (Me-19) and carbon resonances at δ 40.4 (C-9), 36.6 (C-5) and 37.0 (C-1) [18]. Using a combination of 1D-TOCSY and DQF-COSY spectral analysis, the sugar chain has been identified to be composed of one unit of β–D-glucopyranoside. A glycosidation shift was observed for $C\text{-}3_{Agl}$ (δ 77.6), a downfield shift from δ 66.9. The HMBC spectrum showed key correlation peaks between the proton signal at δ 4.98 (H-1Glc) and the carbon resonance at δ 77.6 (H-3 Agl). On the basis of the above results, the structure of chamaedroside A was deduced as 3-O-β-D-glucopyranoside-(25S)-5β-spirostan-3β-ol (Fig.1). Compound **1** was isolated from *Veronica chamaedrys L.* for the first time and has been previously reported in the literature [19].

The ^{1}H-NMR spectrum of **2** displayed signals for four steroidal methyl groups at δ 1.15 (3H, s, H–18), 0.89 (3H, s, H–19), 1.50 (3H, d, J=6.0 Hz, H–21) and 1.20 (3H, d, J=6.9 Hz, H–27), as well as signals for two anomeric protons at δ 4.98 (1H, d, J=7.07 Hz) and 4.84 (1H, d, J=7.5 Hz). The above ^{1}H-NMR data, an acetalic carbon signal at δ 110.7 in the ^{13}C-NMR spectrum, indicated chamaedroside B to be a furostanol saponin with two monosaccharides. The ^{13}C NMR spectrum of **2** showed C–5 at δ 36.6, C–9 at δ 40.3, and C–19 at δ 23.9, characteristic of 5β-steroidal sapogenins. On the basis of the HSQC and HMBC correlations, the aglycone moiety of compound **2** was identified as (25S)-5β-furostan-3β, 22α, 26-triol. One glycosyl unit was shown to be linked to the C-26 hydroxy group of the aglycone by an HMBC correlation of the anomeric proton at δ 4.84 with C-26 of the aglycone at δ 72.2. The HMBC spectrum also showed key correlation peaks between the proton signal at δ 4.98 (H-1Glc) and the carbon resonance at δ 77.8 (C-3 Agl). Thus, chamaedroside B was determined to be 3-O-β-D-glucopyranoside-(25S)-5β-furostan-3β, 22α, 26-triol-26-O-β-D-glucopyranoside (fig.1). Compound **2** was isolated from *Veronica chamaedrys L.* for the first time and has been previously reported in the literature [20].

Compound **3** was obtained as an amorphous powder. Its HR-ESI-MS showed a major ion peak at *m/z* 763.9176 $(M+Na)^{+}$, and significant fragments at *m/z* 601 $(M+Na–162)^{+}$, attributable to the loss of a hexose unit. The molecular formula of 3 was determined as $C_{39}H_{64}O_{13}$ by the HR-ESI-MS (*m/z* $(M)^{+}$). Furthermore, the prominent fragments were observed at *m/z*: 578.7$(M–162)^{+}$, 416.6 $(M–162–162)^{+}$ attribute to the sequential loss of two hexose residues, respectively. The ^{1}H-NMR spectrum of chamaedroside C showed two singlet methyl signals at δ 0.90 (3H, s, Me-18) and 1.08 (3H, s, Me-19), and two doublet methyl signals at δ 1.27 (3H, d, J=7.0 Hz, Me-27), and 1.33 (3H, d, J=7.2 Hz, Me-21), which were recognized as typical spirostanol saponin methyls. 5β configuration was deduced by HMBC correlation between the methyl signal at δ 1.08 (Me-19) and carbon resonances at δ 40.2 (C-9), 36.8 (C-5) and 37.0 (C-1). Moreover, signals for two anomeric protons at δ 4.99 (1H, d, J=7.4 Hz) and 5.45 (1H, d, J=7.4 Hz) could be readily assigned. The J values (>7 Hz) of two anomeric protons indicated the β-orientation at the anomeric centre for the hexose. The ^{13}C-NMR spectrum of **3** showed two anomeric carbon signals at δ 101.9 and 105.8. The HMBC spectrum showed key correlation peaks between the proton signal at δ 4.99 (H–1 Glc) and the carbon resonance at δ 77.8 (C–3 of the aglycone), the proton signal at δ 5.45 (H–1 Glc') and the carbon resonance at δ 78.7 (C–4 Glc). On the basis of the above results, the structure of chamaedroside C was determined as 3-O-β-D-glucopyranosyl(1→4)-β-D-glucopyranoside-(25S)-5β-spirostan-3β-ol. Chamaedroside C is a new compound earlier indescribable in the literature.

Compound **4** was obtained as a colorless powder. Its HR-ESI-MS showed a major ion peak at *m/z* 944.0735 $(M+Na)^{+}$ and significant fragments at *m/z* 782 $(M+Na–162)^{+}$, attributable to the loss of a hexose unit. The molecular formula of **4** was unequivocally established to be $C_{45}H_{76}O_{19}$ by HR–MALDIMS (*m/z* 942 $[M+Na]^{+}$). Positive coloration reactions were observed when **4** was subjected to Ehrlich and Sannie tests, which suggested that **4** have a steroidal saponin skeleton. The ^{1}H-NMR data of chamaedroside E contained two singlet methyl groups at δ 1.003 and 0.89 (each s), two doublet methyl groups at δ 1.22 (d, J=7.0 Hz) and 1.33 (d, J=7.0 Hz) and a methenyl proton at δ 4.98 (m), attributable to a steroidal aglycone moiety. Furthermore, the furostanol glycosidic nature of chamaedroside E suggested by the strong absorbtion bands at 3300 and 900 cm^{-1} in the IR spectrum, and a semiketal carbon signal at δ 110.63 in the ^{13}C-NMR spectrum.

The above ^{1}H-NMR spectral data and a comparison of the ^{13}C-NMR signals of the aglycone moiety of chamaedroside E with those described in the literature [18] showed the structure of the aglycone to be (3β, 22α, 25S)-5β-furostan-3, 22, 26-triol. The α-configuration of C–22 hydroxyl group of the aglycone moiety was deduced from the semiketal carbon signal at δ 110.64, instead of δ 115.5 for β-configuration, and it was further confirmed by the ROESY correlation between H–20 (2.21, dq, J=6.5, 7.5 Hz) and H–23 (1.33, m). The 25S-stereochemistry was established by the resonance of H–27 methyl protons at δ 1.22, a few bigger than 1.00 [18], and also by the resonance difference between equatorial proton signal (3.48, m, J=6.5 and 9.5 Hz) and axial proton signal (4.13, m) of H–26: 0.64 ppm, a few bigger than 0.57 ppm [18]. 5β configuration was deduced by HMBC correlation between the methyl signal at δ 1.1 (Me-19) and carbon resonances at δ 40.4 (C-9), 36.7 (C-5) and 37.1 (C-1).

In the ^{13}C-NMR spectrum, among the 45 carbon signals, 27 signals were assignable to the aglycone, the remaining 18 signals were indicative of the presence of three glucose moieties, in good agreement with three anomeric proton signals appearing at δ 4.82 (d, J=7.49 Hz), 4.98 (d, J=7.07 Hz), 5.43 (d, J=7.48 Hz), and the corresponding anomeric carbon signals at δ 105.13, 101.9 and 105.9, respectively.

A sugar chain was determined to be attached to C–26 by an observation of glycosidation shift of C–26 signal from δ 66.0 to 71.4, and this linkage was further indicated by the cross peak between the ^{13}C signal at δ 71.4 and the anomeric proton signal at δ 4.82 of β-glucopyranosyl moiety in the HMBC spectrum of **4**.

Similarly, a cross peak between the C–3 signal of aglycone at δ 77.91 and the anomeric proton signal at δ 4.98 in the HMBC spectrum of **4,** indicated that another sugar chain was located at the C–3 position of aglycone. A 1→4 linkage

of the one sugar moiety to another was revealed by a cross peak between the C–4 signal of the first glucose at δ 78.58 and the anomeric proton signal of the second glucose at δ 5.43 in the HMBC spectrum. The β-orientation of the anomeric centres of the sugar moieties were supported by the relatively large J values of their anomeric protons (J=7.0–7.8 Hz).

On the basis of all evidences, chamaedroside E was identified as 3-O-β-D-glucopyranosyl (1→4)-β-D-glucopyranoside-(25S)-5β-furostan-3β, 22α, 26-triol-26-O-β-D-glucopyranoside (fig.1).

Chamaedroside E is a new steroidal glycoside isolated and reported for the first time.

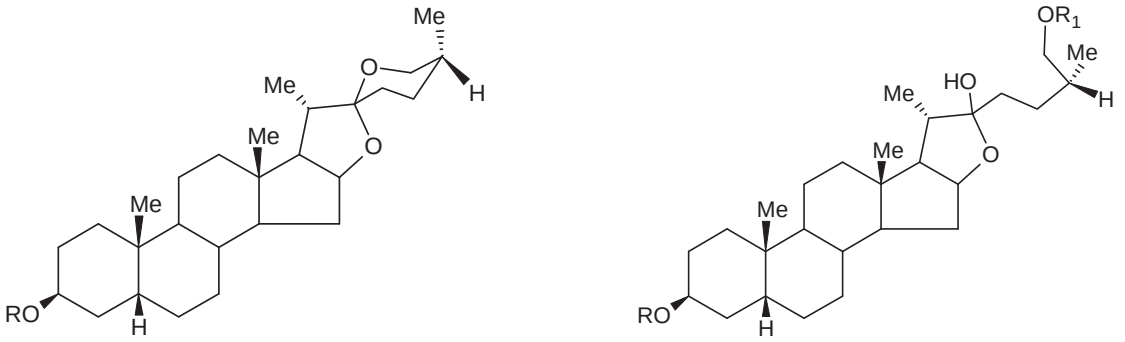

1. R=Glc
2. R=Glc; R_1=Glc
3. R=Glc(1→4)Glc
4. R=Glc(1→4)Glc; R_1=Glc

Fig. 1

Experimental

General experimental procedures

Melting points were measured on a Boetius table. Optical rotations were recorded with a Perkin-Elmer 243 spectropolarimeter. IR spectra were measured on a Bruker FT-IR IFS 66/s instrument as sample in pressed KBr disks. 1D and 2D NMR spectra were recorded on NMR Bruker Advance 600 MHz spectrometer (Bruker BioSpin GmBH, Rheinstetten, Germany) at 300 K dissolving all the samples in C_5D_5N (Carlo Erba, 99.8 %). The standard pulse sequence and phase cycling were used for DQF-COSY, HSQC and HMBC spectra. The NMR data were processed using UXNMR software. The chemical shift values are reported as parts per million (ppm) units relative to tetramethylsilane (δ 0.00 ppm in both cases) for ^1H and ^{13}C, and coupling constants are in hertz (in parentheses).

ESI-MS in the positive ion mode was performed using a Finnigan LCQ Deca ion trap instrument from Thermo Finnigan (San Jose, CA) equipped with Xcalibur software. Samples were dissolved in MeOH (Baker) and infused in the ESI source by using a syringe pump. The capillary voltage was 43 V, the spray voltage 5 kV, and the tube lens offset 30 V. The capillary temperature was 280ºC.

HPLC separations were carried out on a Waters 590 system equipped with a Waters R401 refractive index detector, a Waters XTerra Prep MSC_{18} column (300 x 7.8 mm i.d.) and a Rheodyne injector.

TLC was performed on silica gel plates (Merck precoated silica gel 60 F_{254}). Gel filtration was performed on the Sephadex G–50 (Loba Feinchemie) and G–25 (Pharmacia, Fine Chemicals). Column chromatography was performed over Silica gel Merck 60 (70–230 mesh, Merck, Chemapol). Solvent systems: chloroform/methanol (4:1), chloroform-methanol-water (65:35:3). All solvents for chromatographic separation were of analytical grade. HPLC grade water (18 mΩ) was prepared using a Millipore Milli-Q purification system (Millipore Corp., Bedford, MA).

Plant material has been collected in the scientific research field of the Institute of Genetics and Plant Physiology in May 2009 year. The voucher specimen has been deposited in the Laboratory of Genetics and Physiology of Plant Stability.

Extraction and separation

Fresh plant material of *Veronica chamaedrys L*. (1600 g) was extracted three times at 100ºC with water for 4 hours. Water extracts were combined and extracted with n-butanol, after that n-butanol was evaporated under reduced pressure to give a mixture of saponins (10.3 g). This mixture was subjected to purification on Sephadex G–50 and G–25 and then has been chromatographied on silica gel column (70–230 mesh, Merck). The column was eluted with system chloroform-methanol-water (4:1:0–13:7:1). After monitoring by TLC [Si gel plates, chloroform-methanol (4:1)] fractions showing identical characteristics were combined to give A (105 mg) and B (120 mg).

Fractions A and B were submitted to HPLC on a Waters XTerra Prep MSC_{18} column (300 x 7.8 mm i.d., the flow rate was 1.5 μL/min), using a MeOH:H_2O in the ratio 80:20 for A, and 85:15 for B (isocratic conditions). Pure **1** (20.2 mg) and **2** (26.6 mg) were obtained from A, **3** (40 mg) and **4** (52.2 mg) from B.

Table 1

^{13}C-NMR spectral data (600 MHz , C_5D_5N, ppm) of glycosides (1–4)

	Aglycone					Monosaccharides			
	carbon					carbon			
	1	2	3	4		1	2	3	4
					Glc				
1	37.0	37.1	37.0	37.1	1	101.9	101.8	101.9	101.9
2	30.5	30.7	30.6	30.7	2	75.3	75.2	74.8	74.9
3	77.6	77.8	77.8	77.9	3	78.2	78.0	77.1	77.1
4	34.9	34.6	34.8	34.4	4	71.6	71.0	78.7	78.6
5	36.6	36.6	36.8	36.7	5	78.5	78.5	77.3	77.6
6	27.1	27.0	27.1	27.01	6	62.7	62.6	62.5	62.6
7	32.4	32.3	32.4	32.42	Glc’				
8	35.4	35.4	35.3	35.5	1’			105.8	105.9
9	40.4	40.3	40.2	40.4	2’			75.1	75.2
10	35.9	35.8	35.5	35.6	3’			77.7	77.9
11	21.3	21.2	21.2	21.1	4’			71.7	71.6
12	40.2	40.2	40.1	40.2	5’			78.6	78.6
13	40.5	40.6	40.5	40.6	6’			62.8	62.7
14	56.3	56.3	56.4	56.4	Glc’’				
15	32.3	32.4	32.3	32.4	1’’		105.2		105.1
16	81.1	81.3	81.2	81.2	2’’		75.2		75.4
17	63.7	63.9	63.8	64.0	3’’		78.0		78.2
18	16.5	16.5	16.7	16.7	4’’		71.6		71.7
19	23.9	23.9	24.0	24.0	5’’		78.3		78.5
20	41.0	41.1	41.1	41.2	6’’		62.5		62.8
21	16.3	16.4	16.4	16.5					
22	110.5	110.7	110.6	110.6					
23	36.6	36.8	36.8	36.8					
24	28.3	28.2	28.3	28.3					
25	34.3	34.4	34.4	34.4					
26	65.4	72.2	65.6	71.4					
27	17.3	17.3	17.2	17.5					

1. Amorphous powder. M. p. 290–292ºC, $[\alpha]^{20}_D$: –65 (CH_3OH, c 0.34). IR υ_{max}^{KBr} cm^{-1}: 3402.5 (OH), 980, 910.5, 850, 757.3 (intensity 915>896, 25S-spiroketal). HR MS, *m/z* 578.7771 [calcd for $C_{33}H_{54}O_8$ $(M)^+$]; 416.6 $[M–162]^+$; ^{1}H NMR (aglycone) δ 4.98 (1H, m, H–16), 4.30 (1H, m, H–3), 1.1 (3H, s, Me–19), 0.89 (3H, s, Me–18), 1.5 (3H, d, H–21), 4.13 (1H, m, H–26a), 3.48 (1H, m, H–26b), 1.19 (3H, d, Me–27); (sugar) δ 4.98 (d, J=7.07 Hz, H–1 Glc), 4.06 (dd, J=7.5 and 9.0 Hz, H–4 Glc), 4.11 (dd, J=9.0 and 9.0 Hz, H–3 Glc), 4.22 (dd, J=9.0 and 9.0 Hz, H–4 Glc), 3.81 (ddd, J=2.5, 4.5 and 9.0 Hz, H–5 Glc), 4.57 (dd, J=4.5 and 11.5 Hz, H–6a Glc), 4.35 (dd, J=2.5 and 11.5 Hz, H–6b Glc). For ^{13}C NMR data see Table.

2. Amorphous powder. M. p. 183–184ºC, $[\alpha]^{20}_D$: –107 (Py, c 0.34). IR υ_{max}^{KBr} cm^{-1}: 3350 (OH), 900 (large band). HR MS, *m/z* 758.9329 [calcd for $C_{39}H_{67}O_{14}$ $(M)^+$]; 596.7 $[M–162]^+$; 434.6 $[M–162–162]^+$; ^{1}H NMR (aglycone) δ 4.96 (1H, m, H–16), 4.29 (1H, m, H–3), 1.15 (3H, s, Me–19), 0.89 (3H, s, Me–18), 1.5 (3H, d, H–21), 4.132 (1H, m, H–26a), 3.5 (1H, m, H–26b), 1.20 (3H, d, Me–27); (sugars) δ 4.98 (d, J=7.07 Hz, H–1 Glc), 4.26 (dd, J=7.5 and 9.0 Hz, H–2 Glc), 4.13 (dd, J=9.0 and 9.0 Hz, H–3 Glc), 4.28 (dd, J=9.0 and 9.0 Hz, H–4 Glc), 3.85 (ddd, J=2.5, 4.5 and 9.0 Hz, H–5 Glc), 4.52 (dd, J=4.5 and 11.5 Hz, H–6a Glc), 4.36 (dd, J=2.5 and 11.5 Hz, H–6b Glc). 4.84 (d, J=7.5 Hz, H–1 Glc’’), 3.978 (dd, J=7.5 and 9.0 Hz, H–2 Glc’’), 4.216 (dd, J=9.0 and 9.0 Hz, H–3 Glc’’), 4.273 (dd, J=9.0 and 9.0 Hz, H–4 Glc’’), 3.985 (ddd, J=2.5, 4.5 and 9.0 Hz, H–5 Glc’’), 4.559 (dd, J=4.5 and 11.5 Hz, H–6a Glc’’), 4.339 (dd, J=2.5 and 11.5 Hz, H–6b Glc’’). For ^{13}C NMR data see Table.

3.

4. Amorphous powder. M. p. 292–294ºC, $[\alpha]^{20}_{D}$: –58 (CH_3OH, c 0.34). IR υ_{max}^{KBr} cm^{-1}: 3398 (OH), 980, 914, 892, 850 (intensity 915>896, 25S-spiroketal). HR MS, *m/z* 740.9176 [calcd for $C_{39}H_{64}O_{13}$ $(M)^+$]; 578.7 $[M–162]^+$; 416.6 $[M–162–162]^+$; ^{1}H NMR (aglycone) δ 4.96 (1H, m, H–16), 4.32 (1H, m, H–3), 1.08 (3H, s, Me–19), 0.90 (3H, s, Me–18), 1.33 (3H, d, H–21), 4.17 (1H, m, H–26a), 3.5 (1H, m, H–26b), 1.27 (3H, d, Me–27); (sugars) δ 4.99 (d, J=7.4 Hz, H–1 Glc), 4.27 (dd, J=7.5 and 9.0 Hz, H–2 Glc), 4.12 (dd, J=9.0 and 9.0 Hz, H–3 Glc), 4.25 (dd, J=9.0 and 9.0 Hz, H–4 Glc), 4.27 (ddd, J=2.5, 4.5 and 9.0 Hz, H–5 Glc), 4.56 (dd, J=4.5 and 11.5 Hz, H–6a Glc), 4.30 (dd, J=2.5 and 11.5 Hz, H–6b Glc). 5.45 (d, J=7.4 Hz, H–1 Glc'), 4.12 (dd, J=7.5 and 9.0 Hz, H–2 Glc'), 4.10 (dd, J=9.0 and 9.0 Hz, H–3 Glc'), 4.21 (dd, J=9.0 and 9.0 Hz, H–4 Glc'), 3.48 (ddd, J=2.5, 4.5 and 9.0 Hz, H–5 Glc'), 4.56 (dd, J=4.5 and 11.5 Hz, H–6a Glc'), 4.28 (dd, J=2.5 and 11.5 Hz, H–6b Glc'). For ^{13}C NMR data see Table.

5. Amorphous powder. M. p. 187–189ºC, $[\alpha]^{20}_{D}$: –76 (H_2O, c 0.34). IR υ_{max}^{KBr} cm^{-1}: 3300 (OH), 900 (large band). HR MS, *m/z* 921.0735 [calcd for $C_{45}H_{76}O_{19}$ $(M)^+$]; 758.9 $[M–162]^+$; 596.7 $[M–162–162]^+$; ^{1}H NMR (aglycone) δ 4.98 (1H, m, H–16), 4.28 (1H, m, H–3), 1.003 (3H, s, Me–19), 0.89 (3H, s, Me–18), 1.33 (3H, d, H–21), 4.128 (1H, m, H–26a), 3.48 (1H, m, H–26b), 1.22 (3H, d, Me–27); (sugars) δ 4.98 (d, J=7.07 Hz, H–1 Glc), 4.26 (dd, J=7.5 and 9.0 Hz, H–2 Glc), 4.10 (dd, J=9.0 and 9.0 Hz, H–3 Glc), 4.24 (dd, J=9.0 and 9.0 Hz, H–4 Glc), 4.27 (ddd, J=2.5, 4.5 and 9.0 Hz, H–5 Glc), 4.58 (dd, J=4.5 and 11.5 Hz, H–6a Glc), 4.34 (dd, J=2.5 and 11.5 Hz, H–6b Glc). 5.43 (d, J=7.48 Hz, H–1 Glc'), 4.12 (dd, J=7.5 and 9.0 Hz, H–2 Glc'), 4.10 (dd, J=9.0 and 9.0 Hz, H–3 Glc'), 4.22 (dd, J=9.0 and 9.0 Hz, H–4 Glc'), 3.50 (ddd, J=2.5, 4.5 and 9.0 Hz, H–5 Glc'), 4.56 (dd, J=4.5 and 11.5 Hz, H–6a Glc'), 4.27 (dd, J=2.5 and 11.5 Hz, H–6b Glc'). 4.82 (d, J=7.49 Hz, H–1 Glc''), 3.98 (dd, J=7.5 and 9.0 Hz, H–2 Glc''), 4.22 (dd, J=9.0 and 9.0 Hz, H–3 Glc''), 4.26 (dd, J=9.0 and 9.0 Hz, H–4 Glc''), 3.98 (ddd, J=2.5, 4.5 and 9.0 Hz, H–5 Glc''), 4.53 (dd, J=4.5 and 11.5 Hz, H–6a Glc''), 4.34 (dd, J=2.5 and 11.5 Hz, H–6b Glc''). For ^{13}C NMR data see Table.

Conclusion

Two steroidal glycosides of spirostane series chamaedroside A and chamaedroside C, and two steroidal glycosides of furostane series chamaedroside B and E have been isolated for the first time from the plants of *Veronica chamaedrys L*. During the investigation the structure of chamaedroside A was elucidated as 3-O-β-D-glucopyranoside-(25S)-5β-spirostan-3β-ol, chamaedroside B – 3-O-β-D-glucopyranoside-(25S)-5β-furostan-3β, 22α, 26-triol-26-O-β-D-glucopyranoside, chamaedroside C – 3-O-β-D-glucopyranosyl(1→4)-β-D-glucopyranoside-(25S)-5β-spirostan-3β-ol and chamaedroside E – 3-O-β-D-glucopyranosyl (1→4)-β-D-glucopyranoside-(25S)-5β-furostan-3β, 22α, 26-triol-26-O-β-D-glucopyranoside. Chamaedrosides C and E are new compounds, and chamaedrosides A and B are known steroidal glycosides identified in *Veronica chamaedrys L*. plants for the first time.

Acknowledgments

The authors are grateful to the members of the analytical group of Department of Chemistry, Adam Mickiewicz University in Poznan, for recording the IR and MS experiments.

References

[1]. Lahloub, M. F. Thesis, ETH Nr. 7340, Zurich 1983.
[2]. Socolov, P.D. *Rastitelinie resursi.* «Nauka».1990, pp. 173–182.
[3]. Tomassini, L.; Brkic, D.; Serafini, M. *Fitoterapia* 1995, **66**, 382.
[4]. Su, B.; Zhu, Q.; Jia, Z. *Tetrahedron Lett.* 1999, **40**, 357–358.
[5]. Graham, J.G. *J. Ethnopharmacol.* 2000, 73, 347–377.
[6]. Lahloub, M. F.; Zaghloul, M. G.; Afifi, M. S.; Sticher, O. *Phytochemistry* 1993, **33,** 401–405.
[7]. Taskova, R.; Handjieva, N.; Peev, D.; Popov, S. *Phytochemistry* 1998, **49**,1323–1327.
[8]. Taskova, R.; Handjieva, N.; Evstatieva, L.; Popov, S. *Phytochemistry* 1999, **52**,1443–1445.
[9]. Ozipek, M.; Saracoglu, I.; Kojima, K.; Ogihara, Y.; Calis, I. *Chem. Pharm. Bull*. 1999, **47**, 561–562.
[10]. Aoshima, H.; Miyase, T.; Ueno, A. *Phytochemistry* 1994, **37**, 547–550.
[11]. Saracoglu, I.; Harput, U.; Inoue, M.; Ogihara, Y. *Chem. Pharm. Bull*. 2002, 50, 665–668.
[12]. Chari, V. M.; Grayer-Barkmeijer, R.J.; Harborne, J.B.; Osterdahl, B. G. *Phytochemistry* 1981, **20**, 1977–1979.
[13]. Harput, S.; Saracoglu, I.; Ynoue, M.; Ogihara, Y. *Chem.Pharm.Bull.* 2002, **50**, 869 – 871.
[14]. Marchenko A.; Kintia, P.; Mashcenco, N.; Basarello, C.; Piacente, S.; Pizza, C. *Chem. J. Mold.* 2008, **3(2)**, 101–104.
[15]. Sannie, C.; Lapin, H.; Heitz, S. *Compt. Rend.* 1952, 1082.
[16]. Kiyosawa, S.; Huton, M. *Chem. Pharm. Bull.* 1968, **16**, 1162.
[17]. Agrawal, P.K.; Jain, D.C.; Gupta, R.K.; Thakur, R.S. *Phytochemistry* 1985, **24**, 2479–2496.
[18]. Agrawal, P.K.; Jain, D.C.; Pathak, A.K. *Magn. Reson. Chem.* 2004, **42**, 990–993.
[19]. Tori, K.; Seo, S.; Terui, Y.; Nishikawa, J.; Yasuda, F. *Tetrahedron Lett.* 1981, **22**, 2405–2408.
[20]. Hostettmann, K.; Marston, A. *Saponins* 1995, 548.

OBSERVATIONS ON THE ANTIOXIDANT ACTIVITY OF NOVEL DIHYDROXYFUMARIC ACID DERIVATIVES

N. Secara, Gh. Duca, L. Vlad, F. Macaev*

Institute of Chemistry of the Academy of Sciences of Moldova,
Academy str. 3, MD-2028, Chisinau, Moldova
Tel +373-22-739-754, Fax +373-22-739-954, E-mail: flmacaev@cc.acad.md

Abstract: The paper describes the syntheses of new derivatives of dihydroxyfumaric acid and investigations of their antioxidant activities using the DPPH method.

Keywords: dihydroxyfumaric acid derivatives, DPPH test, antioxidant activity.

1. Introduction

The interest in plant metabolites as sources of antioxidants appeared a long time ago. One of the leaders, due to its potential, in the series of natural reductons is the dihydroxyfumaric acid **1** [1].

The dihydroxyfumaric acid **1** proved to be an efficient reducing compound in several applications, and has been suggested as an intermediate species in the biosynthesis of sugars, uronic acids, and vitamin C [2,3]. DHF was observed to improve wine taste and flavor, leaving out turbidity and inhibiting catechol and phenol oxidation [4]. Also, DHF is used as a disinfectant in contact lenses, in treated municipal sewage or effluents from paper or food-processing industries, as color destabilizing in cleaning products, as an ingredient in highly efficient tobacco smoke filter [5-7]. Maleic acids and the DHF o-acetyl derivatives are used as analgesic and antipyretic drugs [8].

Also, dihydroxyfumarate proved to be a very efficient inhibitor of N-nitrosamines formation in model systems [9], in vitro [10] and in vivo [11].

Due to its structure, very similar to that of ascorbic acid, bearing two hydroxyl groups at vicinal carbons, linked by a double bond, dihydroxyfumaric acid **1** is a good radical scavenger and has high antioxidant properties. However, due to very high reaction rates between dihydroxyfumaric acid **1** and free radicals, there is very little data in the literature concerning the kinetic investigation of such reactions.

A perspective direction of obtaining new compounds with mentioned above properties is the synthetic transformation of known metabolites.

2. Results and discussion

Previously it was shown that compound **1**, having in its structure carboxyl, hydroxyl and olefin fragments can be used to create porphyrinic macrocycles or pyrimidines [12,13]. However, despite the obvious progress in this direction, the chemistry of dihydroxyfumaric acid **1**, remains a poorly studied area in many aspects. Among the works on modifying dihydroxyfumaric acid **1** there is limited data on the synthesis of aminated derivatives, including with a heterocyclic fragment [14].

Creation of new compounds based on the natural dihydroxyfumaric acid **1**, the search for new synthons for targeted synthesis and study of the relationship "structure-property" seem an actual task, to which is devoted this work.

2.1 Design and development of novel dihydroxyfumaric acid derivatives

In developing synthetic approaches to obtaining new substances we took into account advances regarding the transformation dihydroxyfumaric acid **1**, among which there were no synthesis of benzimidazole (Scheme 1). They may be obtained as a result of the interaction of o-phenylenediamine with dihydroxyfumaric acid **1**. By adjusting the reactants ratio it is possible to synthesize mono-and bisbenzimidazoles. An alternative approach to symmetric and not symmetric congeners can be the selective amidation reaction of dihydroxyfumaric acid **1**. The choice of substrates is, above all, due to the practical interest, which is manifested in the development of methods for the synthesis of the corresponding derivatives of dihydroxyfumaric acid 1, as well as to the interest in the chemical processes in terms of forming the desired products.

Nitrogen containing derivatives of dihydroxyfumaric acid **1** may open new possibilities in organic synthesis: selecting of appropriate combinations of substituents may allow adjusting the polarity in wide ranges, the solvating ability, catalytic properties and thereby influence the depth and selectivity of the reaction. Data of this study are shown below.

Scheme 1

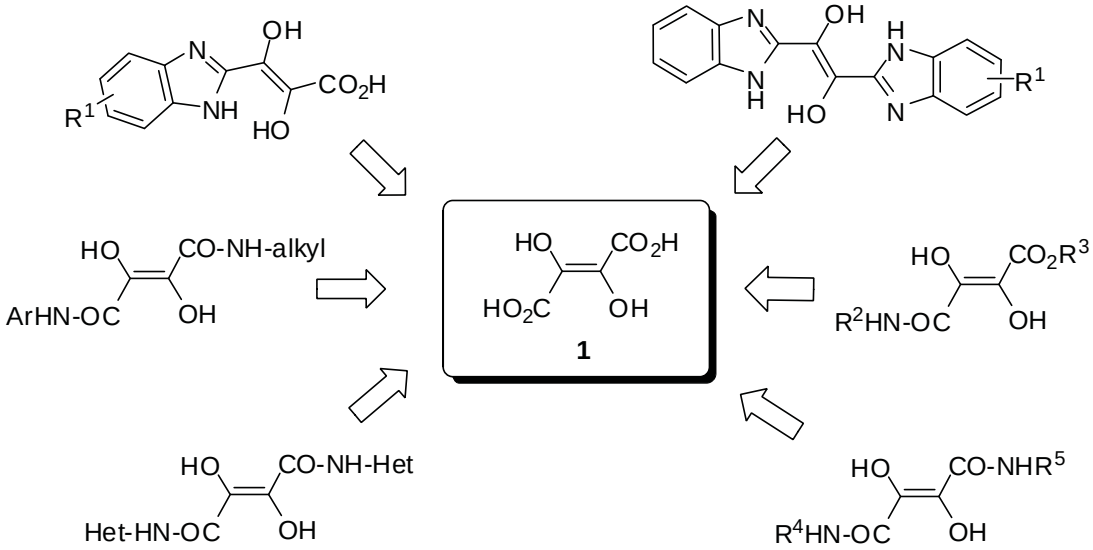

The dihydroxyfumaric acid **1** was first identified (as the *trans* isomer of the dihydroxymaleinic acid) in the 1950's [15]. Few reports are published concerning the chemistry of DHF was, which is rather surprising considering that research was strongly supported during last few decades, and novel technologies were introduced and applied to improve productivity. DHF proved to be an efficient reducing compound in several applications, and has been suggested as an intermediate species in the biosynthesis of sugars, uronic acids, and vitamin C [2]. Moreover, the DHF o-acetyl derivatives are used as analgesic and antipyretic drugs [8].

The interest in the mechanism of oxidation and isomerisation of *trans* **1** and *cis*-enediols **4** prompted us to attempt the preparation of different isomers in this series.

Scheme 2

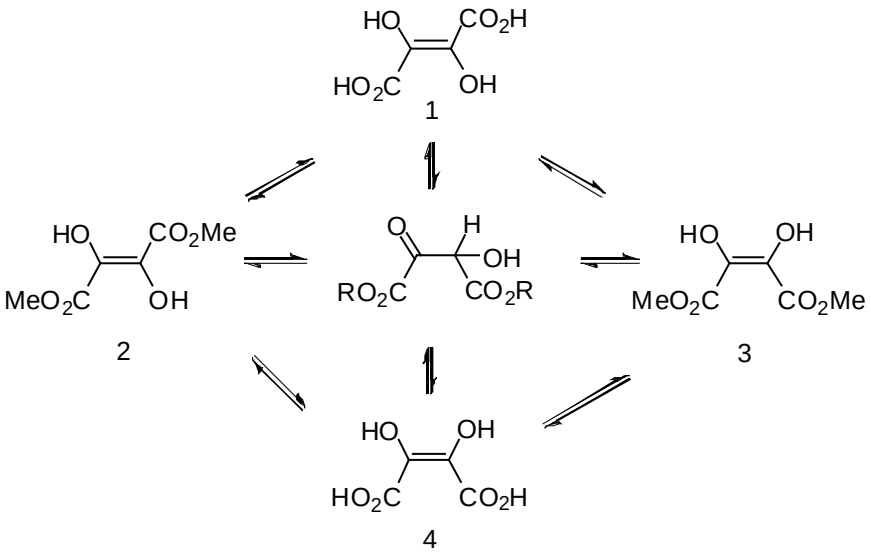

It is known that methylation of dihydroxyfumaric acid **1** can be realized *via* action of the MeOH/acids or diazomethane. In both cases, the configuration of esters **2** is *trans* [15,16].

We performed a new esterification of DHF with methanol under the action of trimethylsilyl chloride.

In this case, the ester had m.p. 149^{0}C although [15,16] give 173^{0}C. Our registered Infrared spectra were very similar with literature data for compound **2**. It is worth mentioning one important difference in the shift of the ester band (*trans*- at 1677.8 cm^{-1} *cis* – at 1670.7 cm^{-1}), the absence of any differences in C=C bands and a small difference of the shift of the OH band at 3164.5 cm^{-1} and at 3168.2 cm^{-1}, respectively.

In ^{1}H NMR spectrum of compound **2** the signal of both methyl groups are located in characteristic region for methyl esters (at 3.94 ppm). Moreover, the signal of the hydroxyl groups was observed as singlet at 9.36 ppm. In the mass spectrum of the investigated compound, the mass of the molecular ion M^+ is 176.03. These data, in combination with the data of elemental analysis specify the structure **2**.

The conversion of esters to amides is a useful reaction, and different amides can be prepared this way from appropriate amine. The reaction is particularly useful because ester **2** is easily prepared, even in cases where the corresponding acyl halide or anhydride are not. Although more studies have been devoted to the mechanism of acylation of amines with esters than with other reagents, the mechanistic details are not yet entirely clear.

Under the normal alkaline conditions, the reaction is base-catalyzed, indicating that a proton is being transferred in the rate-determining step and that two molecules of amine are involved.

Heating of the diester **2** in aniline solution during two hours leads to the formation of the sole product, its structure was determined on the basis of spectral data. The specific feature of ^{1}H NMR spectrum of the investigated compound, in comparison with those for a product **2**, is the presence of two singlet at 3.62 ppm (OMe), 7.82 ppm (OH) and signals of aromatic group in region 6.48-7.88 ppm. These data are supported by the IR-spectrum having characteristic bands at 1474, 1496, 1595 см$^{-1}$ (Ar), 1568, cm^{-1} (CONH), 1665 cm^{-1} (CO_2).These data, in combination with the results of the elemental analysis, confirm the structure **5**.

Scheme 3

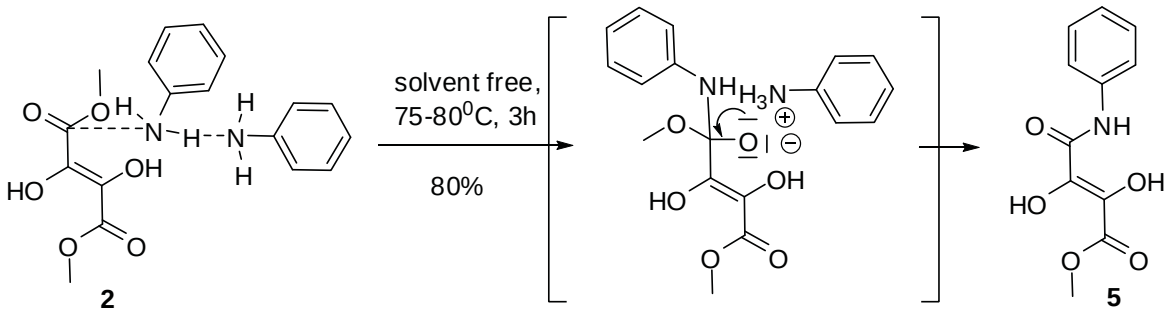

Increasing the reaction time and temperature to the boiling point of aniline didn't lead to the formation of bis-anilide. It should be mentioned that the tentative of synthesis of the mixed amide by heating ester 5 with monoethanolamine wasn't successful, either.

An interesting result in the reaction of amidation of diester 2 was obtained when replacing aniline with its nitrogen-containing analogue – 2-aminopyridine (Scheme 4).

Scheme 4

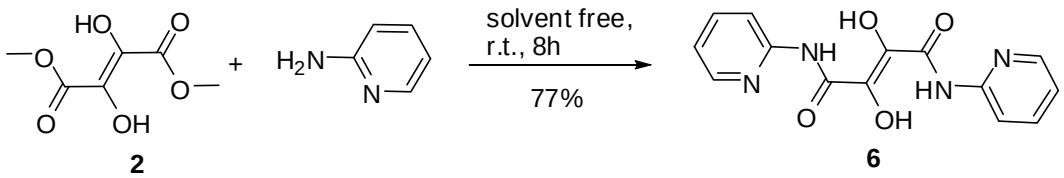

A crystalline substance was separated with melting temperature of 145^{0}C, i.e. four degrees lower than in the case of the initial compound 2. In the IR spectrum of investigated sample**,** appear the characteristic bands for Py, -CO-NH- and OH groups. In comparison with ^{1}H NMR spectrum of compound **5** the signal of CO_2Me group was not observed. In the weak area of its ^{13}C NMR spectrum, the seven signals of carbon atoms at 157.32, 148.81, 141.76, 141.20, 138.87, 113.41 and 112.36 ppm. These data, in combination with the data of elemental analysis specify the structure **6**.

Therefore, replacing of the carbon atom in the benzene ring with nitrogen in the initial amine, had a significant influence on the character of the formed compound.

It was mentioned earlier that attempts of synthesizing mixed amides using monoethanol amine and ether **5,** proved to be unsuccessful.

If the amidation is carried out at room temperature by using ester 2 and monoethanolamine, the reaction product is bis-amidoalcohol **7**.

In its IR-spectrum there are bands characteristic to the amide and hydroxyl groups (see exp.). ^{1}H NMR spectrum of compound **7** contains singlet signal of primary and tertiary hydroxyl groups (in the region 3.3-3.45 and 4.5-5.0 ppm, respectively), quartet (at 3.2 ppm) and triplet (at 3.44 ppm) signals of methylene groups, which are completed by the signal of amide proton at 8.57 ppm. In the high area of its ^{13}C NMR spectrum two signals of carbon atoms are evidenced (see exp.), which are completed by two signals in the weak area at 154.9 and 160.49 ppm. In the mass spectrum of the investigated compound, the mass of the molecular ion M^+ is 234.08.

Scheme 5

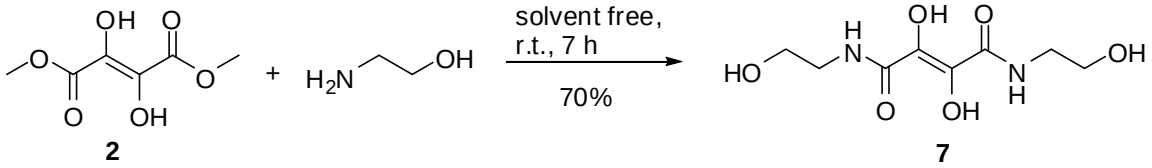

2 **7**

The influence of the nature of homologues of monoethanolamine on the reaction rate and physico-chemical properties of dihydroxymaleinic acid amides was investigated.

Increasing the alkyl radical by one methylene fragment in the initial aminoalcohol gave the decrease of the total output of the reaction, as well as of the melting point from 158-160^{0}C to 142-143^{0}C.

The homologue **8** was spectrally characterized. The presence of an additional methylene group in the structure of compound **8**, as compared to structure **7**, is demonstrated by the characteristic signal in its ^{1}H NMR spectrum (in the region 1.5-1.61 ppm), which is in accordance with the signal in its ^{13}C NMR spectrum at 32.77 ppm. In the mass spectrum of the investigated compound, the mass of the molecular ion M^+ is 262.11.

Scheme 6

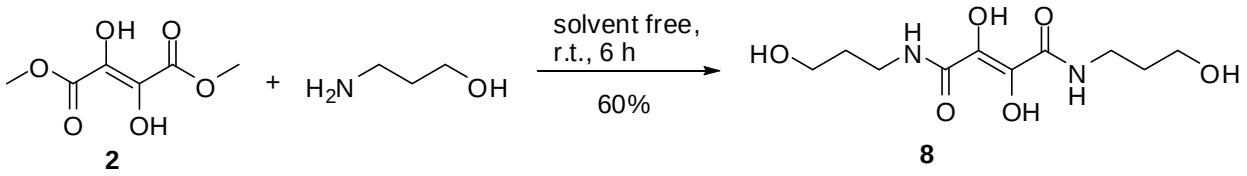

2 **8**

The presence of two methyl groups in the α-position with respect to the amino group in the initial 2-amino-2-methylpropan-1-ol didn't decrease the yield of the target diamide **9**. Analogically to the previous synthesis, this reaction was performed at room temperature.

Scheme 7

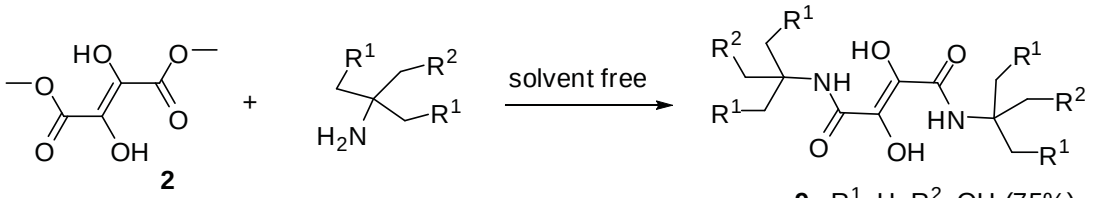

2

9 R^1=H, R^2=OH (75%)
10 R^1=OH, R^2=OH (69%)
11 R^1=R^2=H (70%)

The transformation into the 2-amino-2-(hydroxymethyl)propane-1,3-diol decreased the reactivity of the amine. According to TLC data, only in the case of fusion of initial reagents at 50^{0}C the formation of one single product was observed. Following processing of the reaction mass with yield of 69%, was separated N^1,N^4-bis(1,3-dihydroxy-2-(hydroxymethyl)propan-2-yl)-2,3-dihydroxyfumaramide **10**, and its structure was proved by spectral and physico-chemical methods. Thus, in its ^{1}H NMR spectrum there are multiplet signals of six methylene groups in the region 3.37-3.62 ppm. The signals of six hydroxyl groups are registered in the region from 3.62 to 5.3 ppm.

It should be mentioned that the homologue **11** may be synthesized at room temperature by mixing of tert-butyl

amine with diester **2**. In this case, the yield of the reaction product is practically the same with the mentioned above. As opposed to homologue **9,** the separated product **11,** analogically to compound **10** represents a crystalline substance.

Following the syntheses of a series of amides of the dihydroxyfumaric acid **1,** were decided to continue with the synthesis of heterocyclic derivatives.

The benzimidazole nucleus has been of considerable interest since it was noted that benzimidazole inhibits the growth of certain yeasts and bacteria. Such heterocyclic systems can be modified not only by changing the nature and the number of the connecting atoms but by changing the nature of the substituents in the benzimidazole nuclei as well. In literature revealed the fact that a number of bis-benzimidazoles have been reported but apparently none of them have been synthesized from dihydroxyfumaric acid **1**.

In the present investigation methods were developed to synthesize novel mono and bis-benzimidazoles where the both benzimidazole nuclei are united through their 2-positions either through ethen-1,2-diols.

The benzimidazole was synthesized by hydrochloric acid-catalyzed condensation of the o-phenylenediamine with a dihydroxyfumaric acid **1** an oil bath at 135° under N_2. The same procedure can be used to prepare bis-benzimidazoles by refluxing two moles of diamine with one mole of a dihydroxyfumaric acid **1** in 4 *N* hydrochloric acid.

Scheme 8

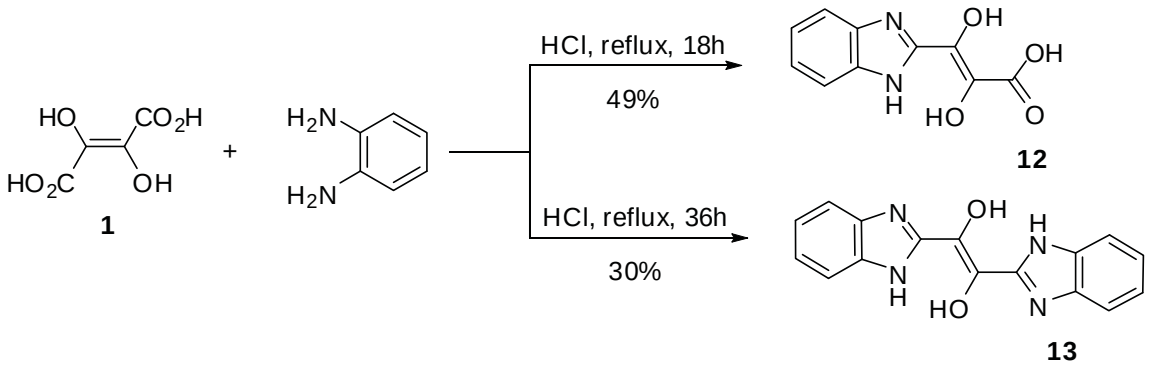

Table1

Analytical results of Synthesized Compounds

Compound/ Molecular formula	Aggregation/ Color/ M.p. °C	Method[a]/ Yield (%)	IR (Nujol) ν, cm^{-1}	Elemental analysis Requires /Found		
				C	H	N
2 $C_6H_8O_6$	Solid/ White/ 149 °C	A/66	691, 771, 879, 893, 1021, 1184, 1213, 1243, 1300, 1396, 1442, 1460, 1516, 1671, 2822, 2887, 2963, 3168, 3376.	40.92/ 40.79	4.58/ 4.98	-
5 $C_{11}H_{11}NO_5$	Solid/ Yellow/ 202-203 °C	C/80	778, 794, 868, 902, 958, 1003, 1029, 1078, 1143, 1162, 1193, 1223, 1240, 1317, 1330, 1437, 1475, 1497, 1558, 1595, 1665, 1729, 3301, 3337.	55.70/ 55.56	4.67/ 4.88	5.90/ 6.04
6 $C_{14}H_{12}N_4O_4$	Oil/ Yellow	A/77	724, 770, 848, 867, 938, 989, 1022, 1051, 1100, 1151, 1162, 1242, 1299, 1329, 1382, 1434, 1485, 1522, 1547, 1572, 1589, 1629, 1668, 2011, 2712, 3081, 3147, 3310.	56.00/ 56.20	4.03/ 4.16	18.66/ 16.78
7 $C_8H_{14}N_2O_6$	Solid/ Colourless/ 158-160 °C	A/70	660, 745, 761, 825, 1013, 1035, 1055, 1106,1205, 1240, 1299, 1315, 1391, 1445, 1476, 1534, 1651, 2824, 2881, 2941, 2985, 3287.	41.03/ 41.22	6.03/ 5.95	11.96/ 13.79

8 $C_{10}H_{18}N_2O_6$	Solid/ Colourless/ 142-143 °C	A/60	745, 761, 822, 862, 913, 943, 1029, 1046, 1072, 1113, 1201, 1241, 1252, 1300, 1312, 1324, 1361, 1441, 1476, 1532, 1650, 1740, 2859, 2893, 2933, 2952, 2981, 3067, 3300, 3336, 3400.	45.80/ 45.99	6.92/ 6.73	10.68/ 10.49
9 $C_{12}H_{22}N_2O_6$	Oil/Yellow	A/75	739, 761, 769, 791, 846, 860, 901, 934, 977, 1011, 1080, 1121, 1183, 1206, 1228, 1228, 1259, 1294, 1319, 1374, 1403, 1454, 1487, 1511, 1546, 1560, 1588, 1637, 1678, 1742, 2115, 2316, 2428, 2559, 2647, 2738, 2839, 2909, 2974, 3375.	49.65/ 49.85	7.64/ 7.77	9.65/ 9.61
10 $C_{12}H_{22}N_2O_{10}$	Solid/ Colourless/ 142-143 °C	B/69	683, 773, 825, 870, 909, 984, 1023, 1042, 1119, 1179, 1227, 1262, 1279, 1368, 1383, 1425, 1461, 1515, 1663, 1735, 2887, 2944, 3252, 3336.	40.68/ 40.49	6.26/ 6.41	7.91/ 8.02
11 $C_{12}H_{22}N_2O_4$	Solid/ Colourless/ 120-122 °C	A/70	777, 873, 906, 1023, 1049, 1110, 1169, 1231, 1268, 1369, 1381, 1419, 1515, 1669, 1723, 2899, 2935, 3248, 3330.	55.80/ 55.96	8.58/ 8.77	10.84/ 11.03
12 $C_{10}H_8N_2O_4$	Solid/ Brown/ 250 °C dec.	C/49	672, 754, 831, 952, 1048, 1135, 1310, 1463, 1490, 1525, 1610, 1677, 2299, 2577, 2791, 3341, 3737.	54.55/ 54.38	3.66/ 3.78	12.72/ 12.71
13 $C_{16}H_{12}N_4O_2$	Solid/ Brown/ 250 °C dec.	C/30	726, 754, 838, 893, 953, 1049, 1079, 1132, 1149, 1238, 1260, 1368, 1396, 1449, 1480, 1527, 1570, 1618, 1643, 1686, 1777, 2803, 2989, 3031, 3118, 3306.	65.75/ 65.91/	4.14/ 4.13	19.17/ 18.88

[a]Method: **A** – Reaction at room temperature; **B** - Reaction at 50-55^{0}C; **C**-Reaction at 75-80^{0}C. **D** - Reaction at 125-135^{0}C.

Due to the fact that the initial dihydroxyfumaric acid possesses maximal absorption at 295 nm (ε = 7100 in aqueous methanol) it was decided to register the spectra of the synthesized compounds in 70% aqueous methanol in order to determine the correlation between the UV absorption and the structure of the molecule and the antioxidant activity (see Table 2).

Table2

UV-Absorption of Synthesized Compounds

No.	Compound	λ_{max}, nm	ε
1	**2**	300	3500
2	**5**	285	10365
3	**6**	299	9825
4	**7**	215	18900
5	**8**	214	9965
6	**9**	211	6245
7	**10**	210	7305
8	**11**	296	315
9	**12**	267	7960
10	**13**	261	17880

Substitution of the carboxyl group with the ester group shifts absorption towards shorter wavelengths. The bathochromic shift is registered for all amides and benzimidazoles. The value λ_{max} for tert-butylamides **11** is most equal to that for acid **1**, whereas the structural differences of these substances produce almost 20 fold changes in ε_{max}: from 7100 to 315. Saturated substituents, which include other heteroatoms such as oxygen and nitrogen, contain nonbonding electrons besides the σ-electrons. Amides 7-**10** with a free hydroxyl group absorb at wavelengths less than the original ether **2**. Increasing the length of the carbon skeleton, or substitution of two hydrogen atoms on the methyl or carbinol group in compound **7** leads towards longer wavelengths in the chain of **7** → **8** → **9** → **10**. The mean values of λ_{max} of these three types of compounds listed in Table 2 indicate their decrease in the same sequence.

As expected, the absorption of aromatic and heterocyclic compounds of the investigated series are different from saturated derivatives of linear structure. The values λ_{max} of compounds **5,6,12** and **13** are higher than those of the discussed above substances, except for compound **11**. There wasn't noticed a correlation between the values λ_{max} and ε_{max}.

It should be noted that probably such generalizations cannot be used in all cases, because these data apply only to alicyclic derivatives of acid **1**.

Next, our attention has been focused on the study of antioxidant properties of synthesized compounds.

It was determined that all amides of alicyclic structure showed a weak desired activity (see Table 3).

The presence of nitrogen atoms in the molecules of compounds **6** and **13** has a negative effect on the antioxidant activity in comparison with the activity of anilide **5** or mono-benzimidazole **12**. Bis-benzimidazole **13** showed antioxidant activity at the same level as the ether **2**. The highest antioxidant activity was exhibited by mono-benzimidazole **12**.

Table 3

Antioxidant properties of Synthesized Compounds

Compound	Number of DPPH molecules reduced by one antioxidant molecule
2	1.07
5	0.63
6	0.25
7	0.02
8	0.05
9	0.031
10	0.066
11	0.009
12	2.1
13	1

Summary

A new method was developed for the synthesis of the dimethyl ether of dihydroxyfumaric acid and its aminated derivatives. The correlation between the structure of the molecule, the UV absorption and the antioxidant activity was investigated.

Increasing the length of the carbon skeleton of the amide fragment, or substitution of two hydrogen atoms with the methyl or carbinol, shifts UV absorption towards longer wavelengths. The mean values of λ_{max} of these three types of derivatives decrease in the same sequence. The presence in the molecules of amides or heterocyclic derivatives of additional nitrogen atoms has a negative effect on the antioxidant activity in comparison with the activity of anilide or mono-benzimidazole. Benzimidazole with a free carboxyl group showed antioxidant activity to two times higher than the ether 2.

The obtained data suggest that generalizations are not of a general nature and are applicable only to discuss types of acid derivatives 1.

4. Experimental methods

All used solvents were of reagent quality, and all commercial reagents were used without additional purification. Removal of all solvents was carried out under reduced pressure. Analytical TLC plates were Silufol® UV-254 (Silpearl on aluminium foil, Czecho-Slovakia). IR spectra were recorded on a Spectrum 100 FT-IR spectrophotometer (Perkin –Elmer) using the universal ATR sampling accessory. Melting points (uncorrected) were determined on a Boetius apparatus. The mass spectra (ES) were measured on Thermo Scientific Exactive mass spectrometer using Advion Travesra Nanomate automated injection system. ^{1}H and ^{13}C NMR spectra have been recorded for $(CD_3)_2SO$ 2-% solution on a "Bruker -Avance III" (400.13 and 100.61 MHz).

UV spectra were recorded on a Perkin Elmer Lambda 25 UV/Vis spectrometer.

Antioxidant activity of investigated compounds was determined according to the method described earlier [17] with

several modifications. Briefly, DPPH and all other compounds were dissolved in 70% aqueous methanol, exact initial concentrations were determined using linear regression equations for each compound. Absorbance was read at 217 nm. For each antioxidant, different mollar ratios (MR), expressed as moles of investigated compound per mole of DPPH, were tested. For each MR, the remaining percentage of DPPH at the plateau was determined and graphed, and EC_{50} was determined as the MR which reduces half of the initial DPPH concentration.

2,3-Dihydroxyfumaric acid, aniline, pyridin-2-amine, 2-aminoethanol, 3-aminopropan-1-ol, 2-amino-2-methylpropan-1-ol, 2-amino-2-(hydroxymethyl)propane-1,3-diol and **2-methylpropan-2-amine** – reagents from Aldrich Chemical Company.

Synthesis of the dimethyl 2,3-dihydroxyfumarate 2.

The mixture of 2,3-dihydroxyfumaric acid **1** (1.48 g, 0.01 mole), Me_3SiCl (0.324 g, 0.03 mole) and 5 ml of MeOH was stirred for 3 days. Excess of Me_3SiCl and MeOH was removed in vacuum. Compound **2** was separated as white crystals by precipitation with mixture hexane/Et_2O and filtration. Yield: 1.16g. Spectrum ^{1}H NMR: 3.94 s (6H, $2CH_3$), 9.36 s (2H, 2OH). MS *m/z* 231.0472 (M^++Na).

Synthesis of the (*E*)-methyl 2,3-dihydroxy-4-oxo-4-(phenylamino)but-2-enoate 5.

The mixture of esters **2** (1.76 g, 0.01 mole) and 2 ml of aniline was stirred at 75-80^{0}C for 3 hours. Excess of amine was removed in vacuum. Compound **2** was separated by column chromatography. Yield: 1.90g, 66%. Spectrum ^{1}H NMR: 3.62 s (3H, CH_3), 7.82 s (2H, 2OH), 6.48-7.87 m (5H, arom).

Synthesis of the 2,3-dihydroxy-N^1,N^4-di(pyridin-2-yl)fumaramide 6.

The mixture of esters **2** (1.76 g, 0.01 mole) and pyridin-2-amine (0.940 g, 0.01 mole) was stirred at room temperature for 8 hours. After completion (TLC analysis), the reaction mixture was directly loaded on a silica gel column and eluted with hexane-ethyl acetate to afford the product **6**. Yield: 2.31g, 77%. Spectrum ^{1}H NMR: 7.69 br s (2H, 2OH), 6.67-7.92 m (8H, arom). Spectrum ^{13}C NMR: 157.32, 148.81, 141.76, 141.20, 138.87, 113.41, 112.36.

Synthesis of the 2,3-dihydroxy-N^1,N^4-bis(2-hydroxyethyl)fumaramide 7.

The mixture of esters **2** (1.76 g, 0.01 mole) and 2-aminoethanol (2 ml) was stirred at room temperature for 6 hours. After completion (TLC analysis), the excess of 2-aminoethanol was removed in vacuum. Compound **7** was separated as white crystals by crystallization from EtOH and filtration. Yield: 1.64g, 70%. Spectrum ^{1}H NMR: 3.25 t (4H, $2CH_2N$, *J*=6.0), 3.44 t (4H, $2CH_2N$, *J*=6.0), 4.5-4.85 s (2H, 2C=OH), 8.57 t (2H, 2 NH, *J*=4.0). Spectrum ^{13}C NMR: 160.49, 154.9, 59.68, 42.13. MS *m/z* 257.0711 (M^++Na).

Synthesis of the 2,3-dihydroxy-N^1,N^4-bis(2-hydroxypropyl)fumaramide 8.

The mixture of esters **2** (1.76 g, 0.01 mole) and 2 ml of 3-aminopropan-1-ol was stirred at room temperature for 6 hours. After completion (TLC analysis), the excess of 3-aminopropan-1-ol was removed in vacuum. Compound **8** was separated as white crystals by crystallization from EtOH and filtration. Yield: 1.57g, 60%. Spectrum ^{1}H NMR: 1.56-1.62 m (4H, 2 $CH_2\underline{CH_2}CH_2$), 3.16-3.25 m (4H, $2CH_2N$), 3.39-3.42 m (2H, $2CH_2\underline{OH}$), 3.5-4.0 br s (4H, 4 OH), 8. 7 t (2H, 2 NH, *J*=4.0). Spectrum ^{13}C NMR: 172.18, 160.47, 59.18, 37.01, 32.77. MS *m/z* 285.1041(M^++Na).

Synthesis of the 2,3-dihydroxy-N^1,N^4-bis(1-hydroxy-2-methylpropan-2-yl)fumaramide 9.

The mixture of esters **2** (1.76 g, 0.01 mole) and 2-amino-2-methylpropan-1-ol (0.890 g, 0.01 mole) was stirred at room temperature for 12 hours. After completion (TLC analysis), the reaction mixture was directly loaded on a silica gel column and eluted with hexane-ethyl acetate to afford the product **9**. Yield: 2.18g, 75%. Spectrum ^{1}H NMR: 1.06 s (12H, 4 CH_3), 3.25 s (4H, $2CH_2$), 4.7-5.2 br s (4H, 4 OH), 7.81 s (2H, 2 NH). Spectrum ^{13}C NMR: 164.76, 159.86, 69.29, 53.83, 24.82.

Synthesis of the N^1,N^4-bis(1,3-dihydroxy-2-(hydroxymethyl)propan-2-yl)-2,3-dihydroxyfumaramide10.

The mixture of esters **2** (1.76 g, 0.01 mole) and 2-amino-2-(hydroxymethyl)propane-1,3-diol (1.21 g, 0.01 mole) was stirred at 50-55^{0}C for 12 hours. After completion (TLC analysis), compound **10** was separated as white crystals by crystallization from MeOH and filtration. Yield: 2.44g, 69%. Spectrum ^{1}H NMR: 3.29-3.62 m (12H, $6CH_2$), 4.0-5.3 br s (8H, 8 OH), 7.79 s (2H, 2 NH). Spectrum ^{13}C NMR: 175.3, 159.90, 65.37, 56.50.

Synthesis of the N^1,N^4-di-tert-butyl-2,3-dihydroxyfumaramide 11.

The mixture of esters **2** (1.76 g, 0.01 mole) and 2-methylpropan-2-amine (0.73 g, 0.01 mole) was stirred at room temperature for 8 hours. After completion (TLC analysis), compound **11** was separated as white crystals by crystallization

from EtOAc and filtration. Yield: 1.81g, 70%. Spectrum ^{1}H NMR: 1.23 s (18H, 6CH_3), 5.0-6.3 br s (2H, 2 OH), 7.61 s (2H, 2 NH). Spectrum ^{13}C NMR: 173.5, 160.60, 50.89, 28.76.

Synthesis of the (*E*)-3-(1H-benzo[*d*]imidazol-2-yl)-2,3-dihydroxyacrylic acid 12.

The mixture of acid **1** (1.48 g, 0.01 mole) and *o*-phenylenediamine (1.08 g, 0.01 mole) were refluxed for 18 hours in 20 ml of **4** *N* hydrochloric acid. The reaction mixture was cooled, the crystalline dihydrochloride separated by filtration. Product was treated with hot 20% aq NH_4OH and washed with water. Acidification of the ammoniacal filtrate with AcOH gave the corresponding monobenzimidazole. Attempts to recrystallize the product from EtOH gave a gum **12**, which solidified on standing. Yield: 1.07g, 49%. It decomposes at 250 °C. Spectrum ^{1}H NMR: 5.0-6.3 broad s (3H, 2OH, NH), 7.15-7.6 m (2H, arom), 7.7-7.81 m (2H, arom), 10.06 s (1H, CO_2H).

Synthesis of the (E)-1,2-di(1H-benzo[d]imidazol-2-yl)ethene-1,2-diol 13.

The mixture of acid **1** (1.48 g, 0.01 mole) and *o*-phenylenediamine (2.16 g, 0.02 mole) were refluxed for 36 hours in 50 ml of 5 *N* hydrochloric acid in an oil bath at 135^{0}C under N_2. The mixture was cooled in an ice bath to separate the HCl salts of the bisbenzimidazole **13.** In this case the crude product was treated with hot sodium bicarbonate solution in place of aqueous ammonia. Recrystallization of product from ethylene glycol or EtOH in both cases gave a gum **13**, which solidified on standing. Yield: 0.876g, 30%. It decomposes at 250 °C. Spectrum ^{1}H NMR: 4.7-6.9 br s (6H, 4OH, 2NH), 7.16-7.68 m (8H, arom).

References

[1]. Дука, Г.; Гаина, Б.; Ковалева, О.; Ковалев, В.; Гонца, М. Экологически чистое винодельческое производство. Ştiinţa, 2004.
[2]. Hough, L.; Jones, J. K. N. Nature, 1951, 167, 180.
[3]. Sychev, A.; Duka, G. G. Sadovod. Vinograd. Vinodel. Mold. 1985, 12, 34.
[4]. Nelson, Eric L., Richard L. United States Patent 4490389
[5]. Verachtert, H. United States Patent 4311598
[6]. Michelson, A.M.; Rotter, P. United States Patent 4088595
[7]. Irimi, S.; Molnar A.; Gabor J.; Toke L. United States Patent 5060672.
[8]. D'Amico, A.; Chiesa, F.; Montaldi, D.; Quarenghi, F. Bull. Soc. Chim. Fr. 1962, 101, 903.
[9]. Gonţa M., Duca M., Porubin D., Voloc N. Anale Ştiinţifice ale USM, Chişinău 2003, 419-425
[10]. Porubin Diana. Chemistry Journal of Moldova. 2007, 2, 3-7.
[11]. Porubin, D.; Hecht, S. S.; Li, Zh.; Gonta, M.; Stepanov, I. Journal of Agricultural and Food Chemistry, 2007, 55, 7199-7204.
[12]. Bellec, N.; Garrido Montalban, A.; Williams D. B. G.; Cook, A.S.; Anderson, M. E.; Xidong Feng, Barrett, A. G. M.; Hoffman, B.M. J. Org. Chem. 2000**,** 65, 1774-1779.
[13]. Goldberg, D.P.; Michel, S.L. J.; White, A.J. P.; Williams, D. J.; Barrett, A. G. M. ; Hoffman B. M. Inorg. Chem. 1998, 37, 2100-2101.
[14]. Dreher, D.D. United States Patent 0090668.
[15]. Hartree E. F., J. Am. Chem. Soc., 1953, 75, 6244-6249.
[16]. Goodwin S., Witkop B., J. Chem. Soc., 1954, 76, 5599-5603.
[17]. Brand-Williams, W.; Cuvelier, M.E.; Berset, C. Lebensm. Wiss. Technol. 1995, 28, 25-30.

COMPARATIVE KINETICS STUDY OF THE THERMAL AND THERMO-OXIDATIVE DEGRADATION OF A POLYSTYRENE-CLAY NANOCOMPOSITE BY TGA AND DSC

Ion Dranca*, Nicon Ungur, Tudor Lupascu, Oleg Petuhov

Institute of Chemistry, ASM, Center of Physical Chemistry and Nanocomposites
3 Academiei Str., Chisinau MD2028, Moldova
Tel. +37322 739 781 Fax. 37322 725 490
drancai@yahoo.com

Abstract: The methods of thermogravimetry (TGA) and differential scanning calorimetry (DSC) have been used to study the thermal and thermo-oxidative degradation of polystyrene (PS) and a PS-clay nanocompoiste. An advanced isoconversional method has been applied for kinetic analysis. Introduction of the clay phase increases the activation energy and affects the total heat of degradation, which suggests a change in the reaction mechanism. The obtained kinetic data permit a comparative assessment of fire resistance of the studied materials.

Keywords: degradation; fire resistance; nanocomposites; thermogravimetric analysis (TGA); differential scanning calorimetry (DSC);

Introduction

Alexandre and Dubois found that implanting layered silicates into polymers is known[1] to modify dramatically various physical properties including thermal stability and fire resistance.[2] A great deal of attention has been focused on the thermal behavior of polystyrene (PS) clay nanocomposites[3-9] as studied by using cone calorimetry as well as standard thermal analysis methods such as thermogravimetric analysis (TGA), differential scanning calorimetry (DSC), and dynamic mechanical analysis (DMA). It has been found that compared to virgin PS the clay nanocomposites have somewhat higher glass transition temperature, [4,6],decompose at significantly greater temperatures, [4-9] and demonstrate a substantial decrease in the maximum heat release rate on combustion. [5-9] It should be stressed that even when clay content is as little as 0.1% the initial decomposition temperature is increased by 40°C and the peak heat release rate is decreased by about 40% relative to virgin PS. [7] The mechanism of such remarkable effect is not yet well understood. The effect is most commonly rationalized in terms of the barrier model that suggests the enhanced fire resistant properties to arise due to a carbonaceous-silicate char that builds up on the surface of the polymer melt and provides the mass and heat transfer barrier. [5-11]. It has also been suggested that the effect may be associated with radical trapping [8] by the structural iron in clays.

Although the thermal behavior of polymer clay nanocomposites has been studied extensively, the kinetic aspects of the thermal and thermo-oxidative degradation remain practically unknown. The importance of reliable kinetic analysis cannot be overestimated as it may provide information on the energy barriers of the process as well as offer mechanistic clues. Finding a reliable approach to kinetic analysis presents a certain challenge as the thermal analysis literature describes a great number of kinetic methods that make use of either single or multiple heating rate data. The shortcomings of the single heating rate methods have been repeatedly stressed. [12-13] The recent publication [14] summarizing the results of the ICTAC Kinetics Project has recommended the use of multiple heating rate methods such as isoconversional methods.[12]

In this paper, we employ Vyazovkin, advanced isoconversional method, [15,16] in order to obtain reliable kinetic information on the thermal and thermo-oxidative degradation of a PS-clay nanocomposite. We demonstrate that the obtained kinetic information provides important mechanistic conclusions about the effect of the clay phase on degradation of the polymer composites.

Experimental part

The PS clay nanocomposite was prepared by intercalating a monocationic free radical initiator into montmorillonite clay and the subsequent solution surface-initiated

polymerization (SIP), where the chain growth was initiated in situ from clay surfaces. The initiator we synthesized was an azobisisobutyronitrile (AIBN)-analogue molecule with a quaternized amine group at one end. The intercalation process was realized by cation exchange reaction in which the cationic end of the initiator was ionically attached to the negatively charged clay surfaces. The structure of the initiator and details regarding the preparation and characterization of the intercalated clay can be found in the paper [17]. The subsequent SIP with the clay that had been intercalated by the initiator was performed in THF solvent with styrene as the monomer, resulting in a PS-clay nanocomposite by the in situ polymerization. The molecular weight (~90,000) and polydispersity (~2.3) of the product were measured by size

exclusion chromatography (SEC) using PS standards. Details of the initiator synthesis and similar procedures of the SIP process and product analysis can be found in another publication, [18] in which the results have shown that this free radical SIP strategy can achieve exfoliated PS-clay nanocomposites with even higher clay loading by using the same monocationic initiator. The obtained material will be referred to as nPS90. For comparison purposes, we have used virgin PS that was purchased from Alfa Aesar and used as received. Its Mw value is 100,000 and it will be referred to as PS100.

The degradation kinetics have been measured as the temperature dependent mass loss by using a Mettler-Toledo TGA/SDTA851^e module. Polymer samples of ~5mg have been placed in 40μL Al pans and heated from 30 to 600^{o}C at the heating rates 2.5, 5.0, 7.5, 10.0, and 12.5 ^{o}C min^{-1}. Thermal and thermo-oxidative degradations have been respectively performed in the flowing atmosphere of N_2 and air at a flow rate of 70 mL min^{-1}. The buoyancy effect in TGA has been accounted for by performing empty pan runs and subtracting the resulting data from the subsequent sample mass loss data. DSC measurements have been conducted by using a Mettler-Toledo DSC 822^e module. The conditions of DSC runs have been similar to those of TGA except that DSC runs have been carried at a single heating rate 10 ^{o}C min^{-1}. Both instruments have been calibrated by using an Indium standard. The amount of residue has been ~1%.

Kinetic method

The overall rate of polymer degradation is commonly described by the following equation [12]

$$\frac{\mathrm{d}\alpha}{\mathrm{d}t} = A\exp\left(\frac{-E}{RT}\right) f(\alpha) \tag{1}$$

where α is the extent of polymer conversion, t is the time, T is the temperature, R is the gas constant, A is the pre-exponential factor, E is the activation energy, and $f(\alpha)$ is the reaction model. The latter is frequently taken in the form of the reaction order model $(1-\alpha)^n$. The deficiencies of such model-based approach are well known. [12] In addition to the difficulty of determining a unique reaction model, degradation of polymers tends to demonstrate complex kinetics [19] that cannot be described by single eq. 1 throughout the whole temperature region. [20, 21]

In order to adequately represent the temperature dependence of degradation, one may use a model that involves several steps such as recombination, random scission, and end chain scission each of which is represented by the respective eq. 1. [22] However, simultaneously solving of three kinetic equations presents a considerable computational problem. A simpler alternative is to use a model-free isoconversional method. The method is based on the isoconversional principle that states that at a constant extent of conversion the reaction rate is only a function of the temperature:

$$\left[\frac{\mathrm{d}\ln(\mathrm{d}\alpha/\mathrm{d}t)}{\mathrm{d}T^{-1}}\right]_\alpha = -\frac{E_\alpha}{R} \tag{2}$$

Henceforth the subscript α indicates the values related to a given conversion). While based on eq. 1, the method assumes that E_α is constant only at a given extent of conversion and the narrow temperature region related to this conversion at different heating rates. In other words, the isoconversional methods describe the degradation kinetics by using multiple eq. 1 each of which is associated with a certain extent of conversion and has its own value of E_α. By using the integral form of Equation (2) Vyazovkin [15,16] has developed an advanced isoconversional method. The method offers two major advantages over the frequently used methods of Flyn and Wall[27] and Ozawa.[28] The first advantage is that the method has been designed to treat the kinetics that occur under an arbitrary variation in temperature, *T(t),* which allows one to account for self-heating/cooling detectable by the thermal sensor of the instrument. For a series of n experiments carried out under different temperature programs, *T(t),* the activation energy is determined at any particular value of α by finding E_α, which minimizes the function [Equation (3)].

$$\phi(E_\alpha) = \sum_{i=1}^{n} \sum_{j\neq i}^{n} \frac{J[E_{\alpha,} T_i(t_\alpha)}{[E_{\alpha,} T_j(t_\alpha)]} \tag{3}$$

where [Equation (4)]:

$$J[E\alpha, Ti(t_\alpha)] \equiv \int_{t_\alpha-\Delta\alpha}^{t_\alpha} \exp[\frac{-E\alpha}{RT_i(t)}]dt \tag{4}$$

The second advantage is associated with performing the integration over small time segments (Equation (4)), which allows the elimination of a systematic error [16] occurring in the Flynn and Wall and Ozawa methods when E_α varies significantly with α.

Results and discussion

Figure 1 provides a comparison of the mass loss curves for degradation of virgin polymer and nanocomposite under nitrogen and air. PS100 degrades without forming any residue. Degradation of nPS90 leaves some residue in amount of ~1% that remains practically constant up to 1000°C. Assuming PS has been completely volatilized; this number represents the amount of the clay phase in the nanocomposite. As seen in Figure 1, in both nitrogen and air the mass loss curves for nPS90 are found at markedly greater temperatures than the curves for PS100. The decomposition temperature increases by as much as 30-40°C that is consistent with the results of other workers.[7-9] Given the small amount of the clay phase, this obviously represents a dramatic increase in thermal stability.

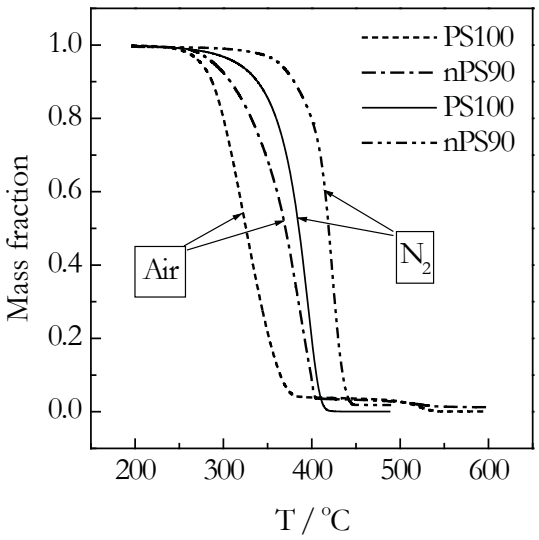

Figure 1. TGA curves for degradation of PS100 and nPS90 at heating rate 5°C min^{-1} in air and nitrogen.

Figure 2 displays the results of the isoconversional kinetic analysis for the thermal degradation of PS100 and nPS90 in the atmosphere of nitrogen. For PS100 the effective activation energy increases from ~100 to ~200 kJ mol^{-1} throughout degradation. The variation suggests a change in a limiting step of the process. It has been suggested [25, 26] that PS degradation is initiated at weak link sites inherent to the polymer itself. Similar increases from smaller values of E_α have been observed for degradation of other polymers (PE, PP, and PMMA). [20, 21]The values of E_α for nPS90 also show an increase with the extent of degradation that suggests a change in the rate limiting step. That latter occurs at the early stages of degradation ($\alpha < 0.25$) after which the effective activation energy practically levels off at 220 – 230 kJ mol^{-1}. The whole process of

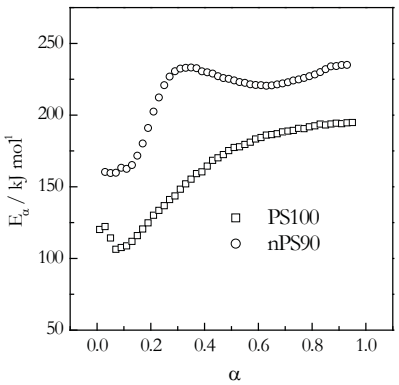

Figure 2. Dependence of the effective activation energy on the extent of conversion for the thermal degradation of PS100 and nPS90 in nitrogen.

nPS90 degradation demonstrates markedly larger effective activation energy as compared to that of PS100 degradation. According to our DSC data the degradation of PS100 and nPS90 demonstrates single endothermic peaks whose respective heats are –990 and –670 J g^{-1}.

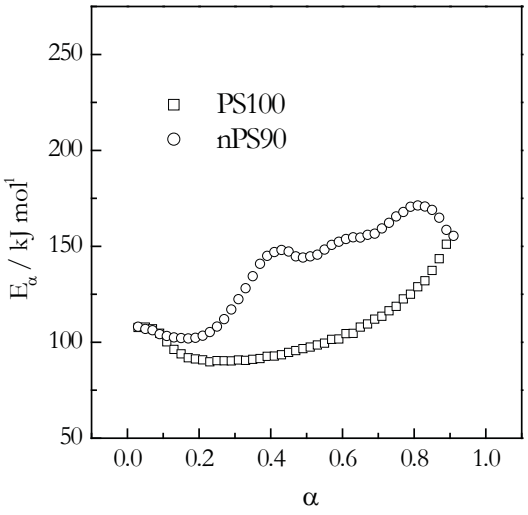

Figure 3. Dependence of the effective activation energy on the extent of conversion for the thermo-oxidative degradation of PS100 and nPS90 in air.

Figure 3 presents variations in E_α for thermo-oxidative degradation of PS100 and nPS90. For PS100 the initial stages of degradation occur with lower activation energy of ~90 – 100 kJ mol^{-1} that later ($\alpha > 0.6$) rises to ~150 kJ mol^{-1}. This behavior is consistent with the mechanism of thermo-oxidative degradation of PS that assumes [19,27] the initial formation of hydroperoxide radicals whose decomposition determines the degradation at early stages. At later stages and higher temperatures these radicals are no longer stable so that the degradation rate becomes controlled by unzipping. This mechanism is consistent with our DSC data that show that initial stages of thermo-oxidative degradation are exothermic, whereas the later ones are endothermic. Putting the above results together we may conclude that the introduction of the clay phase into PS causes a considerable increase in the effective energy of degradation. The enhanced thermal stability of the PS clay nanocomposites is likely to be associated with this increase.

It does not seem that this result can be easily rationalized in terms of the barrier model that suggests that the degradation rate of a polymer clay nanocomposite should be limited by diffusion of gaseous decomposition products through the surface barrier of the silicate char. However, diffusion of gases in liquids and solids, including polymers tends to have a low activation energy of about 40 – 50 kJ mol^{-1}.[28] Also the presence of the surface barrier cannot affect the total value of the heat of degradation. Nevertheless, the degradation of the nanocomposite in nitrogen demonstrates a more than 30% smaller endothermic effect than that for virgin PS. In air, the degradation of nPS90 shows an exothermic effect followed by an endotherm as is observed for PS100. However, the exothermic effect appears somewhat smaller and endothermic effect is almost twice larger than the respective effects observed for PS100. These facts suggest that introduction of the clay phase in PS is likely to change the concentration distribution of degradation products and/or maybe cause the formation of some new products of degradation. This suggestion appears to correlate with the results of cone calorimetry experiments [5-9] which indicate that the clay enhanced PS composites tend to burn with releasing a significantly smaller amount of the total heat. This may be because for the clay enhanced PS the concentration distribution of the polymer degradation products changes toward the formation of less combustible products.

Although the barrier model makes sense from both experimental [9, 10] and theoretical standpoint,[11] the barrier formation does not seem to be the only reason that contributes to the enhanced thermal and fire stability of polymer clay nanocomposites. Indeed, there is still a lot to learn about the mechanism of enhancing these important properties. In particular, experimental comparison of the concentration distribution of degradation products in virgin polymer and in polymer clay composite should be of fundamental importance.

Conclusions

The application of the advanced isoconversional method allows one to obtain meaningful information on the kinetics of the thermal and thermo-oxidative degradation of PS clay nanocomposites that, in particular, can be used for comparative assessment of fire resistance. The kinetic analysis suggests that enhanced thermal stability of nanocomposites is associated with the increase of the effective activation energy of their degradation.

Acknowledgement: Partial support for this work from the *State Program of Moldova* under grant 169. PA/09.836.05.04A is gratefully acknowledged.

REFERENCES

[1]. M. Alexandre, P. Dubois, *Mater. Sci. Eng., R*, **2000**, *28*, 1.
[2]. D. Porter, E. Metcalfe, M. J. K. Thomas, *Fire Mater*. **2000**, *24*, 45
[3]. R. A. Vaia, H. Ishii, E. P. Giannelis, *Chem. Mater.* **1993**, *5*, 1694
[4]. M. W. Noh, D. C. Lee, *Polym. Bull.* **1999**, *42*, 619.
[5]. J. W. Gilman, C. L. Jackson, A. B. Morgan, R. Harris, E. Manias, E. P. Giannelis, M.
[6]. M. Okamoto, S. Morita, H. Taguchi, Y. H. Kim, T. Kotaka, H. Tateyama, *Polymer* **2000**
[7]. J. Zhu, C. A. Wilkie, *Polym. Int*. **2000**, *49*, 1158.
[8]. J. Zhu, F. M. Uhl, A. B. Morgan, C. A. Wilkie, *Chem. Mater.* **2001**, *13*, 4649
[9]. A. B. Morgan, R. H. Harris, T. Kashiwagi, L. J. Chyall, J. W. Gilman, *Fire Mater*. **2002**, *26*, 247.
[10]. J. Wang, J. Du, J. Zhu, C. A. Wilkie, *Polym. Degrad. Stab.* **2002**, *77*, 249.
[11]. M. Lewin, *Fire Mater.* **2003**, *27*, 1.
[12]. J.H. Flynn, In *Encyclopedia of Polymer Science and Engineering*; H.F. Mark, N.M. Bikales, C.V.Overberger, J.I. Kroschwitz, Eds.; J. Wiley & Sons, New York, 1989, Suppl. Vol., p. 690.
[13]. S. Vyazovkin, N. Sbirrazzuoli, *Macromol. Chem. Phys.* **1999**, *200*, 2294.
[14]. M.E. Brown, M. Maciejewski, S. Vyazovkin, R. Nomen, J. Sempere, A. Burnham, J. Opfermann, R. Strey, H.L. Anderson, A. Kemmler, R. Keuleers, J. Janssens, H.O. Desseyn, C-R. Li, T.B.Tang, B. Roduit, J. Malek, T. Mitsuhashi, *Thermochim. Acta* **2000**, *355*, 125.
[15]. Vyazovkin, S. *J. Comput. Chem.* **1997,** *18,* 393.
[16]. Vyazovkin, S. *J. Comput. Chem.* **2001,** *22,* 178.
[17]. Fan, C. Xia, R. C. Advincula, *Collids and Surfaces: A* **2003**, *219*, 75
[18]. X. Fan, C. Xia, R. C. Advincula, *Langmuir* **2003**, *19*, 4381
[19]. J. H. Flynn "Polymer Degradation" in "*Handbook of Thermal Analysis and Calorimetry"*, Vol.3, S. Z. D. Cheng, ed., Elsevier, 2002, p. 587.
[20]. J. D. Peterson, S. Vyazovkin, C. A. Wight, *J. Phys. Chem. B*, **1999**, *103*, 8087.
[21]. J.D. Peterson, S. Vyazovkin, C. A.Wight, *Macromol. Chem. Phys*. **2001,** *202*, 775.
[22]. Y. Kodera, B. J. McCoy, *Energy & Fuels* **2002**, *16*, 119.
[23]. H. Flynn, L. A. Wall, *J. Res. Nat. Bur. Standards: A* **1966**, *70*, 487.
[24]. T. Ozawa, *Bull. Chem. Soc. Japan* **1965**, *38*, 1881.
[25]. S. L. Madorsky, "*Thermal Degradation of Organic Polymers"*, Interscience Publishers, New York 1964.
[26]. N. Grassie, G. Scott, "*Polymer Degradation and Stabilisation",* Cambridge University Press, Cambridge 1985.
[27]. M. Celina, D. K. Ottesen, K. T. Gillen, R. L. Clough, *Polym. Degrad. Stabil.* **1997**, *58,* 15.
[28]. W. Jost, "*Diffusion in Solids, Liquids, Gases*", Academic Press, New York, 1960.

METALLIC COMPOUNDS IN THE PHASE OF THE RETICULATED IONIC POLYMERS

Vasile Gutsanu[a]*, Constantin Turta[b], George Filoti[c]

[a] *Department of inorganic and physical Chemistry, State University of Moldova, 60 A.Mateevich str., MD-2009 Chisinau, Moldova *Email: gutsanu@gmail.com*
[b] *Institute of Chemistry, Academy of Sciences of Republic of Moldova, 3, Academiei str.. MD-2028, Chisinau, Moldova*
[c] *National Institute of Materials Physics, Atomistilor str.105 bis, PO Box MG.7, Magurele, Bucharest, Romania, 077125*

Abstract: In this review there are described the results of studying of iron ions state in the ion-exchange resins (KU-2, AN-31, AV-17, Varian – AD, EDE-10P), obtained by Mossbauer spectroscopy. The iron ions have been sorbet on ion exchangers, from aqueous solutions at different temperatures and air conditions. The iron state in polymer phase depends of nature of electron donor groups - amine or carboxylic. To explain the form and temperature dependence of Mossbauer spectra of polymer phase containing iron it was proposed the presence of different compounds like β-FeOOH, α-Fe_2O_3, and jarosite mineral type compounds: $(R_4N,H_3O)[Fe_3(OH)_6(SO_4)_2]$ or coordination modes: {RCOO-Fe(L_4)-OOCR}$^{1+}$, {R-CO_2=Fe(X_2)=O_2C-R}n, {R-COO-Fe(X_4)-OOC-R}n, and {(-NCH2CH2N-)= Fe(X_2) =(-NCH_2CH_2N-)}, where X= H_2O, OH-, SO_4^{2-}., n= from 3- to 1+. In special conditions the ultrafine superparamagnetic particles of Fe_2O_3 have been obtained.

Keywords: ion exchangers, Mossbauer spectra, iron, superparamagnetic, complexes, polymer phase.

Introduction

Reticulated ionic polymers produced in large amounts by chemical industry are widely used as ion exchangers in the water treatment of thermal and nuclear electric power plants, in waste-water and gas purification, in separation and concentration of substances, as well as in acid-basic catalysis. The ion exchange process is conditioned by electrostatic Coulomb interactions between atoms with definite electrical charges located in the polymer matrix and mobile ions (contrioni). Therefore, this process is virtually no selective in retention of micro-molecular ions.

In many cases the ion exchange is accompanied by other secondary, often uncontrolled, processes that affect polymers during their use. The ion exchangers are frequently poisoned by iron compounds, which results in reduction their service life and involve considerable additional expenses on chemical reagents and water for their regeneration [1-3]. Often the processes of the ion exchangers "poisoning" are irreversible [3]. All types of ion exchangers are "poisoned" by iron compounds. Poisoning via iron compounds presence can occur even during exchangers' production [4] by acids or bases solutions, not enough pure [5].

Reticulated ionic polymers containing electron donor atoms (amino groups, phenolic, carboxylic, etc..) can simultaneously participate to complexing mechanisms besides ion exchange process, too. Complexing metal cations by poly-ligands is a relatively new direction in the chemistry active polymers [6.7].. The synthesis of metal compounds in the form of ultrafine particles in the polymer phase is considered to be a new direction in physical chemistry of chemically active polymers [8, 9]. Polymers loaded with metallic compounds significantly change their physico-chemical properties. They can become catalysts [10], selective sorbents [11-14], biochemical models of transport substances [15] as well as models for experimental research of relaxation processes [16]. In order to use the metal containing polymers in different physical or chemical processes – it is necessary to know and to control the conditions of loading these metal compounds and, especially to induce the right metal cation state in the polymer phase. Knowing exactly the ions' state in polymer phase is quite difficult for several reasons. Firstly, the polymers of this class are amorphous and reticulated, which limits the number of suitable investigation methods. Secondly, the loading processes of reticulate ionic polymers with metal compounds gives simultaneously rise to other concurrent processes, and an ion exchange is generally required.

These processes depend on several factors such as nature and concentration of electrolyte, temperature, pH of the solution, contact time with the polymer solution. The processes evolve either in static or in dynamic conditions, while the presence of air in the system, nature and concentration of organic solvent, could directly or indirectly influence the processes of formation of metal compounds inside the polymer. The best methods of studying metal and non-metal ions parameters and properties in the reticulated polymer phase are the Mossbauer spectroscopy, ESR, IR, and magnetic measurements.

Results and Discussion

State of ions in the ionic reticulated polymer phase containing carboxylic groups

As a results of the investigations using potentiometric method and IR spectroscopy [17] it is known that in carboxylic polymer SG-1 type at contact with a solution of 0.003 - 0.5 M Fe (NO_3) 3 in 0.5 M $NaNO_3$ in a pH range 1-2.5 the complexes of the typeare formed.

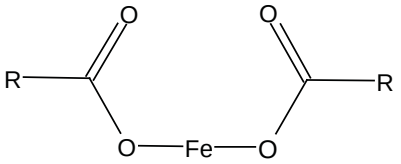

They are stable in the pH range 2.5 ~ 5.0. These complexes decompose in solutions with pH> 7 and γ-FeOOH phase is formed. According to [18], a Fe^{3+} ions from the solution of $FeCl_3$ are retained by the KB-4 polymer as a result of complexing process via carboxylic groups with final formation of a precipitate.

The presence of solvent in the polymer phase leads to increasing of Fe^{3+} ions oscillation amplitude and electric field gradient (EFG) on their nucleus. The solvent (H_2O), which molecules coordinate to metal ions, primarily affects the ion oscillations in chemical bond with ligand, as well as the oscillation of the polymer chain. The non-polar solvent influences primarily, on chain oscillation. Various measurements [19] show that the Mossbauer spectra (MS) of Fe^{3+} ions in carboxylic polymer phase (КБ-2 and others) exhibit doublet patterns. The observed differences, often essential, of iron ions state in carboxylic polymer phase [18-20] confirm that it depends on many factors, which are not always taken into account.

It is surprising that the nature of anions (Cl^-, SO_4^{2-}) influence Fe^{3+} cations complexation with carboxylic groups of cationite. Increasing of the concentration of either Cl^- or SO_4^{2-}anions have induced a diametrically opposite influence on the sorption of Fe^{3+} ions by KB-2 cationite [21].

Sorption of Fe(II) from tartaric acid solutions (0.005 N of Mohr salt, 10 mmol / L of tartaric acid) by KB-2 polymer occurs in the pH range 3-9 with a maximum at pH 6.5. In the polymer phase almost all Fe^{2+} ions being oxidized up to Fe^{3+} [22].

The Fe^{2+} and Fe^{3+} ions in cationite KB-2 phase retained from solutions of 0.005 N $^{57}Fe_2(SO_4)_3$ (pH 2), $FeSO_4$ (inert gas atmosphere, pH = 5), $(NH_4)_2Fe(SO_4)_2$ in 0,01M tartaric acid (pH 5) are found in the high-spin state and in octahedral environment [19]. By keeping in air atmosphere, the oxidation of Fe^{2+} ions in the KB-2 polymer phase ends up to Fe^{3+} is occurred. But the state of oxidized ions differs from the state of Fe^{3+} ions absorbed from the $Fe_2(SO_4)_3$ solution as described in the followings. The Fe^{2+} ions retained from $FeSO_4$ solutions are complete oxidized, and those retained from $(NH_4)_2Fe(SO_4)_2$ solutions are only partially oxidized. Existence of tartaric acid in the system from where the Fe^{2+} ions were detained from contributes to their oxidation during the storage of polymer in the air [19]. Asymmetrical lines in Mossbauer spectra of KB-2 samples, containing Fe^{3+} obtained as a result of air oxidation of Fe^{2+} ions, may be as the results that some Fe^{3+} ions are in the form of precipitate and need supplemental investigation. Although the presence of Cl^- and SO_4^{2-} anions influence in different mode on Fe^{3+} sorption by KB -2, the stabilized state of Fe^{3+} ions practically does not depend on the nature of anions in polymer phase. It is assumed that in polymer phase one part of Fe^{3+} ions is in the form of γ-FeOOH. Fe^{3+} ions from the $Fe_2(SO_4)_3$ solution with pH 1.2 are retained by the KB-2 polymer due to of their complexation with carboxylic groups only. The parameters of Mossbauer spectra of KB-2 samples retained Fe^{3+} ions from solution with pH 1.2 differ for relevancy from those who have retained cations from solution with pH 1.7 - 2.0 [19]. The effected investigations using IR spectroscopy [19] showed that the retention of Fe^{3+} cations from $Fe_2(SO_4)_3$ solutions the complexes of type I are formed in polymer KB-2 phase, but from $FeCl_3$ solutions - complexes of type I and II co-exist.

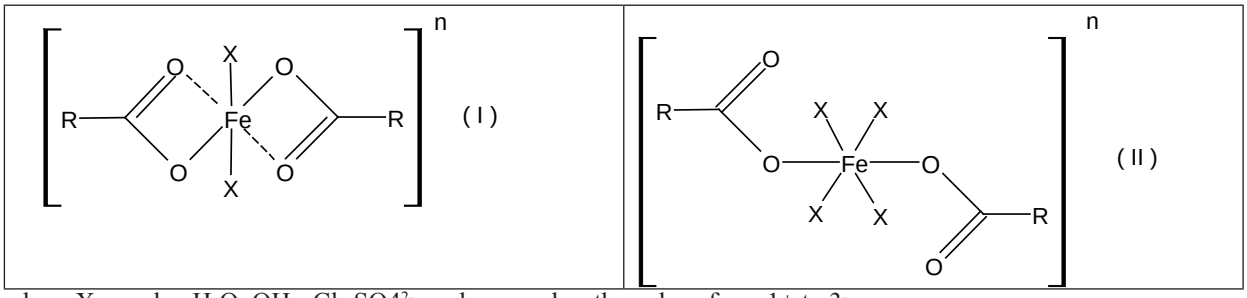

where X may be H_2O, OH-, Cl-,$SO4^{2-}$, and n may has the values from 1+ to 3^-.

State of iron ions in the phase of the anion exchangers containing amine groups

Anion exchangers containing amine groups, are able to retain both hidroxycationes of Fe^{2+} and Fe^{3+} [21], as well as their complexes from the solutions containing tartaric acid [22.23]. Opportunity to observe Mössbauer spectra at 300 K of a wet sample anion exchanger EDE-10P demonstrates unequivocally coordination of ions with amine groups of polymer [24]. The parameters of Mössbauer spectra (δNa+ = 0.62-0.72 mm/s, ΔEQ = 0.72 - 0.79 mm/s (δNa+ - isomer shift relative to sodium nitroprusside as reference substance, ΔE_Q- quadrupol splitting) shows that Fe3+ ions in polymer phase is in a high-spin state and having a somewhat perceptible distorted octahedral environment.

Relatively small values of spectral lines width Γ = 0.52 - 0.56 mm/s and no diffuse broadening of spectra with increasing temperature, especially at $T > T_{melting}$ of ice, also confirms that Fe^{3+} ions in the EDE-10P polymer phase are coordinated with electron donor atoms of poly-ligand matrix. According to the composition of polymer structural unit [4] and the results of publications [24.25] it may be considered that Fe^{3+} ions form compounds of bis-ethylenediamine type in the anion exchanger EDE-10P phase.

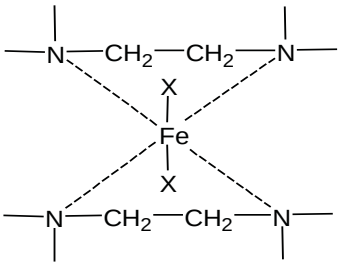

At the retention of iron ions in the anion exchanger AN-2FN phase, containing phenolic groups, secondary and tertiary amines [4.26], from the solution of $Fe_2(SO_4)_3$, Fe^{2+} ions were also detected in the polymer phase, too [27]. The Fe^{2+} and Fe^{3+} ions are in a high-spin state from AN-2FN polymer phase (Table 1).

Table 1

The Mossbauer spectra parameters (± 0.04 mm/s) of plymer AN-2FN after contacting with $Fe_2(SO_4)_3$ solution at different temperatures.

T.K	δ_{Na+}	ΔE_Q	Γ	δ_{Na+}	ΔE_Q	Γ	α f´	Fe^{2+}(%)
	Fe^{2+}					Fe^{3+}		
333	-	-	-	0.67	0.65	0.52	1.0	-
295	1.32	2.68	1.56	0.69	0.78	0.69	2.0	-
273	1.33	2.75	1.55	0.69	0.78	0.7	2.3	-
234	1.56	3.14	0.62	0.75	0.79	0.8	3.3	23
198	1.57	3.19	0.55	0.77	0.79	0.77	3.5	23
173	1.61	3.29	0.45	0.77	0.80	0.76	3.5	21
123	1.60	3.29	0.53	0.79	0.81	0.78	3.6	27
80	1.64	3.37	0.54	0.82	0.85	0.80	3.5	28

Note: α f´- a prportional value of Mossbauer effect probability (f´) for integral spectrum.

For Fe^{2+} (Tab.1) ions the sharp and essential increasing of line width (Γ) at T> 273 K is related to diffusion of these ions to the active centers of polymer.

The shape of Mössbauer spectra and their evolution with temperature (Fig. 1), seems at the first glimps to correspond to mixed valence iron complexes ($Fe^{2,5+}$). However a thorough analysis of the results does not confirm this assumption. The sharp diminution of the Mössbauer effect probability for Fe^{2+} at T> 273 K is probably determined by increasing of amplitude of oscillation of the polymer chain (scheme A) affecting the Debye temperature of the whole entity. The Fe^{3+} cations form compounds with a reduced occurrence of chain oscillation (Scheme B) in the polymer.

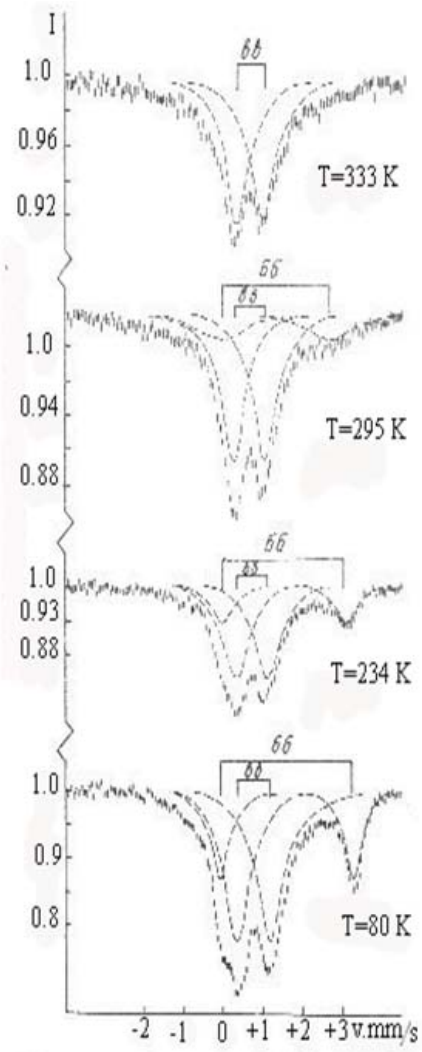

Fig. 1. The Mossbauer spectra of polymer AN-2FN retaiting the iron ions from the solution of $Fe_2(SO_4)_3$ at different temperatures.

At treating of polymer sample by 3% H_2O_2 solution a part of Fe^{3+} ions is reduced up to Fe^{2+}. In this case the Mössbauer effect fraction is not zero at 300 K. So, the vibration amplitude of Fe^{2+} in the coordinative node B is lower than in A, i.e strongest bonded in composite lattice.

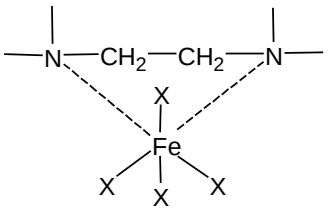

(A)

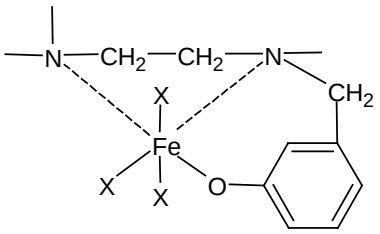

(B)

,

where X may be H_2O, OH^-, SO_4^{2-}.

Putting in contact a water - acetone solution and the sample of polymer EDE-10P, which contains Fe^{3+} from solution of $FeCl_3$, the Mossbauer spectra parameters δ_{Na+} and ΔE_Q have constant values both at 80 as well as 300 K [24], in the whole range of concentration of acetone from 0 to 100%. When dealing with the EDE-10P sample and water - ethanol solution the ΔE_Q value remains virtually constant throughout the all range of concentrations of ethanol, but the δ_{Na+} value is noticeable changed, especially at ~ 10-15% of ethanol [24].

Perhaps this change in δ_{Na+} value at this peculiar concentration of ethanol, is determined by the change of the solution structure [28.29]. The Mossbauer fraction data f'_{300}/f'_{80} (where f'_{300} şi f'_{80} is expressing Mossbauer effect probability at 300 and 80 K respectively) indicate that with increasing the acetone concentration and, especially, the ethanol ones in their solution with water the vibration amplitude of Fe^{3+} ions is decreased [24]. Enhancing the organic component concentration in solution gives rise to augmentation of the relaxation time, which, considering the low iron content in the polymer phase (15 mg / g), it seems to be most probably of spin-lattice type. This rezoning is confirmed by comparing Γ_{80K} = 0.57 mm / s and Γ_{300K} = 0.40 mm/s for EDE-10P probe containing Fe^{3+} after its treatment with 100% acetone.

The experimental data show that the nature and concentration of anions in solution influence on Fe^{3+} ions sorption by anion exchangers containing weak basic groups [21.30]. Taking into account the high concentration of anions in the anion exchangers phase (up to 5-8 M) one may assume that some anions coordinate to Fe^{3+} ions bounded with groups-ligands of polymer. But the performed investigations using Mossbauer spectroscopy [31] did not provide clear detection of any influence of anions ClO_4^-, NO_3^-, Cl^-, SO_4^{2-} on electronic state of Fe^{3+} ions retained by the polymer EDE-10P. This fact does not exclude anions coordination to Fe3+ ions in the anion exchanger comprising weak basic groups. The state of Fe^{3+} ions in the EDE-0P polymer phase is determined by ethylenediamine groups and presence of water molecules or OH^- ions in solution and practically doesn't change it. A similar trend for δ_{Na+} values was observed for the addition of ethylenediamine to solutions of Sn(IV) halides [32].

Anions possessing red-ox or complexion character could change essentially the state of iron ions in the anion exchanger phase. When processing with Na_2S solution the majority of Fe^{3+} cations from the EDE-10P polymer phase to Fe^{2+} [33]. Reduction of Fe^{3+} ion the complexes with EDE-10P poly-ligand is blocked when FeS is formed. The FeS compounds appears as ultra fine particles which freely diffuse into the liquid phase of polymer and at $T > T_{melt}$ of ice, f' = 0. After prolonged exposure to air a part of Fe^{2+} ions are again oxidized to Fe^{3+}. If one assume that the parameter f' has the same value in the initial wet sample, for Fe^{2+} and Fe^{3+} at 80 K, then the Fe^{2+} ions are 74% and Fe^{3+} - 26%. Checking

sample storage in air after 6 days, 1 and 6 months the amount of Fe^{2+} is continuously decreased to 62, 55.5 and 46%, respectively.

In the polymer phase during the storage of a sample in air the processes (1) – (3)

$$2\,[(R_3N)nFe]^{3+} + 3S^{2-} = 2FeS + S + 2n\,R_3N. \quad (1)$$

$$4FeS + 3O_2 + 2\,H_2O = 4FeOOH + 4S \quad (2)$$

$$2FeOOH + 3H_2S = 2FeS + 4H_2O + S \quad (3)$$

take place analogous to those described in [35]:

Depositing in air the EDE-10P sample processed with Na_2S solution the increase of particle size and modification of structure of compounds containing iron has involved a change the Mossbauer parameters δ_{Na+}, ΔE_Q, Γ and f′ as deduced from experimental spectra.

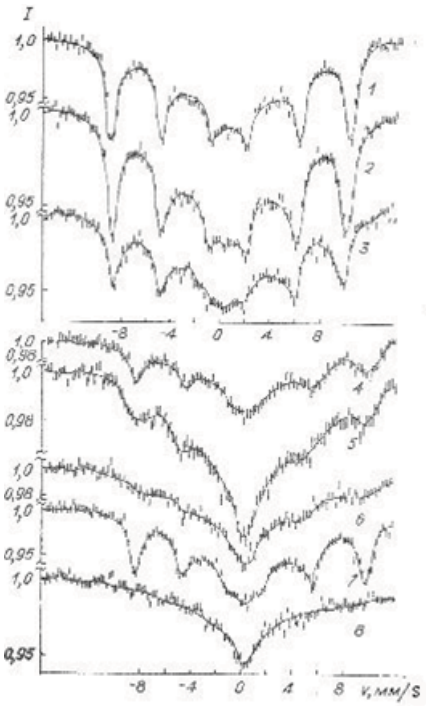

Fig.2. Mossbauer spectra of wetted EDE-10P polymer containing Fe(III) after treated with NaF solution at 80 (1), 116 (2), 150 (3), 172 (4), 209 (5) and 230 K (6), and a dry sample in air at 80 (7) and 300 K (8).

The low temperature Mossbauer spectra of EDE-10P sample, that retained iron ions from the $Fe_2(SO_4)_3$ solution after treating with NaF solution, are characterized by appearance of the magnetic hyperfine structure (MHS) [33]. In the EDE-10P polymer phase the paramagnetic Fe^{3+} ions are in spin blocking state and in this case the magnetic hyperfine structure is evidenced through a slow relaxation of the electronic spin [35]. With increasing temperature T> 80 K the electronic spin relaxation time of Fe^{3+} ions in the wetted EDE -10P polymer phase is diminished and from T> 230 K the MHS lines merge into a singlet component (Fig. 2) reflecting a very fast and complete relaxation of spins.

The ground term (^6S) of Fe^{3+} ions in the polymer processed by solution of NaF is spitted due to ligands crystalline field into three Kramers doublets S = ±5/2, ± 3/2 and ±1/2, which all are populated by electrons. With increasing temperature the spectral lines of the magnetic hyperfine structure (MHS) sextets became larger, but do not change sensibly their position. Since the Fe content in the EDE-10P polymer phase is small, around 2%, and taking into account the results from [16], it may be as above inferred that the evolution of MHS is characterized by a spin – lattice relaxation type.

Fluor anions completely destroy the Fe(III) compounds with groups-ligands of EDE-10P polymer as derived from Mossbauer spectra (at T> 230 K, f′ = 0 for damp sample) [34]. For air dry sample of EDE-10P the relaxation time remains quite high. In this case the formed Fe(III) compounds are located near the functional groups of the polymer. The values of δ_{Na+} = 0.70 ± 0.15 mm / s and H_{ef} = 580 ± 10 kOe (H_{ef} - effective magnetic field intensity on Fe^{3+} nucleus) indicate that iron compounds with F-anions in the polymer phase contain Fe^{3+} ions in the high-spin state and hexagonal coordination environment according to the data from [36]. Furthermore, the symmetrical ESR spectrum, with the relatively narrow spectral line (ΔH = 104 Oe at semi height) and g = 2.005 (77 K) [33], allows, according to [37], to consider that in the EDE 10P polymer phase which contains Fe (III) when processing it by the NaF solution then the $[FeF_4\,(H_2O)_2]^-$ ions are formed and subsequently are retained by the polymer as a result of Coulomb interactions.

The iron ions state in outspent ion exchangers during water treatment

Using Mossbauer spectroscopy it has been investigated the ion exchangers KU-2 and AN-31 which were depleted in water treatment in the first step and the AV-17, Varion - AD - in the second step of the Moldavian thermoelectric station [37.38]. Since the iron content in these polymers was relatively small (0.5 to 2.75 mg / g) the polymer samples were thermally treated in air at different temperatures up to 550 °C. The Mossbauer spectra of AV-17 sample are shown in Fig. 3, and the parameters of Mossbauer spectra of AV-17 and Varion-AD samples in the Table 2.

The MS parameters show that in the phase of mentioned-up polymers iron is in the ultrafine particles of β-FeOOH, which during the thermal processing of polymer are transformed in γ- then α-Fe_2O_3. According to [39] the transformation of iron(III) oxohydroxide to α-Fe_2O_3 passes across the formation step of a paramagnetic phase x-Fe_2O_3 particles with $d_c = 80 \pm 20$ Å (d_c – is critical diameter). When the particles have $d > d_C$ the x-Fe_2O_3 is transformed to γ - Fe_2O_3, and when the particles become more massive (~ 300 Å) - to α-Fe_2O_3. With decreasing of particle size of Fe(III) -oxide at $d < d_C$, in case of presence of superparamagnetism, outer sextet lines of the Mossbauer spectra became wider but reduced their intensities and are moving inward to the center until a broad relaxing singlet is formed [40]. Since the superparamagnetic state depends not only of particle size but also of temperature. In the case when the particles dimensions are slightly larger than the d_C the superparamagnetic state of magnetic ordered particles appears when the temperature is increasing. Such a situation was observed in the MS with increasing temperature from 300-370 K for used-up Varion -AD sample previously thermally treated at 550°C (Fig. 4) [37].

Therefore it can be concluded that there are ultrafine particles of Fe_2O_3 in the used-up and heat treated at 550°C Varion -AD polymer phase as well as there are β-FeOOH ultrafine particles in the exhausted but not heat-treated polymer.

It is known [41], that β-FeOOH is chemically more inert than other FeOOH allotropic forms, which makes difficult for regeneration of ion exchangers. The chemical stability of β-FeOOH can be explained not only by its special structure, but also due to the fact that the Cl-ions enter in its composition [41.42]. The investigations [43] have demonstrated that in this case the composition of precipitate consist of "β-FeOOH + β-FeOOH(CL)" and has the anion exchange properties. The anions with 1- charge (NO_3^-) substitute the Cl^- ion from β-FeOOH easier than anions with larger charge (SO_4^{2-}).The anion exchange capacity of β-FeOOH depends on pH and at pH 3 it is a 1 mmol (Cl^{1-})/ g [44].

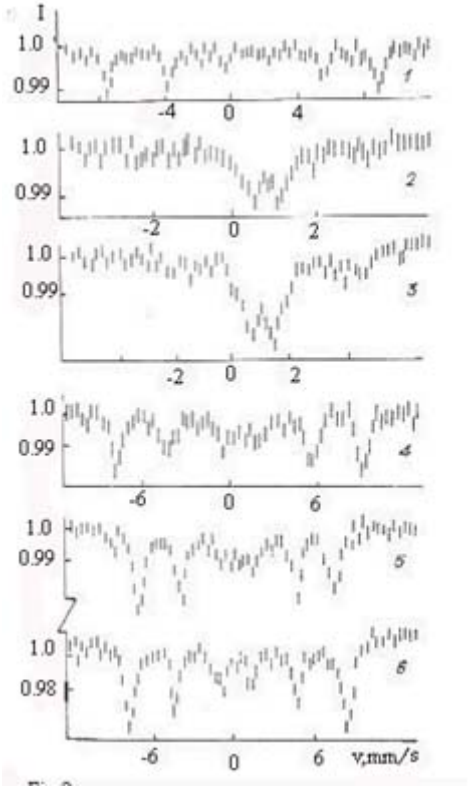

Fig. 3. Mossbauer spectra at 80 (1,4) and 300 K(2,3,5,6) of outspent AV-17 sample after thermo processing at 20 (1,2), 160 (3), 260 (4,5) şi 550°C (6).

It is necessary to mention, that after clearing the cause of earlier used-up limit for ion exchangers, the water source alimentation at the Moldavian thermoelectric station was changed.

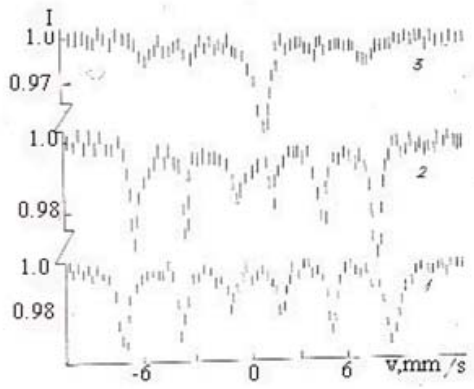

Fig.4. The Mossbauer spectra obtained at 80(1), 300 (2), and 370 K(3) of exhaustive Varion–AD anionit thermoprocessing at 550°C.

Table 2

The Mossbauer spectra parameters of termo processing anionites at 300 and 80 K (in brackets).

t, ^{0}C	δ_{Na+}, mm/s	H_{ef} , kOe	δ_{Na+}, mm/s	H_{ef} ,kOe	compusul
AV-17			Varion-AD		
20	0,62 (0,62)	0 (492,5)	0,62 (0,62)	0 (480)	β-FeOOH
160	0,74 (0,68)	0 (448)	0,63 (0,70)	0 (486)	β-FeOOH
260	0,63 (0,71)	492 (518)	0,69 (0,71)	477 (512)	γ-, α- FeOOH
350	0,70 (0,65)	515 (543)	0,55 (0,60)	492 (540)	γ-, α- FeOOH
450	0,84 (0,77)	508 (546)	0,86 (0,98)	497 (528)	α- FeOOH
550	0,72 (0,78)	517 (512)	0,74 (0,69)	528 (528)	α- FeOOH

The iron ions state in the ion reticulate exchangers phase containing strongly basic groups

The monofunctional anion exchangers containing strongly basic groups (R_4N^+), do not containing in their matrix the atoms with negative charge or electron donors. In this case, theoretically, they are not entitled to retain cations from solution in static conditions. But in dynamic conditions, being in OH^- form, they can retain the metal cations which are readily hydrolyzed and forming hydroxides [31]. However, surprisingly, it was demonstrated [8.21], that such polymers can retain hydroxocations of Fe (III) in the static conditions from the sulphate solutions with pH = 2.0 at equilibrium. In the same conditions these polymers do not retain hydroxocations of Fe(III) from the solutions of $FeCl_3$ or $Fe(NO_3)_3$. The curve of the Fe (III)-containing cations sorption from sulphate solutions on anion exchangers AV-17 (containing R_4N^+ group) and Varion-AD (containing R_4N^+ and ROH groups) vs. temperature passes through maximum Fig. 5) [45].

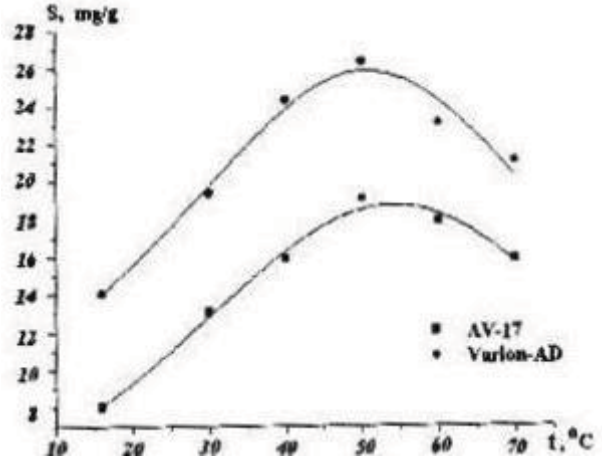

Fig. 5. The temperature dependence of Fe(III) sorbtion by AV-17 and Varion – AD polymers.

Anyhow, it can be affirmed that the retention of cations by anion exchangers containing strongly basic groups is a chemical process and not a physical one. Sorption of Fe(III) cations by strongly basic polymers takes place in a medium (polymer phase) with relatively high concentration of SO_4^{2-}anions, and in principle could form anionic complexes inside the polymer phase, which will be electrostatically retained. But it is well known that the ion exchange is the process which almost does not depend on temperature.

As it is shown in [8] in the AV-17 polymer phase which was in contact with $Fe_2(SO_4)_3$ solution (pH 1.7 and concentration from 0.03 to 0.06 N), there is a solid iron(III) compound (doublet in the Mossbauer spectrum) and $[Fe(H_2O)]^{3+}$, $[FeOH(H_2O)_5]^{2+}$ (sextets in the spectrum). The dimmer ions of oxo-or hydroxocomplexes of Fe (III) ions in polymer phase were not detected. There is only one type of solid Fe (III) compound in the polymer phase after contacting with $Fe_2(SO_4)_3$ solution at pH 1.85 - 2.00. The parameters of Mossbauer spectra of these compounds (ΔE_Q = 1 mm / s) are close to corresponding parameters which are characteristic to Jarosite mineral: $A[Fe_3(OH)_6(SO_4)_2]$, where A may be = Na^+, K^+, H_3O^+ , NH_4^+ and other cations [46.47], or hydrated compound $FeOHSO_4$ [46-48]. The compounds like Jarosite mineral type are obtained during hydrolytic precipitation of Fe^{3+} ions in the presence of SO_4^{2-} anions [48.50].

The Jarosite mineral is not notably stable in the normal atmospheric environment, partially transforming in to $Fe(OH)_3$ [50]. The $Fe_2(SO_4)_3$ solution interacts with freshly precipitated $Fe(OH)_3$ giving rise, in dependence of

temperature, to soluble or insoluble $FeOHSO_4$ [51.52]. The Jarosite mineral type compounds are stable up to about 230^0C on heating in air, and at T> 230^0C one of the thermodecomposing products is $FeOHSO_4$ [53]. Following the thermal dehydration of $FeOHSO_4$, the ΔE_Q value grows considerably. Boiling in water the iron(III) compounds such as Jarosite are transformed into α-FeOOH in superparamagnetic state [47].

Under thermal treatment in air up to 200^0C of Fe (III) Jarosite mineral type compounds in the AV-17 polymer phase the red-ox processes take place and the Fe (II) compounds as well as stable libber radicals are formed [54]. Mossbauer spectra parameters of AV-17 sample containing Jarosite do not change essential when the sample was heated up to 180^0C. So in the AV-17 polymer phase there is not formed $FeOHSO_4$ when it is in contact with solution of $Fe_2(SO_4)_3$. Furthermore, when boiling in aqueous medium the Jarosite from polymer phase is converted to ultrafine particles of FeOOH showing superparamagnetic state.

During a few cycles "sorption of Fe (III) then boiling in water", one part of the magnetic particles become relatively large and magnetically ordered, while another part remains in superparamagnetic state due to location in narrow pores of the polymer [55]. In the solution of $Fe_2(SO_4)_3$ with pH 2.0 there are $[Fe(H_2O)_6]^{3+}$, $[FeOH(H_2O)_5]^{2+}$ and $[Fe_2(OH)_2(H_2O)_8]^{4+}$ions [55.56]. The dimeric hydroxocomplexes were not detected in the polymer phase via contacting with $Fe_2(SO_4)_3$solution. These complexes are hardly changed to organize in new structural units [57]. The $[Fe(H_2O)_6]^{3+}$ ions does also not directly participate in the formation of compounds like Jarosite mineral. So in the polymer phase the $[FeOH(H_2O)_5]^{2+}$ ions participate to the formation of compounds of Jarosite mineral type:

$$R_4N^+ + 2\ SO_4^{2-} + 3\ [FeOH(H_2O)_5]^{2+} + 3\ OH^- \leftrightarrow R_4N[Fe_3(OH)_6(SO_4)_2] + 15\ H_2O \quad (4)$$

$$H_3O^+ + 2SO_4^{2-} + 3\ [FeOH(H_2O)]^{2+} + 3\ OH^- = H_3O[Fe_3(OH)_6(SO_4)_2] + 15\ H_2O \quad (5)$$

In boiling aqueous solution the iron compounds such as mineral Jarosite decompose according the scheme (6):

$$2\ R_4N[Fe_3(OH)_6(SO_4)_2] = (R_4N)_2SO_4 + 6\ \beta\text{-}FeOOH + 3\ SO_4^{2-} + 6\ H^+ \quad (6)$$

Jarosite mineral formation can take place only in the presence of water. When this mineral was found on Mars it was deduced that water is present there too and latter confirmed.

The Jarosite mineral type compounds are formed as layers of 3 or 6 octahedral cycles [49]. The OH- groups are located in the equatorial plane, forming a bridge between metal ions and SO_4^{2-}groups are located in axial position, each coordinating 3 metal ions of 3 octahedrons.

The Jarosite mineral type compounds presence in polymers phase changes essentially their physical-chemical properties. The R_4N^+ and H_3O^+ ions from compounds can be exchanged with different cations but at the same time the anions SO_4^{2-} connect with different other anions or molecules able to form coordination bonds with the central metal ions.

The alunit type mineral $K[Al_3(OH)_6(SO_4)_2]$ is izostructural with Jarosite mineral. So, at contacting with $Al_2(SO_4)_3$ solution in the phase of strongly basic anion exchangers it may be formed compounds such alunit [13]. Moreover, in the analogical conditions it may be formed compounds like Jarosite mineral type containing other cations species which differ of Fe3+ or Al^{3+} [12].

The reticulated ionic polymers containing in their matrix not only strongly basic groups, but other chemically active functional groups such as - COOH,-CN etc, also may retain metal cations (M^{3+}) from the solutions of sulfate as a result of training compounds like Jarosite mineral, as well as function of coordination with electron donor atoms of the polymer [58].

Conclusions

To understand more deeply the formation of metal compounds in chemical active reticulate polymer phase and the processes connected with utilization in different areas of these composites uploaded with metallic compounds polymers it is imperiously required their investigation using various complementary physical methods, including Mossbauer spectroscopy in special.

Acknowledgements

The authors gratefully thank Silvia Melnic and Dumitru Sirbu for assistance provided in preparation of this manuscript.

References

[1]. Visotskii, S.P.; Peaterikov, V.V.; Kopilova, O.N. Teploenergetika. 1982,.№7, 58-59. (rus.)

[2]. Method of cleaning of sulfonated from iron oxides / AM Dedyukhin / Bul.Izobr.1979,. № 8, 26. (rus.)

[3]. Foshko. Increased reliability and efficiency water chemical conditions, ways to simplify the technological schemes and lowering the cost of water treatment at the units S.K.D. and large TETS S.D.V; Leningrad: CKTI II Polzunova. 1973, 128-134 (rus).
[4]. Saldadze, K.M.; Pashkov, A.B.; Titov V.S High-molecular-weit ion exchange.materials, Goskhimizdat: Moscow, 1960. 356 (rus.)
[5]. Nazarova, R.S.; Sandar, A.A.; Andreev, M.B.; Kovalev, M.P. Plastics. 1974, № 4, 72- (rus)
[6]. Gutsanu V.L. Doct.Habilitat. Thesis, State University of Moldova. Chisinau, 1993 (rus.)
[7]. Saldadze, K.M.; Kopylova-Valova, V.D. Complex-forming ion exchangers (kompleksities). Chemistry: Moscow, 1980. 336. (rus.)
[8]. Gutsanu V.L.; Turta, C.; Gafiiciuc, V.A.; Shofranski, V.N. Russ. J. Phys. Chem. 1988, T.62. pp.2515-2422. (rus.)
[9]. Gutsanu V.L. Chemistry and Technology of Water.1990, T.12. .№12 pp. 1074-1097. (rus.)
[10]. Copylova, V.D.; Astanina, A.H. Ion exchanger complexes in catalysis. Chemistry: Moscow. 1987 . 191 (rus.)
[11]. Guțanu V., Druță R. Procedeu de obținere a ioniților modificați. Brevet de invenție, MD 810. // BOPI, 1997,nr.8, p.24-25
[12]. Guțanu V., Druța R. Procedeu de moificare cu Cr(III) a polimerilor ionogeni reticulați ce conțin grupe R4N+ . Brevet de invenție, MD 1027. // BOPI,1998. nr.9. p.23
[13]. Guțanu V., Druța R. Obținerea sorbenților selectivi pentru sorbția coloranților alimentari din soluții // Materialele I simposion internațoinal "Biochimie şi biotehnologii în îndustria alimentara " .Chişinău. Tehnica –Info.2002. p.210-215
[14]. Guțanu V., Cojocaru L. Procedeu de obținere a sorbentului selectiv care conține compuşi de Bi (III) . Brevet de invenție, 32.95 MD . // BOPI, 2007,nr.4, p.42-43
[15]. Suzdalev, I.P. Gamma-rezonance spectroscopy of proteines and model compounds. Nauca: Moscow. 1988. 262 pp. (rus.)
[16]. Suzdalev, I.P.; Afanasiev, A.N.; Placinda, A.S.; Golidanskii, V.I. Journ.Exper. and Theor. Physics. 1968, 55. 1752-1765 (rus).
[17]. Laskorin, B.N.; Ligvinenko, I.A.; Fedorova, L.A.; Ashurkova, C.B. Journ. Anal. chemistry. 1969.T.42. № 6, s.1320-1325 (rus.)
[18]. Suzdalev, I.P.; Plachinda, A.S.; Makarov, E.F.; Dolgopolova, V.A. Russ. J. Phys. Chem. 1967, V.41, № 11. 2831-2837 (rus.)
[19]. Gutsanu, .VL.; Turte, K.I.; Muntean, S.A. et al Russ. J. Phys. Chem 1990, 64, № 2, 479-487 (rus.)
[20]. Dzevitsky B.E., Zviadadze GN, Margulis, VB et al. Russ. Coord. Chem. 1977,3, № 7, 643 - 647 (rus.)
[21]. Gutsanu, V.L.; Gafiychuk, V.A. Russ. J. Phys. Chem 1986, 60,1824-1826. (rus.)
[22]. Gutsanu, .VL.; Muntean, S.A.; Turte, K.I Bull. AN MSSR, Ser. biol. and chem. science.1980, N:2, 73-79(rus.).
[23]. Gutsanu, .V.L.; Dogaru G.N. Russ. J. Phys. Chem. 1985, 54, №8, 2098-2101 (rus.).
[24]. Gutsanu, .V.L.; Turte K.I.; Stukan, R.A.; Gafiychuk, V.A. Russ. J. Phys. Chem. 1985, 59, № 3, 693-696 (rus.)
[25]. Safin R.Sh.; Gutsanu, .V.L.; Vishnevskaya G.P. Russ. J. Phys. Chem. 1987, 61, №8, 2134 - 2138(rus.).
[26]. Lurie, A,L. Sorbents and chromatographic carriers. Nauka: Moscow. 1972. 320 pp. (rus.)
[27]. Turte KI, Gutsanu, .V.L.; Bobkova, SA etc. The study of complexation of iron ions on the anion exchanger AN-2FN / . Izv.Acad.Nauk MSSR. Ser. biol. and chem. science.1980, 4, 54-60 (rus.).
[28]. Krestov, G.A.; Klopov, V.I.; Patsatsia, K.M. Journ. Strukt. Chemistry .1969, 10, № 3,417-422 (rus).
[29]. Buslaeva, M.N.; Samoilov, O.Y. Journ. Strukt. Chemistry. 1963,4, № 4, 502-505 (rus).
[30]. Gutsanu, .V.L.; Gafiychuk, V.A. Chemistry and Technology of Water. 1989, T.11, № 7, 584-588 (rus). .
[31]. Gutsanu, .V.L.; Stukan, R.A., Turte, K.I., Gaftychuk, V.A. Russ. J. Phys. Chem. 1986, T.60, C.936-940 (rus).
[32]. Gol'danskii, V.I.; Makarov, E.F.; Stukan, R.A. Proc. AS USSR. 1964, T.156, № 2, C.400-403 (rus).
[33]. Gutsanu, .V.L.; Gafiychuk, V.A. Russ. J. Phys. Chem. 1990.64, № 2, 488-494 (rus).
[34]. Astanina, A.N.; Fung, Chi Chi; Rudenko, A.P., etc. Russ. J. Phys. Chem. 1983, 57, № 6, 1397-1399 (rus).
[35]. Chemical Applications of the Messbauer Spectroscopy, Ed. VI Gol'danskii, R.Herber. Mir: Moscow.1970 (rus).
[36]. Edwards, R.P., Johnson, C.E. J.Chem. Phys.1968, v.49, №1, p.211-216.
[37]. Gutsanu, .V.L.; Turte, K.I.; Labunskaya N.Y. Russ. J. Phys. Chem. 1987, 61, № 1, 170-174 (rus).
[38]. Gutsanu, .V.L.; Turte, KI, Labunskaya N.Y. Chemistry and techn. of water. 1987, T.9, № 6, 514-517(rus).
[39]. Krupyansky, Y.F.; Suzdalev, I.P. Journ.exper. and theor. phys. 1973, 65, № 4, 1715-1725 (rus).
[40]. Suzdalev, I.P. Solid State Physics. 1970, 14, № 4, 988-990 (rus).
[41]. Wever, I.E.; May, L.A., Bull. AS Lat. SSR. Ser. Chem.,1979, 2, 147-153 (rus).
[42]. Borggard, O.K. Acta Chem. Scand . 1988, A37, №2, 169-171
[43]. Gutsanu, .V.L.; Labunskaya, N.Y. Russ. J. Phys. Chem.. 1986, 60, №12, 3113-3116(rus).
[44]. Paterson Russeli, Rahman Habibar. J. Colloid. Interface Sci. 1983, 94, №1, 60-69.

[45]. Gutsanu, V., Raisa Drutsa, Rusu V. Reactive and Funct. Polym., 2001, 46, 203-211
[46]. Hrynkiewicz, A.Z., Kubisz, I., Kulgawczuk, D.S. J. Inorg. Nucl. Chem. 1965, 27, №12, 2513-2517.
[47]. Matashige Ohyabu, Iusuke Ujihira .J. Inorg.. Nucl. Chem. 1981, 43, 1948 -1949.
[48]. Morais, P.S.; Neto, K.S. Polyhedron. 1983, 2, № 9, 875-880.
[49]. Archipenko, D .K, Deviatkina, ET, Palchik, NA, Crystallochemical particularities of synthetic jarosites. Novosibirsk, Nauka 1987.
[50]. Betekhtin, AG, Mineralogy. Gos. Acad. Geolog. Litr.: Moscow. 1950. 5-73.(rus.)
[51]. Milner, A.; Zapolsky, A.K.; Ryzhuk, N.P.; Jour.n.Appl. Chem. 1986, 59, 499-504.(rus.)
[52]. Zapolsky, A.K.; Milner, A.; Ryzhuk, N.P. et al. Chem. and Techn. of water.1985, 7, № 6,
[53]. 70-73 (rus).
[54]. Margulis, E.V.; Savchenko, L.A.; Shokarev, M.M.; et al. Russ. J. Inorg. Chem. 1973, 18, № 5, 1263-1269 (rus).
[55]. Gutsanu, V.; Gafiichuk, V.; Shofransky, V.; Turta, C. J. Appl. Polym. Sci., Vol. 99, 59-64.(rus.)
[56]. Fishtik I.F.; Vataman, I.I. Thermodynamics of Metal Ion Hydrolysis. Shtiintsa: Kishinev. 1988) [in Russian].
[57]. Yakubov, J.M.; Ismailov, M.A.; Offengenden E.Y.; Ibragimov, D.C. Hydroxyl complexation in redox systems. Taj. State Univ:: Dushanbe. Issue 3, 5-36 (rus).
[58]. Belozersky, GN, Baikov, M., Boldyrev, VV, et al. Kinetics and Catalysis 1974, 15, № 4, 929-934 (rus).
[59]. Gutsanu, V.; Luca, C.; Neagu, V.; Shofransky, V.; Turta, C. Reactive and Funct. Polym.1999, 40, 123-128.

STOPPED-FLOW SPECTROPHOTOMETRIC STUDIES OF THE KINETICS OF INTERACTION OF DIHYDROXYFUMARIC ACID WITH THE DPPH FREE RADICAL

Natalia Secara

Institute of Chemistry of the Academy of Sciences of Moldova, 3 Academiei str., MD 2028, Chisinau, Moldova
E-mail: natalia_secara@yahoo.com, Phone: 72 97 61

Abstract. The reaction of dihydroxyfumaric acid with the free radical 2,2-diphenyl-1-picrylhydrazyl (DPPH) was studied using the stopped-flow method, in order to describe the reaction kinetics. Dihydroxyfumaric acid reacts very rapidly with DPPH, the reaction being completed in several minutes. This 2-stoichiometric reaction proceeds in two stages, with reaction orders of 1 and 0.76 with respect to DPPH, and 0.5 and 0.3 with respect to DHF, respectively. The rate constant of the two stages of the reaction were found to be 39.1 (L/mol·s) and 0.0012 (s^{-1}) at 20º C and pH 4.0.

Keywords: DPPH; antioxidant activity; stoichiometry; stopped-flow; kinetics; dihydroxyfumaric acid

Introduction

Many studies have reported the carcinogenic and mutagenic implications of oxidative stress or excessive production of reactive oxygen species, resulting in DNA damage [**1**], lipid peroxidation [2], depletion of protein sulfhydryl groups, glutathione levels [3] and other negative effects. Free radical-mediated tissue damage is generally accepted as a major mechanism underlying the occurrence of certain chronic diseases [4].

Antioxidants play an important role in the protection of the cell from oxidants attack by donating hydrogen atoms to the active radicals, while the radicals formed from the antioxidant molecules are stable species that stop the oxidation chain reaction [5]. One of such antioxidants is the dihydroxyfumaric acid (DHF), produced by slow oxidation of tartaric acid. The DHF plays a very important role in nature, as it represents an intermediate compound in the biosynthesis of 3-phosphoglicerinic acid. Also, due to its reducing properties, DHF enhances the taste and odor of wine [6].

In order to estimate the antioxidant activity of many compounds, the DPPH$^{\bullet}$ method has been widely applied during recent years. DPPH$^{\bullet}$ is a stable nitrogen-centered free radical by virtue of the delocalization of the spare electron over the molecule as a whole, so that the molecules do not dimerise, as would be the case of most other molecules [7].

A quantitative analysis of the H-atom transfer reaction from a given antioxidant to DPPH$^{\bullet}$ provides a quite simple way to characterize the reaction kinetics. The H-transfer reactions are monitored by recording the decay of the DPPH$^{\bullet}$ visible absorption band (λ_{max} = 520 nm in 70% methanol at pH 4.0), which reflects the transformation of the DPPH radical into the corresponding hydrazine (DPPH-H) by the antioxidant compound.

In this paper, we explore the kinetic behavior of DHF, in order to build a plausible kinetic model and better understand the mechanism of its interaction with DPPH$^{\bullet}$.

Materials and methods

Reagents

Methanol (>99,8%) was purchased from Fluka. 2,2-Diphenyl-1-picrylhydrazyl (DPPH$^{\bullet}$) was obtained from Sigma and dihydroxyfumaric acid (98%) was from Aldrich.

Spectrophotometric measurements

The H-atom transfer reactions were monitored using an E-100 stopped-flow spectrophotometer (KinTek Corporation, USA). The exact absorbance of each solution was registered before each run using a Lambda 25 UV/VIS spectrophotometer (Perkin Elmer), using 10mm quartz cuvettes. All spectrophotometric data were obtained at room temperature (20 ºC).

Kinetics of reduction of DPPH$^{\bullet}$ by DHF

In order to determine the reaction stoichiometry, different molar ratios, expressed as moles of antioxidant per mole of DPPH$^{\bullet}$, were tested, ranging from 0.1 to 10. For each molar ratio, the remaining concentration of DPPH$^{\bullet}$ at the plateau was determined and graphed, and EC_{50} was read on the graph as the molar ratio which reduces half of the initial DPPH$^{\bullet}$ concentration, was determined from the graph. The number of reduced DPPH$^{\bullet}$ molecules per one molecule of antioxidant was defined as $\sigma = 1/ (2 \times EC_{50})$.

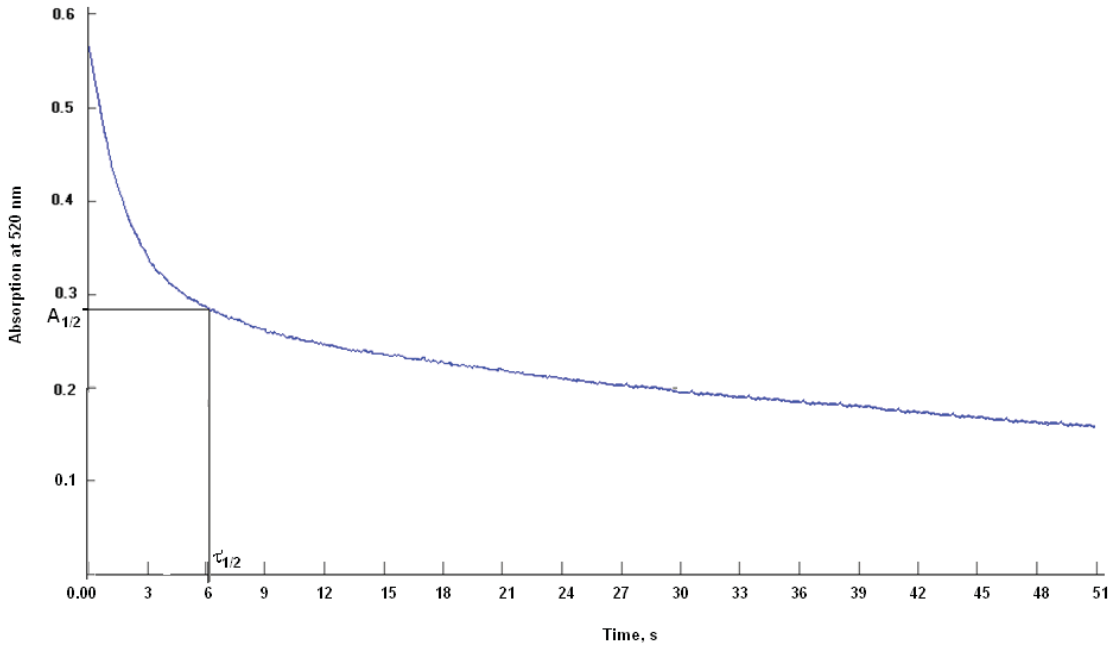

Fig.1. Time evolution of the reaction of DHF and DPPH• when initially Co(DHF) = Co(DPPH•) / σ, where Co(DHF) = $3 \cdot 10^{-5}$ M, and σ = 2.

Fig.1 shows the time evolution of the concentration of DPPH• when it is being reduced by dihydroxyfumaric acid (in the case when initially Co(DHF)= Co(DPPH•)/ σ). As it is observed, the curve which describes the DPPH• decay represents the sum of two consecutive stages. The first stage is similar to that of ascorbic acid [8], corresponding to fast hydrogen atom transfer, while the second stage is somewhat slower. Thus, the stoichiometry of the overall reaction is the sum of two terms: $\sigma = \sigma_{fast} + \sigma_{slow}$, where σ_{fast} and σ_{slow} are the stoichiometric constants for the fast and slow stages of the reaction, respectively.

The rate (v) of a complete reaction between σ moles of DPPH• and one mole of DHF as a function of time (t) is defined by the sum of two terms, describing the fast and slow steps:

$$v = \frac{-dC_{DPPH}}{\sigma \times dt} = k_{fast} \times C^{x}{}_{DPPH} \times C^{y}{}_{DHF} + k_{slow} \times C^{a}{}_{DPPH} \times C^{b}{}_{DHF} \qquad \text{eq.1}$$

where *C* are the initial concentrations, *k* the rate constants, *x, y* and *a, b* the orders with respect to each reactive form. The determination of partial reaction orders is possible using the method of initial rates. Thus, in order to determine the reaction order with respect to DPPH•, the initial reaction rate is determined for various initial concentrations of DPPH•, maintaining the concentration of DHF constant (yet always at least twice lower than the studied concentration of DPPH•). Using eq.1 (for the fast step):

$$v = k_{fast} \times C^{x}{}_{DPPH\cdot} \times C^{y}{}_{DHF} \qquad \text{eq. 1 (a)}$$

after a logarithmic conversion and plotting lg (v) as a function of lg (C_{DPPH}), *x* can be determined from the slope of the linear curve.

Analogically, the reaction order with respect to DHF is determined for various initial concentrations of DHF, maintaining the concentration of DPPH• constant and at least twice greater than the studied DHF concentration. Again, plotting lg (v) as a function of lg (C_{DHF}), *y* can be determined from the slope of the linear curve.

Another way to determine the reaction order with respect to DHF is using eq.1 when initially $C_{DHF} = C_{DPPH}/\sigma$. Using eq.1 (for the fast step):

$$v = \frac{-dC_{DPPH\cdot}}{\sigma_{fast} \times dt} = k_{fast} \times C^{x}{}_{DPPH\cdot} \times C^{y}{}_{DHF} \qquad \text{eq.1 (b)}$$

and after a logarithmic conversion:

$$\lg (v) = \lg (k_{fast} / \sigma_{fast}^{y}) + (x + y) \times \lg C_{DPPH} \quad \text{eq.2}$$

Thus, *y* can be determined from the slope of the linear curve, since *x* is known. Eq.2 makes it possible to determine the rate constant k_{fast}, since $\lg (k_{fast} / \sigma_{fast}^{y})$ is the intersection of the linear curve described by eq.2 and the ordonate axis.

Results and discussion

Experiments were carried out at 20 °C. Taking into consideration the strict requirements for reactions studied by the stopped flow method, the common DPPH• assay was slightly modified: the solvent for the DPPH• and DHF consisted of 70% methanol and 30% of bidistilled water. The solutions of DPPH• and DHF were brought to pH 4.0 by adding acetic acid (respecting the ratio of 70% for methanol). In these experimental conditions, prior to antioxidant activity investigations, calibration curves of absorbance vs. concentration were obtained for the two substances.

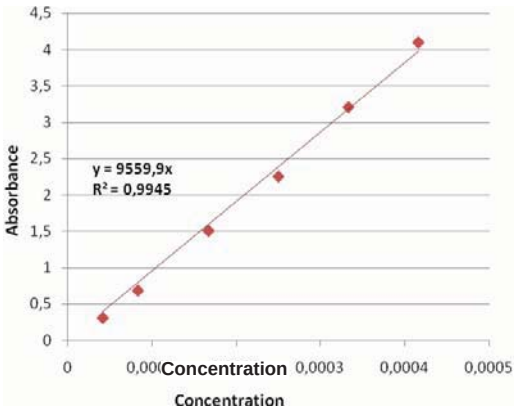

Fig.2.a) Determination of the molar extinction coefficient for the DPPH• radical in the experimental solvent

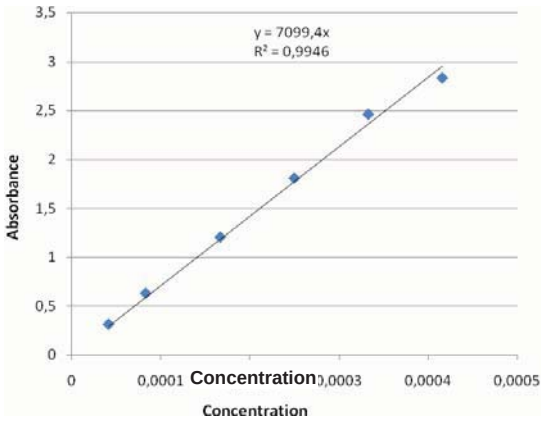

Fig.2.b) Determination of the molar extinction coefficient for the DHF in the experimental solvent

It should be mentioned that DPPH• decay was monitored at 520 nm (not at 515 nm [2] or 517 nm), as in described experimental conditions, the DPPH• absorption spectrum presented a peak at 520 nm.

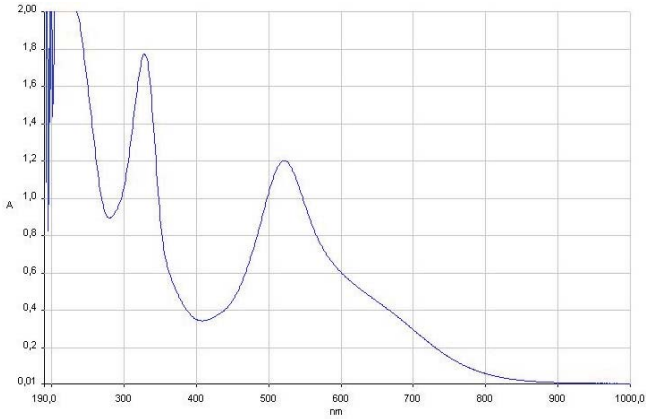

Fig.3. DPPH spectrum in 70% MeOH at pH 4.0

The exact initial concentration of DPPH•, noted Co(DPPH•) (mol/L) was determined using the relationship Co=A/ε, where ε was determined 9560 (Fig.2a). The exact initial concentration of DHF, noted Co(DHF) (mol/L) was determined using the relationship Co=A/ε, where ε in 70% methanol was determined 7100 (Fig.2.b).

The obtained value for EC_{50} was found, according to results presented in Fig.4, EC_{50}=0.24. Therefore, the stoichiometric constant determined for the overall reaction was $\sigma = 1/ (2 \times EC_{50}) = 2.08$, corresponding to the number of freely available OH groups.

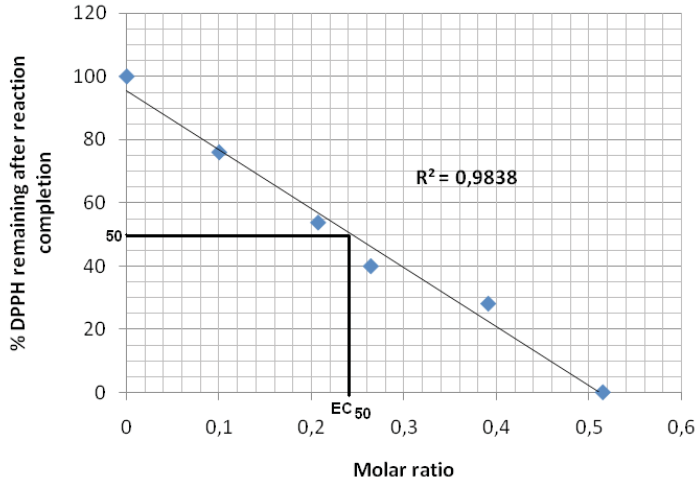

Fig. 4. Determination of the global reaction molecularity

The determined stoichiometric constants for the fast and slow stages of the reaction are σ_{fast}~1 and σ_{slow}~1, i.e. one molecule of DHF interacts very fast with one molecule of DPPH$^{\bullet}$, undergoes transformation and afterwards interacts with a second molecule of DPPH$^{\bullet}$, a lot slower. The chemical structure of dihydroxyfumaric acid suggests the following mechanism of reduction of DPPH$^{\bullet}$:

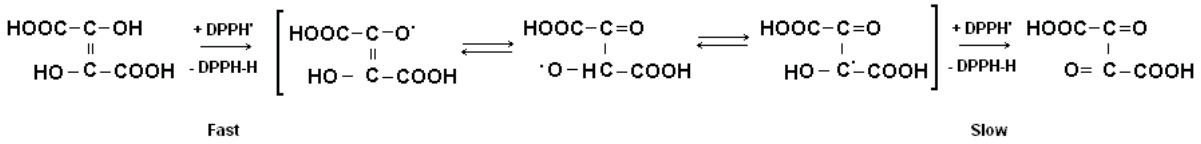

In experiments when initially $C_{DHF} = C_{DPPH} / \sigma$, the fast stage of the reaction was terminated during several seconds (Fig. 1). The reaction orders describing the fast stage of the reaction were found to be x=1 (Fig.5.a) and y~0.5 (Fig.5.b), thus the rate constant was calculated k_{fast} = 39,81 L mol $^{-1}$ s^{-1}. In classical chemical kinetics, the order 0.5 towards DHF implicates the dissociation of this compound prior to the rate determining step [9].

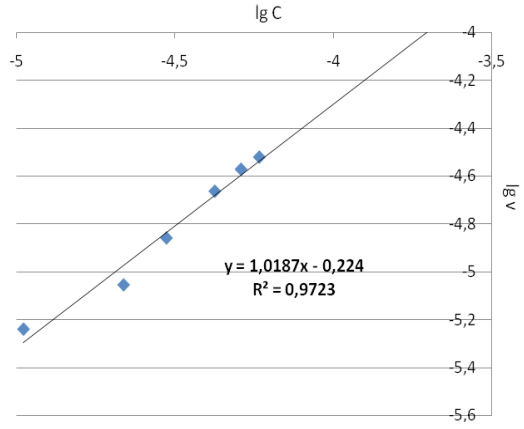

Fig.5.a) Reaction order with regards to initial DPPH$^{\bullet}$ concentration

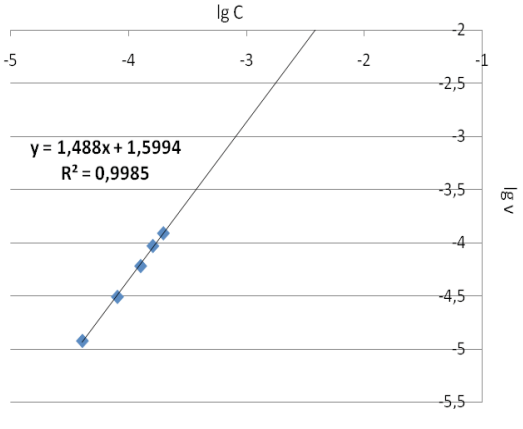

Fig.5.b) Global reaction order for the fast stage of the reaction

The reaction orders describing the slow stage of the reaction were found to be x=0.77 (Fig.6.a) and y=0.28 (Fig.6.b), thus the rate constant is k_{slow} =0.0012 s^{-1}.

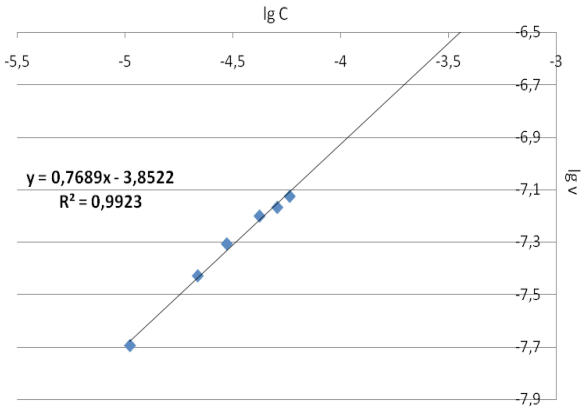

Fig.6.a) Reaction order with regards to initial DPPH• concentration

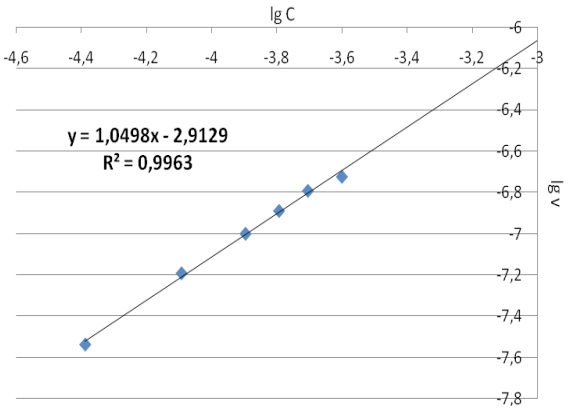

Fig.6.b) Global reaction order for the slow stage of the reaction

Conclusions

The DPPH• assay provides a rapid estimation of the antioxidant activity of chemical compounds. However, in some cases, when the reaction proceeds at a high rate, it is quite difficult (if not impossible) to estimate the reaction kinetic parameters using conventional spectrophotometry. In these cases, the use of stopped flow spectrophotometry allows researchers to get an important insight on the reaction evolution in various conditions.

The dihydroxyfumaric acid proved to have a quite good antioxidant capacity (EC_{50}=0.24). The utilization of stopped flow apparatus allowed us to determine that the reaction of DHF with the DPPH radical proceeds in two consecutive stages, the first being similar to the interaction of ascorbic acid with DPPH•, corresponding to fast hydrogen atom transfer, while the second stage - slower. The overall determined molecularity of the reaction is 2, and the molecularities of the fast and slow stage are each equal to 1. The reaction orders describing the fast stage of the reaction were found to be x=1 (Fig.5.a) and y~0.5 (Fig.5.b), thus the rate constant was calculated 39,81 L mol^{-1} s^{-1}. The reaction orders describing the slow stage of the reaction were found to be x=0.77 (Fig.6.a) and y=0.28 (Fig.6.b), thus the rate constant of the slow stage is 0.0012 s^{-1}.

Acknowledgements: I would like to express my sincere gratitude to my scientific adviser who helped me every step of my research.

References

[1]. Beckman Kenneth B. and Ames Bruce N., The journal of biological chemistry Vol. 272, No. 32, Issue of August 8, pp. 19633–19636, 1997
[2]. Bondet V., Brand-Williams W. and Berset C., Lebensm.-Wiss. u. –Technol., vol 30, pp.609-615, 1990
[3]. Nagy P. and Ashby M. T., Chem. Res. Toxicol. 2007, 20, 79-87
[4]. M. Valko, H. Morris and M.T.D. Cronin, Current Medicinal Chemistry, 2005, 12, 1161-1208
[5]. Ilhami G., Riad E. Akcahan G, Laurent B and Ekrem K., African Journal of Biotechnology Vol.6 (4), pp 410-418, 19 February 2007
[6]. Duca Gh., Gonta M., Mereuta A., Processing and Valorization of Secondary Winery Products, NATO Science for Peace and Security Series C: Environmental Security, Springer Netherlands, 2009, pp 197-207.
[7]. Molyneux, P. Songklanakarin J. Sci. Technol., 2004, 26(2), pp. 211.219.
[8]. Sendra, J.M., Sentandreu E., Navarro, J.L., Eur. Food Res. Technol. 2006, 223, pp. 615-624
[9]. Fremaux, B. Elements de Cinetique et de Catalyse. Paris: Lavoisier, 1989.

ACADEMICIAN CONSTANTIN TURTA - RENOWNED, CONSISTENT, AMBITIOUS, NON-CONFORMIST SCIENTIST.

Mr. Constantin Turta, academician of the Academy of Sciences of Moldova, Professor, Dr. habilitate in chemistry, was born on 20 December 1940, in a hardworking family in the village Buciusca, town New Saharna, district Rezina. This village, according to 2004 census data, is populated by only 263 people.

After graduating the primary school in his native village in 1949 and the school of Rezina in 1956, he is registered at the Faculty of Chemistry, State University of Moldova, and successfully graduates it in 1961. During studentship, he acquires extensive knowledge in all fields of chemistry. But the greatest passion of young Constantin Turta was for inorganic chemistry and physical chemistry.

After graduating the Chemistry Department at SUM, he is assigned to a military unit of the Russian Federation, where he works as a junior scientific researcher (1961-1964). After the expiry of the obligatory work period at the military unit, he returns to Moldova, where he works as an assistant at the Polytechnic Institute of Chisinau. Then he followed PhD studies at the Institute of Chemistry of the ASM and the Institute of Chemical Physics of AS USSR (1966-1969).

After successfully graduating the doctoral studies, he is employed at the Institute of Chemistry of the ASM as senior lab assistant (1969-1971), and is subsequently promoted by competition to the positions of junior scientific researcher (1971-1975), senior scientific researcher (1975-1989) and head of laboratory, since 1989. During 2000-2004 acad. Professor Constantin Turta has worked fruitfully as the General Scientific Secretary of the Presidium of ASM. Throughout his work Professor Constantin Turta proved to be Consistent, Open-minded, Noble, Serious, Talented, Ambitious, Notorious, Trustworthy, Intelligent, Nonconformist (CONSTANTIN), Tireless, Upright, Reliable, Tenacious, Assiduous (TURTA).

Professor Constantin Turta became a world-famous scientist in the fields of bioinorganic chemistry, dynamic effects in coordination chemistry (dynamic electron delocalization in mixed valence iron compounds, the "cross-over" spin transition), in application of Mossbauer spectroscopy in chemistry, magnetochemistry, biologically active coordination compounds, nanomaterials. He founded the scientific school which was further recognized abroad, in the fields of bioinorganic chemistry and use of Mossbauer spectroscopy in chemistry.

Professor Constantin Turta, together with his students, developed new methods of synthesis of coordination compounds with biometals Fe, Co, Mn, Zn, Cu, Ni and carboxylic acids, dioximes, amino acids, Schiff bases, etc. As a result, there have been performed many scientific researches, which were rewarded with valuable results. In order to achieve his goals, advanced scientific equipment was used, which allowed the determination of molecular and crystalline structure, chemical and physico-chemical properties. Thus, the obtained results defined the areas of utilization of new chemicals.

Professor Constantin Turta has worked hard to create the Center for Physical Chemistry and Nanocomposites in 2006 at the Institute of Chemistry of the ASM.

As the executive deputy director of the Center for Physical Chemistry and Nanocomposites, he contributes with his rich experience in solving problems related to studying the processes of obtaining nanoparticles required

in nanoelectronics, development of advanced technologies to obtain the necessary new preparations for the national economy, providing scientific research with performance measurements of various properties of the studied objects from all institutions that deal with chemical research, improving the training of young specialist and highly qualified scientific personnel, through master, doctoral and postdoctoral studies. Academician Constantin Turta prepared 2 Dr. habilitates and 7 PhDs in chemistry.

Special attention was directed by Professor Constantin Turta towards international scientific relations with scientists from Russia, Ukraine, Romania, Spain, Poland, Switzerland, Germany, France, USA etc. Due to these international scientific relations Prof. Constantin Turta obtained through contest and directed 4 research projects with the European Union - INTAS, 4 research projects MRDA-US-CRDF, 1 Swiss research project - Scopes and 1 mobility project in the frames of the European Research Program FP-7.

Sustainable development of society would be impossible without the development and use of new non-polluting energy sources. Everyone knows that the biggest and inexhaustible energy source is the Sun. The main problem consists in finding a way to expand the use of this solar energy, and a way to preserve it. Scientists are working in this field worldwide. Professor Constantin Turta also activates in this field. He synthesized nanocompounds enabling their use in water photolysis, i.e. - to use solar energy to obtain hydrogen and oxygen from water. Addressing this issue would have an enormous positive impact on the global warming phenomenon.

Scientific results obtained by acad. Constantin Turta have been published in over 400 scientific papers, including about 200 scientific articles, published in international journals with impact factor. He is also the author of 28 patents.

Scientific work and practical results of acad. Constantin Turta were deservedly appreciated by superior bodies, being awarded with the Prize of the Presidium of the Academy Award of Science (1995); National Award in Science and Technology (2005); Order of "Labor Glory" (1995); Medal "L. Ciugaev" of the Institute of General and Inorganic Chemistry of Russian AS (2005). Professor Turta is the holder of several national and international exhibitions mentions: Gold Medals - Genius-96, AST-WEST EURO-INTELLECT (Varna, Bulgaria), European Exhibition of Creativity and Innovation, Euro Invent (Iasi, 2009); Silver Medal "European Exhibition of Creativity and Innovation, Euro Invent" (Iasi, 2010), Bronze Medal at the International specialized exhibition INFO-INVENT (Chisinau, 2009), Diploma Genius-96 (Bucharest, 1996), International Exhibition of Inventions " Designs and Trademarks "(Bucharest, 1997).

Dear academician, professor Constantin Turta, on the occasion of Your 70 years anniversary and 50 years of fruitful scientific and teaching activity, on behalf of the scientific community of the Academy of Sciences of Moldova, we address You our best wishes of prosperity, health, welfare, new advances in boinorganic chemistry, nanomaterials and advanced technologies.

Happy Anniversary!

With profound respect, acad. Gheorghe Duca
President of ASM

Dr. hab., Prof. Tudor Lupaşcu,
Director of the Institute of Chemistry of the ASM

SCIENTIST OF AMAZING UPRIGHTNESS AND VALUABLE SCIENTIFIC RESULTS
(dedicated to acad. Constantin Turta 70's anniversary)

Academician T. Furdui
Prime vice-president of ASM

The scientific community marked in December 2010, a special event for local science - 70 years from the date of birth of the great chemist scientist, academician of ASM, doctor habilitate, Professor Constantin Turta, who is considered one of the greatest scholars in inorganic chemistry due to his erudition and fruitful scientific activity.

Acad. Constantin Turta, impassioned by chemistry since middle school, is known and appreciated not only by employees of the Institute of Chemistry of the Academy of Sciences, by several generations of graduates of the State University of Moldova and the Technical University, where he taught and continues to teach inorganic chemistry, but also by specialists from abroad (Romania, Russia, Tajikistan etc.), where he was invited to give lectures. This chemist, so erudite, with an excellent scientific and methodical training, is considered one of the most brilliant chemists by our great chemist, academician Pavel Vlad.

Being a very modest man, he never evoked his own personality. Few people know his biography. Therefore, I considered necessary to say a few words about his life. Constantin Turta was born on December 20, 1940 in the village Buciusca, Rezina, Moldova, in a peasants' family. To fight boredom, as he often remained alone at home, he decided to attend school with his older sister Alexandra. The following year, at the age of 5, he is accepted at the village elementary school, which he graduated in 1949. Since there wasn't any school for further education in the village, he got secondary education in the town Rezina, at School no. 1, which he graduated in 1956.

He was a diligent student, quiet, well noted and eminent almost at all disciplines. He was among those who were to graduate the 10-years school with excellence. But in the tenth grade an unfortunate event happened. Together with a classmate, they decided to visit the classmate's village to celebrate the village festival, being sure that the next morning they would return to school until the beginning of lessons. In the morning, his classmate's parents saw how tight the children were sleeping and decided not to wake them up, thus the boys were late for two hours. Some school teachers have not remained indifferent to that, saying that breach of discipline was committed by some of the best students and insisted for that event to be discussed at the meeting of the teachers' council, as a lesson for the entire school. After all, the biggest injustice to Constantin happened, because conditions have been created to hindrance his graduation with excellence of the secondary school.

Tests with stressful character, naturally, have continued during the entrance examinations at the Faculty of Chemistry, State University of Chisinau. In 1956, when Constantin presented his documents at the State University of Chisinau, there were 12 persons aspiring for each place. Constantin, though he didn't speak Russian very well, passed the test with honor (in those days studies at the Faculty of chemistry and biology and other faculties of exact and life sciences were in Russian) and became a student. Due to the fact that his knowledge of chemistry was quite significant, things at the University in general started to go as he pleased.

A person full of energy, he had several ambitions: to become a dancer in the ensemble "Joc", to form himself as a scientific researcher etc. With great pleasure, in 1957, together with his colleagues at the university, he participated in celery harvesting in Kazakhstan. In a word, just like other students, he was involved in many activities concurrently. But the fact that during that period at the Faculty of chemistry worked so prominent scientists like the future academics of ASM A. Ablov, Gh. Lazurievschi, U. Lealicov, T. Malinovschi, university professors P. Migali, M. Chişineovschi, naturally burst his desire to devote his life to science development. This was also due to the fact that he possessed all the necessary skills of a scientist, from his parents: pedantry, sense of discipline, punctuality, responsibility, diligence, etc. These qualities were what distinguished him among the best students.

After graduating the State University in 1961 he is assigned to work, as junior scientific researcher at a military institute of the Ministry of Defense in the Saratov region, where he dealt with the problems of sorption and filtration of substances. After three years, in 1964, he returned to Moldova, and was hired as an assistant at the Department of General and inorganic chemistry of the Polytechnic Institute of Chisinau. He was actively involved not only in organizing the teaching process of the department, but also in its social life, and therefore he was elected secretary of the Komsomol of the Technological Faculty, Chairman of the Professional Committee of students, assistant secretary of the Komsomol Organization of the Polytechnic Institute. While working at the Polytechnic Institute, he created a family by marrying Hlusova Larisa, also a chemist, and his daughter Ludmila was born in 1964.

In 1964 together with other colleagues working in the Military Institute, he obtained the first patent for invention.

In 1966 he entered the PhD courses at the Institute of Chemistry of the ASM and was delegated to work on

his doctoral thesis at the Institute of Chemical Physics AS USSR (Moscow), where he worked until April 1970. In that institute, whose director was the renowned scientist and Nobel Prize Laureate, Acad. N. N. Simionov, Constantin Turta obtained a deep theoretical and practical training, and became the only specialist in Moldova in the field of application of Mossbauer spectroscopy in chemistry.

The high professional level of the PhD student (future academician) Constantin Turta and the importance of the scientific results obtained in that institute are proved by the publication of his first seven scientific articles between 1970 and 1971 in the most prestigious journals "Reports of AS of USSR", "Theoretical and experimental chemistry", "Journal of inorganic chemistry" and their presentation in two specialty union conferences.

Returning to Chisinau, he was treated just like the other natives – he wasn't appreciated and supported at his fair value, but was employed as senior lab assistant, position held until July 1971. He successfully proved his PhD thesis in 1971, with the title "Study of iron coordination compounds with organic ligands using the Mössbauer method".

After proving the PhD thesis, although he published 10 articles, together with such scientists as A. Ablov, V. Goldanschi etc., in the most prestigious journals and for the first time implemented in our country the magnetochemical method at low temperatures (~ 110 K), gamma resonance spectroscopy, or the so-called Mössbauer spectroscopy, and his family was not very prosperous, the Institute of Chemistry continues to keep him in the position of junior researcher for another four years. And only on 16 December 1975 he was elected and reinforced by the Bureau of the Department of Biology and Chemistry as senior scientific researcher.

In November 1976 he was elected senior scientific researcher in the group of spectral and elemental analysis, which was coordinated by him until 1988, when he was elected through contest in the position of head of the " Bioinorganic Chemistry" Laboratory.

Acad. C. Turta's name is known in the scientific world due to his fundamental pioneering work in the field of application of Mössbauer spectroscopy in chemistry, inorganic and coordinative chemistry. For the first time, he implemented in our country the Mössbauer method with its application in chemistry, which made the majority of his scientific work truly pioneering.

He developed the chemistry of homo- and heteropolynuclear carboxoclusters of iron (III), which allowed him developing new methods of synthesis and obtaining new physiologically active substances. Highly appreciated is the work he devoted to the synthesis and characterization of mixed valence iron compounds, and to the description of dynamic phenomena: phase transition, electronic density delocalization of dynamic time-space type, the phenomenon of spin transition $^6A_1 << {}^2T_2$ for iron ions (III) in thiosemicarbazonates and dioximates of iron (III), to elucidate factors influencing the transition temperature and spin transition type and the velocity of electron transfer in such systems. Based on Mössbauer spectroscopy, a class of substances has been proposed in order to study the intermolecular electron transfer process.

For the first time, he proved that the mixed-valence iron carboxylates possess significant catalytic properties for the reaction of unsaturated hydrocarbons hydrogenation. For the first time he synthesized and studied carboxylates of tetranuclear iron (III) and heterotetranuclear, containing rare earth ions. Also, he developed a unique method of assignment of partial Mössbauer spectra of iron ions with different close surroundings in a polynuclear molecule, which is based on determining the temperature dependence of the projection of amplitude oscillations of iron ions $<x^2>$ from the rest position.

The work of acad. C. Turta got highly appreciated in the scientific world for its originality and the multilateral approach to the studied problems, use of modern methods and deep analysis of scientific results. This may be proved by the cycle of works devoted to iron α-dioximates, whose molecular, crystalline and electronic structures were determined by using Mössbauer spectroscopy, magnetochemistry and quantum-chemical methods. This approach allowed showing that in the class of α-dioximates of iron (II) with octahedral tetragonal distorted structure, introduction in the composition of ligands of groups with different donor-acceptor properties slightly changes the π- and σ-type metal-ligand bonds, leaving unchanged the spin state of the complex generator.

He is among the first researchers who used the data obtained by gamma resonance spectroscopy method to elucidate the topochemical intramolecular redox reaction involving the couple Fe - ligand in iron α-dioximates, described the kinetics of this reaction and studied the electronic state of the dopant Fe in the superconductor of high temperature of type Bi-Pb-Sr-Ca-Cu-O.

Special attention was given to studying the state of iron ions in the phase of ions changes and, also, to transformations of oxidation number and spin state of iron as a result of influence of different reagents and temperature.

The scientific interests of acad. C. Turta extended on the electronic structure of the active center of hemoglobin in different conditions - under the influence of traumatic shock, nitrates and some pesticides.

Based on fundamental scientific results, he synthesized novel coordination compounds - gajazot, galmet, trifeden, difecoden etc., which are used in agriculture and microbiology.

Towards the late 80s of the last century, C. Turta became recognized as the most authoritative scientist in the application of Mössbauer spectroscopy in coordination chemistry and physics, as was widely noted at the ASU Institute

of Chemical Physics (Kiev) while proving his Dr. habilitate thesis "Dynamic effects in complex combinations of mono- and polynuclear iron with polydentate ligands (syntheses, structure, Mossbauer spectra and magnetic properties)".

In 1995 important events took place in the life of C. Turta – he was awarded the title of university professor and elected as corresponding member of the ASM.

Due to his consistency and depth in performing scientific research and its intelligent behavior, scientific achievements and its uprightness, acad. C. Turta's authority in society had become an axiom; therefore his election in 2000 in the position of the general scientific secretary of the ASM was perceived by all as a natural, but also necessary act.

Prof Turta is the author of 517 scientific publications, including nearly 200 articles, published in the most prestigious international journals, 32 patents and a university handbook "Introduction into gamma resonance spectroscopy (Mössbauer spectroscopy)."

He gave lectures not only in local universities in the country (Technical University, State University, Academic University), but in foreign universities, as well (Technical University "Gh. Asachi", Romania, University of Tajikistan, Dushanbe, West University, Timisoara etc.).

C. Turta successfully collaborates with recognized scientific centers in the world - Institute of Chemical Physics "N. N. Semionov" (Moscow), National Institute for Materials Physics (Bucharest), Institute of Physical Chemistry (Bucharest), Institute of Physical Chemistry (Kiev), Institute of Macromolecular Chemistry "P. Poni" (Iasi) etc.

He is the founder of the scientific school in physical chemistry, inorganic and coordinative chemistry. Under the leadership of Prof. Turta were proved 7 PhD theses and 2 Dr. habilitate theses.

Scientific and managerial contributions of acad. C. Turta in the development of science have been recognized at home and abroad, being awarded the Order of "Labour Glory", with the medal "Honor.Glory.Labor" of gr. IV (Ukraine), the Medal "L.S. Ciugaev", awarded the National Prize in Science and Technology etc.

C. Turta stands out among other personalities due to his style of work, his delicate behavior, honesty, pedantry, intelligence. He is appreciated by others as a scientist endowed with great intellectual and moral qualities. Not once I was impressed, as a witness, by his resistance to some temptations, maintaining honesty, good reputation and non-profitable character.

Devoting his life to the study mainly of electronic structure, properties and significance of iron and its coordination compounds, academician, Professor C. Turta has created a lifestyle and uprightness alike the metal he has always studied.

Given such personalities, who willingly sacrifice their lives to science, such people of good faith and great scientists, as is acad. C. Turta, you can be sure about the future of science.

Live healthy for many, many years, dear acad. Constantin Turta, with new achievements in science!